Electronic Supplementary Material (ESI) for Polymer Chemistry.

Supporting information

Oxazolidone formation: myth or fact? The case of biobased polyurethane foams from different epoxidized triglycerides

Julien Peyrton, Luc Avérous*

BioTeam/ICPEES-ECPM, UMR CNRS 7515, Université de Strasbourg,
25 rue Becquerel, 67087 Strasbourg, Cedex 2, France.
*Corresponding author. E-mail address: luc.averous@unistra.fr (Luc Avérous)
Fax: +333 68852716; Tel: +333 68852784

Maximum height of the foam realized with gradual substitution of Pht-DEG by ESO

Figure S1 Pictures of PUF realized with increasing content of ESO at then end of the rise.

FTIR analysis of the ESO foams

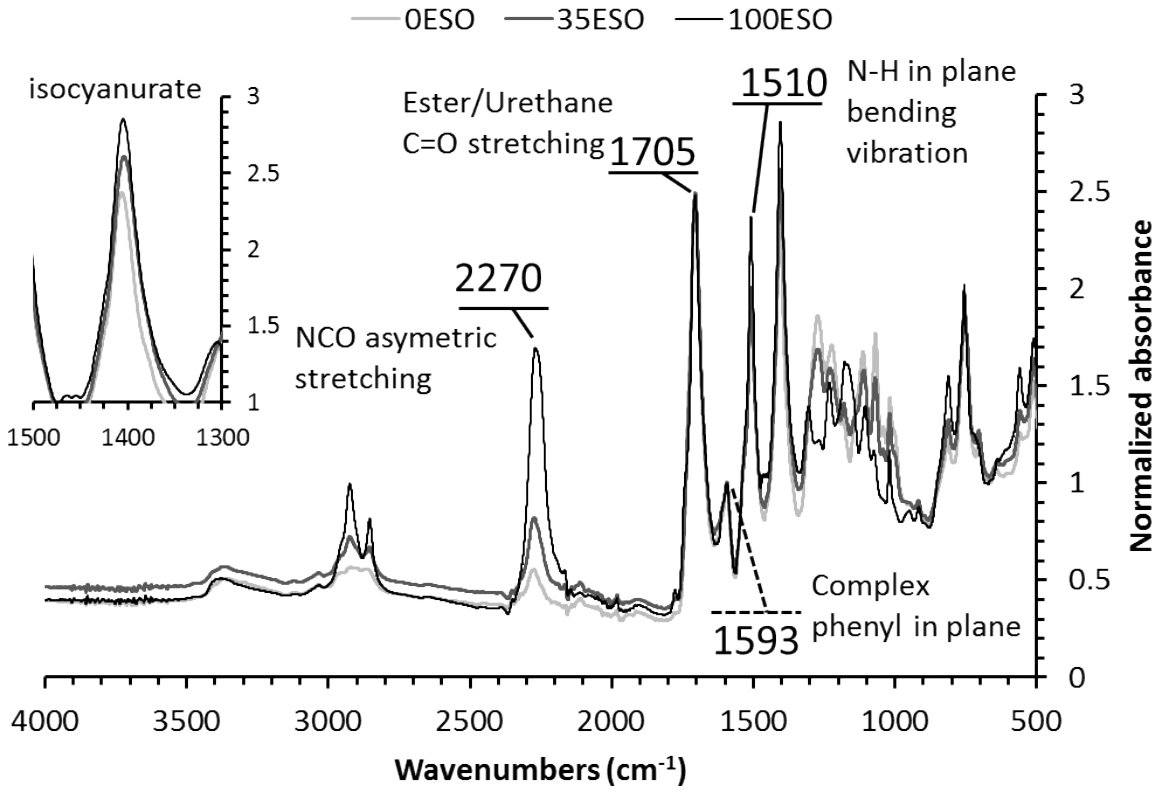

Figure S2 FTIR analysis of 0ESO, 35 ESO and 100ESO with the absorbance normalized on the complex phenyl in plane band at 1593 cm^{-1}.

Identified soluble fractions in freshly synthesized foams

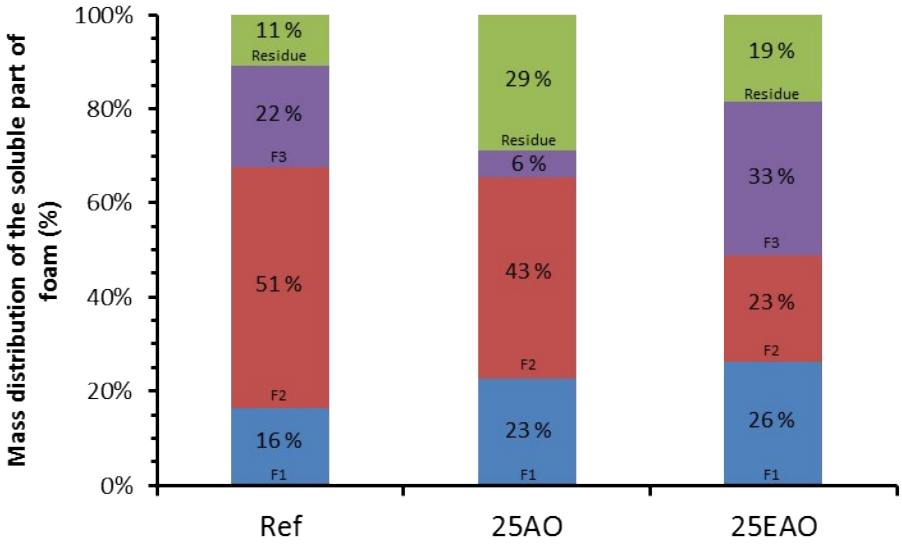

Figure S3 The identified fraction of soluble content of PIR ref, 25AO and 25 EAO foams.

FTIR analysis of formerly synthesized foams

Analysis of F1

The FTIR spectrum of F1-Ref, F1-25AO and F1-25EAO shown in Figure S4A were quasi similar. It was then assumed that the less polar compound was the same for all foams. The F1-Ref, F1-25AO and F1-25EAO extracts also presented carbonyl stretching band at $\tilde{\nu}$=1740 cm^{-1}, the vibration of C-CH_3 at 1460 cm^{-1} and alkane antisymmetric and symmetric CH_2 stretching at $\tilde{\nu}$=2852 and 2921 cm^{-1}, respectively typical of P2H-EG (Figure S4A).[35,36] However, the band related to the ethylene glycol at $\tilde{\nu}$=3350 (OH stretching) and 1400 cm^{-1} (COH vibration) shielded the 2-ethyl hexanoate signals. On the contrary to the EG, the potassium 2-ethyl hexanoate should not be integrated into the PU network during the foam elaboration. The potassium carboxylate identified by the band at $\tilde{\nu}$=1555 cm^{-1} corresponding to the COO-K vibration was potentially transformed into a carboxylic acid ($\tilde{\nu}$=1740 cm^{-1}) during the foam processing.

^{1}H NMR analyses were conducted and presented in Figure S4B to confirm the structure hypothesized in FTIR. In ^{1}H NMR, the alkane protons at δ=1.25 ppm and the end of chain CH_3 at δ=0.88 ppm are identified in the F1 fractions and P2H-EG spectra. The ethylene glycol identified at δ=2.62 ppm in the ^{1}H NMR spectra of P2H-EG (Figure S4B) reacted with isocyanate and was integrated into the polymer network.

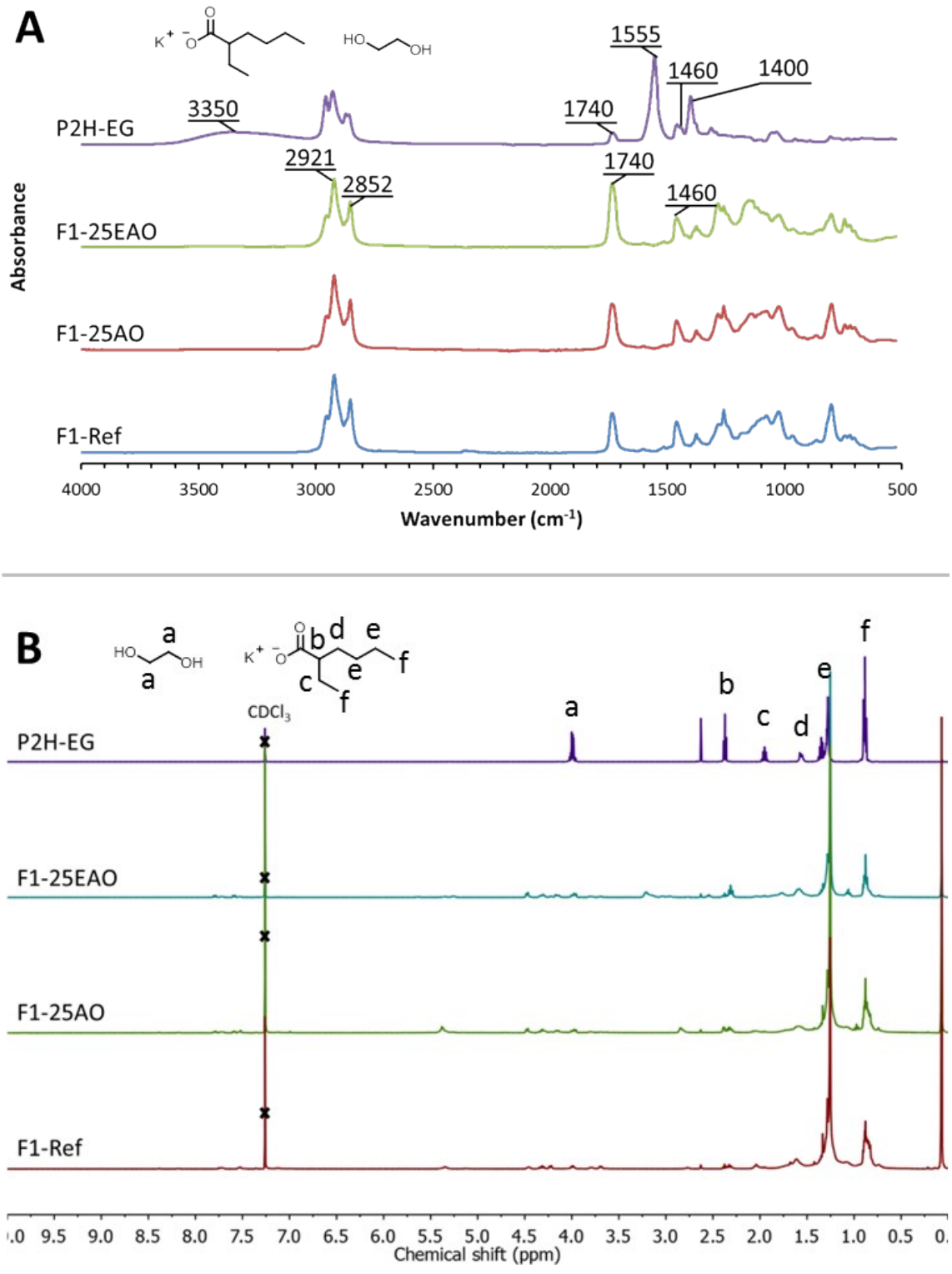

Figure S4 Chemical analysis of F1-Ref, F1-25AO, F1-EAO and P2H-EG by FTIR (A) and ^{1}H NMR (B).

Analysis of F2

The FTIR spectra of F2-Ref, F2-25AO and F2-25EAO were similar (Figure S5A). Surprisingly, the carbonyl stretching at $\tilde{\nu}$=1720 cm^{-1}, ether C-O-C stretching at $\tilde{\nu}$=1290 cm^{-1} and terminal CH_2-CH_2-O at $\tilde{\nu}$=990 cm^{-1} [37] were identified. These bands were also present in the Pht-DEG spectra (Figure S5A).

Therefore, the second fractions could be attributed to unreacted polyol. However, the absence of the characteristic hydroxyl band at $\tilde{\nu}$=3450 cm^{-1} contradicted this hypothesis. The esterification of phthalic acid with diethylene glycol industrially produces Pht-DEG. One of the side-reaction is the formation of cyclic ester, which could explain the similar FTIR spectra of Pht-DEG and the second fractions.

For the second fraction, the ^{1}H NMR (Figure S5B) confirmed the glimpse gave by the FTIR. An aromatic chemical shift matching with the Pht-DEG spectrum appeared at δ=7.80 (a) and 7.58 (b) ppm. It was expected that 100% of the polyol reacted by polyaddition with the polyisocyanate. Therefore, only the side-products without OH groups should be extracted from the foams. The cyclic ester side product of the polyol synthesis was identified in F2-Ref, F2-25AO and F2-25EAO spectra (Figure 2B) by peaks at δ=4.71 (c') and 3.95 (d') ppm. The other peaks observed in the ^{1}H NMR spectra of the second fractions could be explained by some additives such as surfactants, present in the industrially produced Pht-DEG.

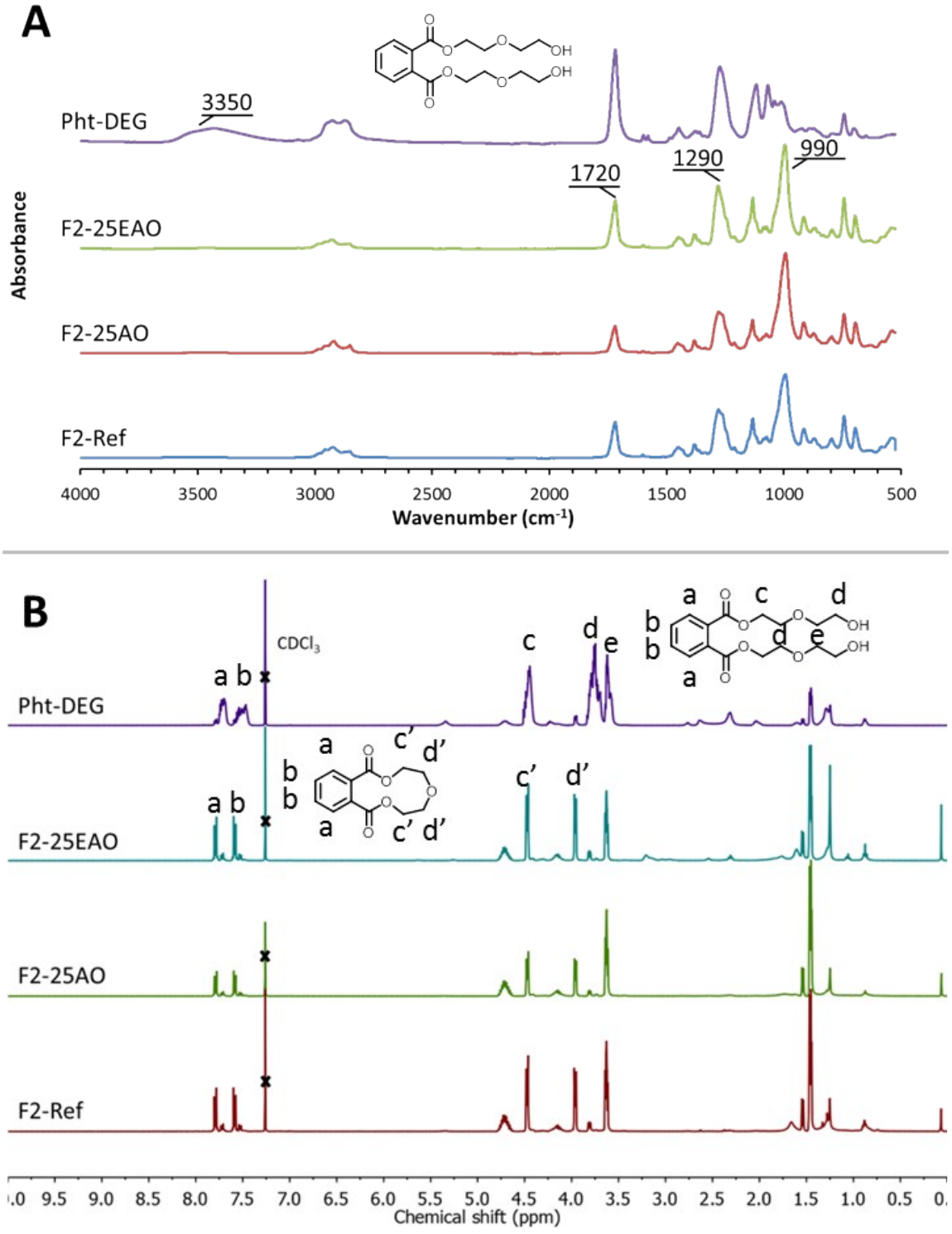

Figure S5 Chemical analysis of F2-Ref, F2-25AO, F2-EAO and Pht-DEG by FTIR (A) and ^{1}H NMR (B).

Analysis of F3

The FTIR spectra of F3-Ref, F3-25AO and F3-25EAO presented in Figure S6A, did not present significant difference compared to F2 fractions spectra. The Pht-DEG derivatives bands of carbonyl stretching at $\tilde{\nu}$=1720 cm^{-1}, ether C-O-C at $\tilde{\nu}$=1290 and 990 cm^{-1} were identified.

Further investigations by ^{1}H NMR were conducted to identify the structure of the third fractions (Figure S6B). Despite the use of strong polar solvents, neither DMCHA nor PoSi signals were detected. The tertiary amine catalyst and the surfactant strongly interact with the silica column and explain the high residue values.

In F3-Ref, the aromatic signals located in the region δ=7.80-7.58 ppm and signals at δ=4.70 and 3.62 ppm in the ^{1}H NMR spectrum, as already stated, indicated the presence of Pht-DEG cyclic ester side-products. Despite the absence of aromatic signals, the Pht-DEG cyclic ester was also identified in F3-AO and F3-EAO (Figure S6B) at δ=4.70 and 3.62 ppm.

In the F3-25EAO, EAO was identified by the chemical shift of the glycerin protons at δ=5.25, 4.31 and 4.15 ppm, the epoxide signal at δ=2.8-3.2 ppm and the methylene protons in between two epoxide groups at δ=1.75 ppm (Figure S6B). The presence of EAO in the F3-EAO indicates that at least one portion of the EAO did not react and was not integrated into the polymer network in freshly synthesized PUF.

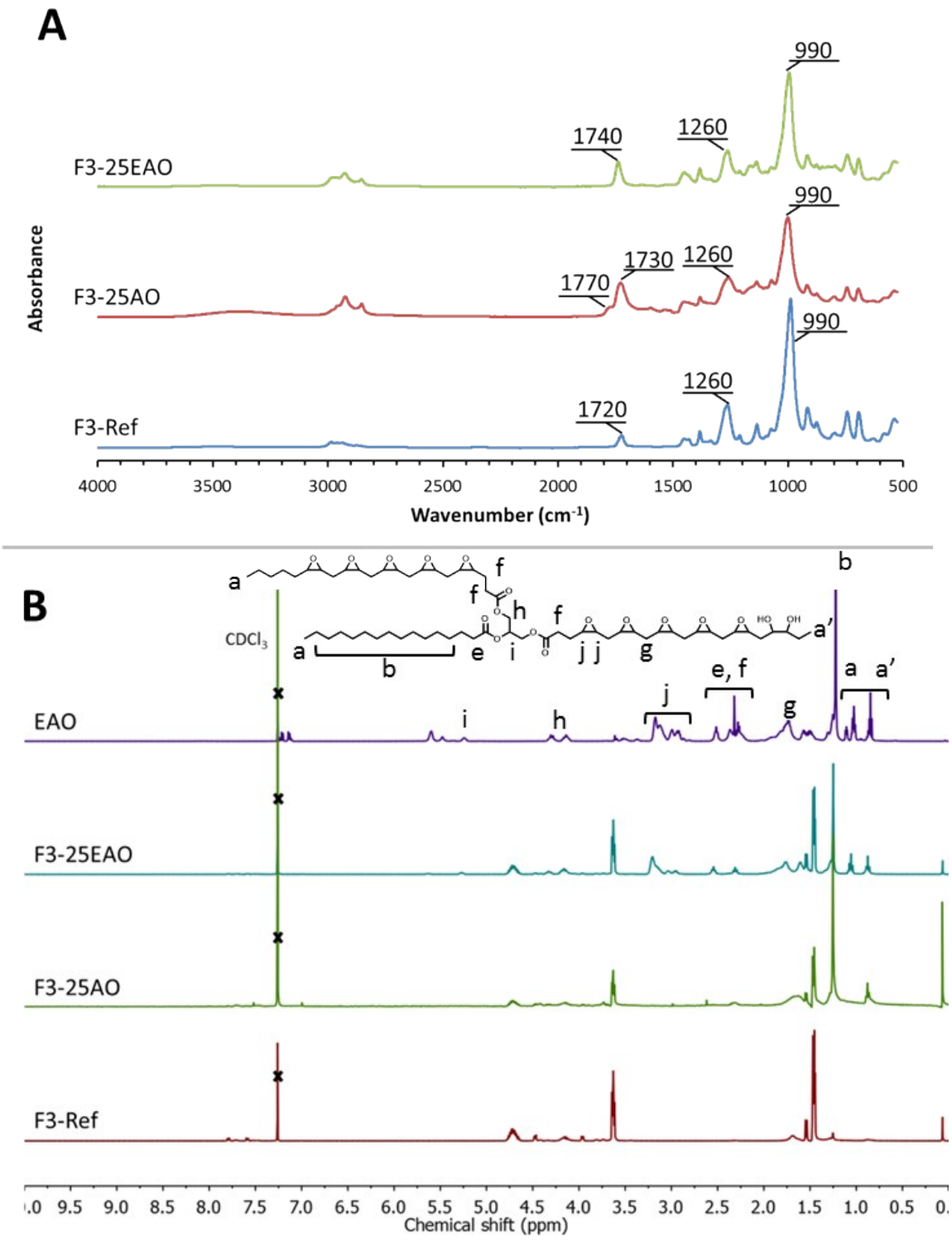

Figure S6 Chemical analysis: (A) FTIR spectra of F3-Ref, F3-25AO, F3-EAO and (B) ^{1}H NMR spectra of F3-Ref, F3-25AO, F3-EAO and EAO-oil.

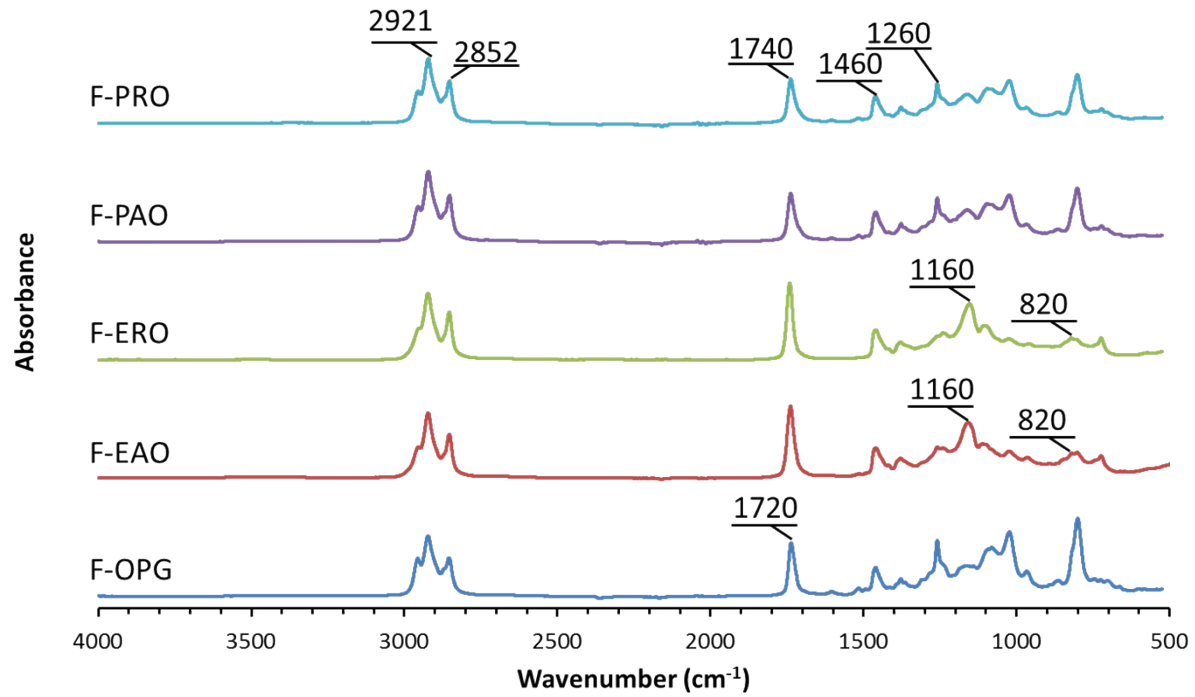

Figure S7 FTIR spectra of F-OPG, F-EAO, F-ERO, F-PAO and F-PRO.

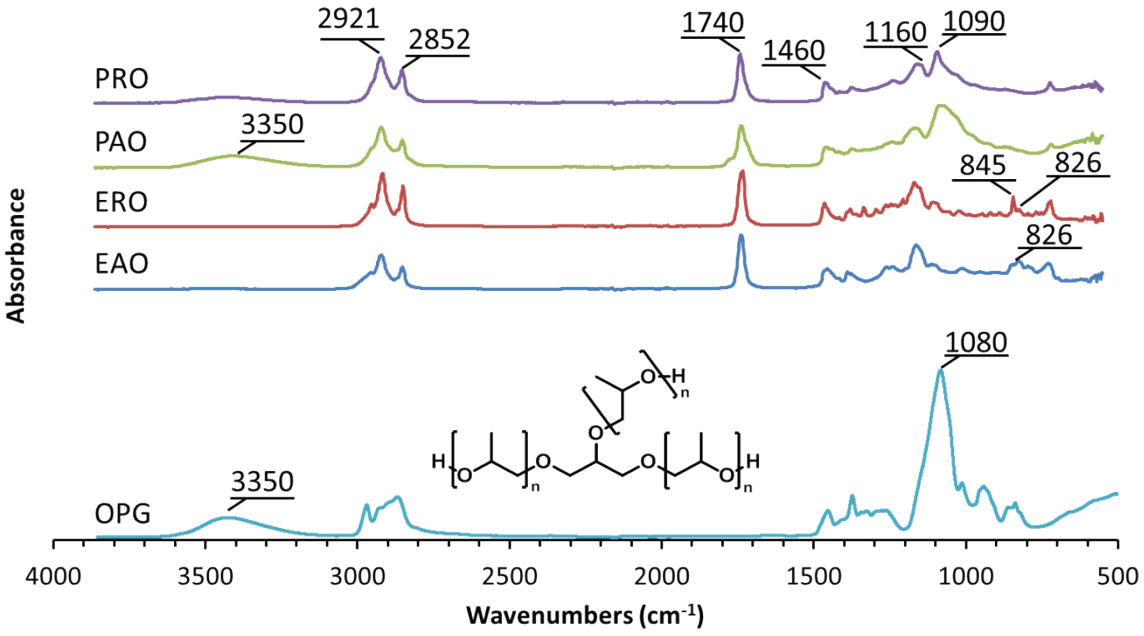

Figure S8 FTIR spectra of OPG, EAO, ERO, PAO and PRO.

NMR Spectra of Mundex synthesis

Undecylenic acid produced in large quantities as intermediate in the synthesis of PA-11 is derived from the pyrolysis of ricinoleic fatty acid. The fatty acid structure is identified by the ester methylene protons at δ=2.33 ppm (f in Figure S9). The terminal double bond protons are located at δ= 5.80 and 4.90 ppm (a and b in Figure S9). Mund was obtained in quantitative yield (98 %wt) by esterification of undecylenic acid with an excess of methanol. The formation of Mund was identified by the methyl ester peak at δ=3.66 ppm in the ^{1}H NMR spectra (g in Figure S9). Mund was further epoxidized with the meta-chloroperoxybenzoic acid, a stable peroxycarboxylic acid, to yield Mundex at 80 wt%. The formation of Mundex was shown by the complete disappearance of the vinyl proton at δ=5.80 and 4.90 ppm, and the presence of the epoxides protons signals at δ=2.89, 2.74 and 2.45 ppm (Figure S9).

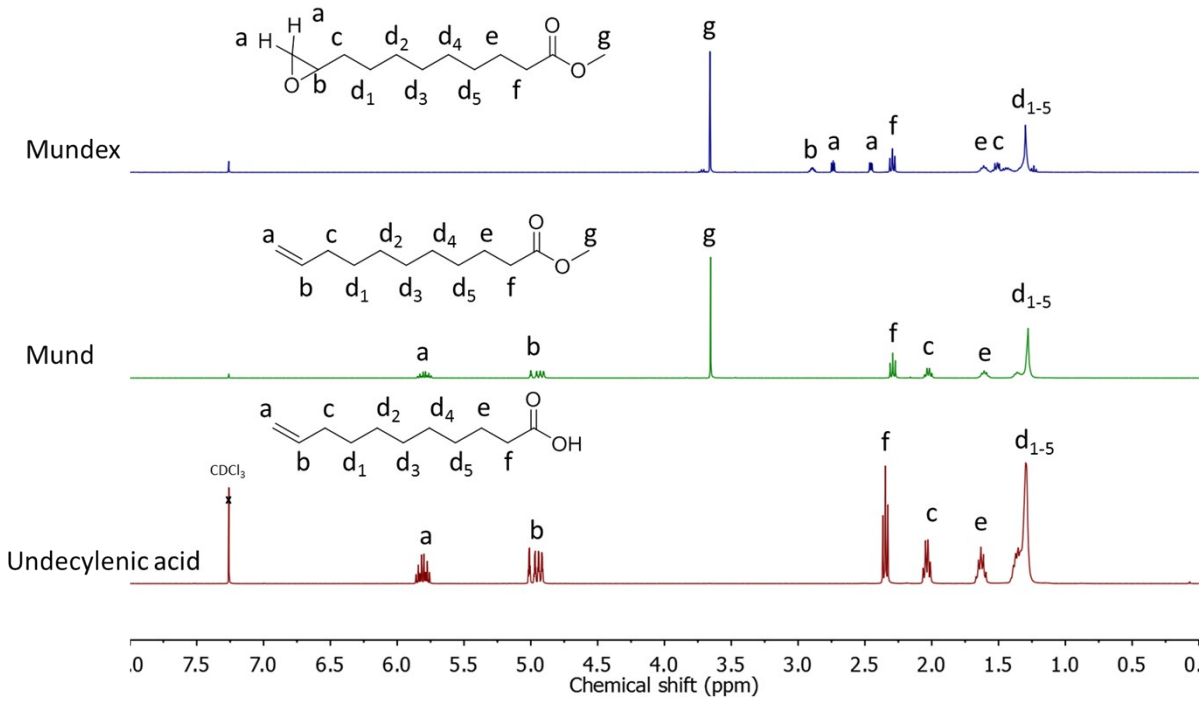

Figure S9 ^{1}H NMR spectra of undecylenic acid, Mund and Mundex.

Repartition of the extracted fraction in model study

Table S1 Weight fraction of products separated by chromatography column of the DGEBA reactions.

DGEBA	F1	F2	F3	Residue	Total
Without cat	73%	25%		2%	100%
BDMA	9%	76%	5%	11%	100%
KOAc	71%			29%	100%
TBAB	26%	47%	15%	12%	100%
$ALCl_3$	5%	57%	24%	14%	100%
Al(salen)2	18%	66%		15%	100%

Table S2 Weight fraction of products separated by chromatography column of the Mundex reactions.

Mundex	F1	F2	F3	F4	Residue	Total
Without cat	54%	6%			39%	100%
BDMA	72%	0.1%	1%	6%	20%	100%
KOAc	73%	1%	3%	2%	21%	100%
TBAB	60%	11%			29%	100%
$ALCl_3$	69%	7%	4%		21%	100%
$Al(salen)_2$	54%	11%	3%		32%	100%

Table S3 Weight fraction of products separated by chromatography column of the EVHOSO reactions.

EVHOSO	F1	F2	F3	F4	Residue	Total
Without cat	58%	10%	11%	17%	4%	100%
BDMA	57%	27%	3%		13%	100%
KOAc	62%	9%	11%	14%	4%	100%
TBAB	69%	4%	3%		25%	100%
$ALCl_3$	58%	11%	4%		27%	100%
$Al(salen)_2$	59%	20%	7%	5%	9%	100%

Determination of the ^{1}H oxazolidone peak for DGEBA

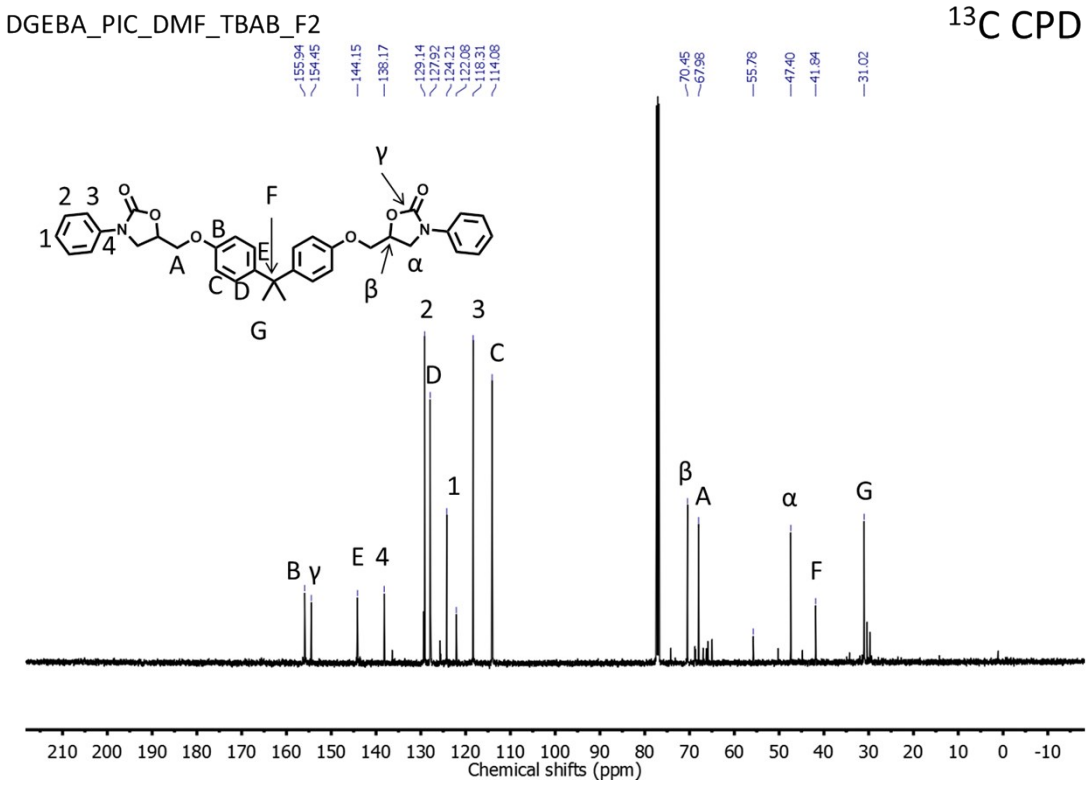

Figure S10 ^{13}C NMR Composite Programmed Decoupling (CPD) spectrum of DGEBA_PIC_DMF_TBAB_F2.

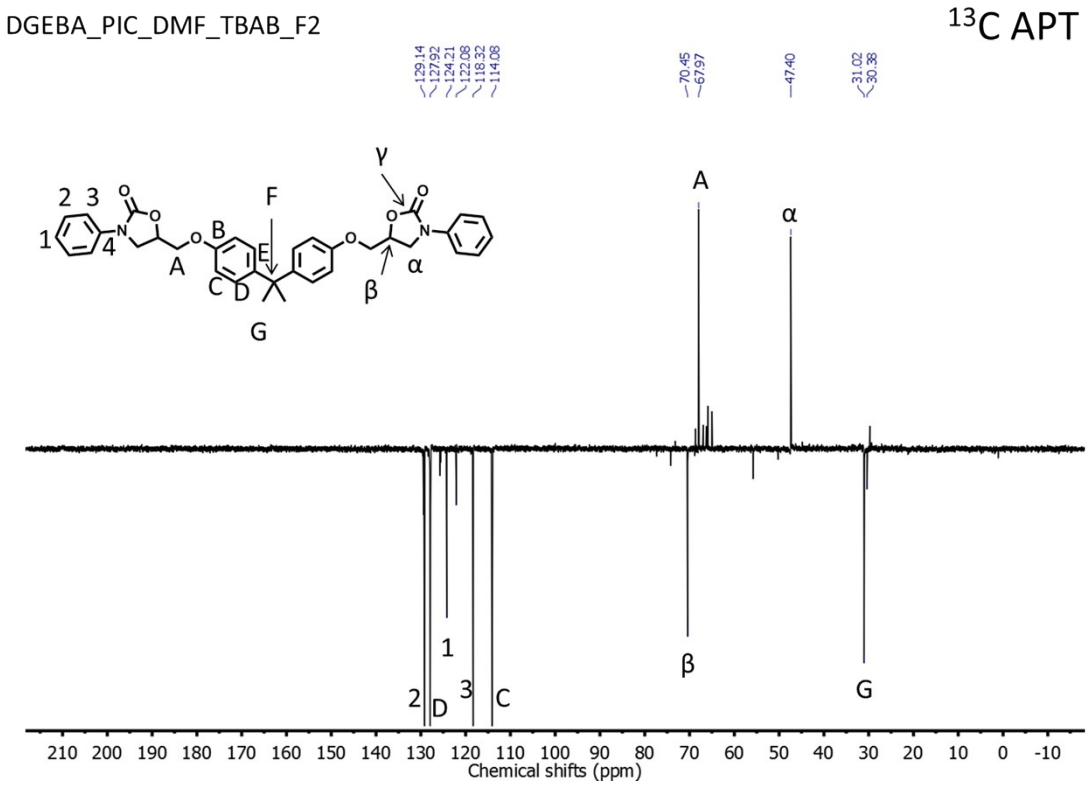

Figure S11 ^{13}C NMR Attached Proton test (APT) spectrum of DGEBA_PIC_DMF_TBAB_F2.

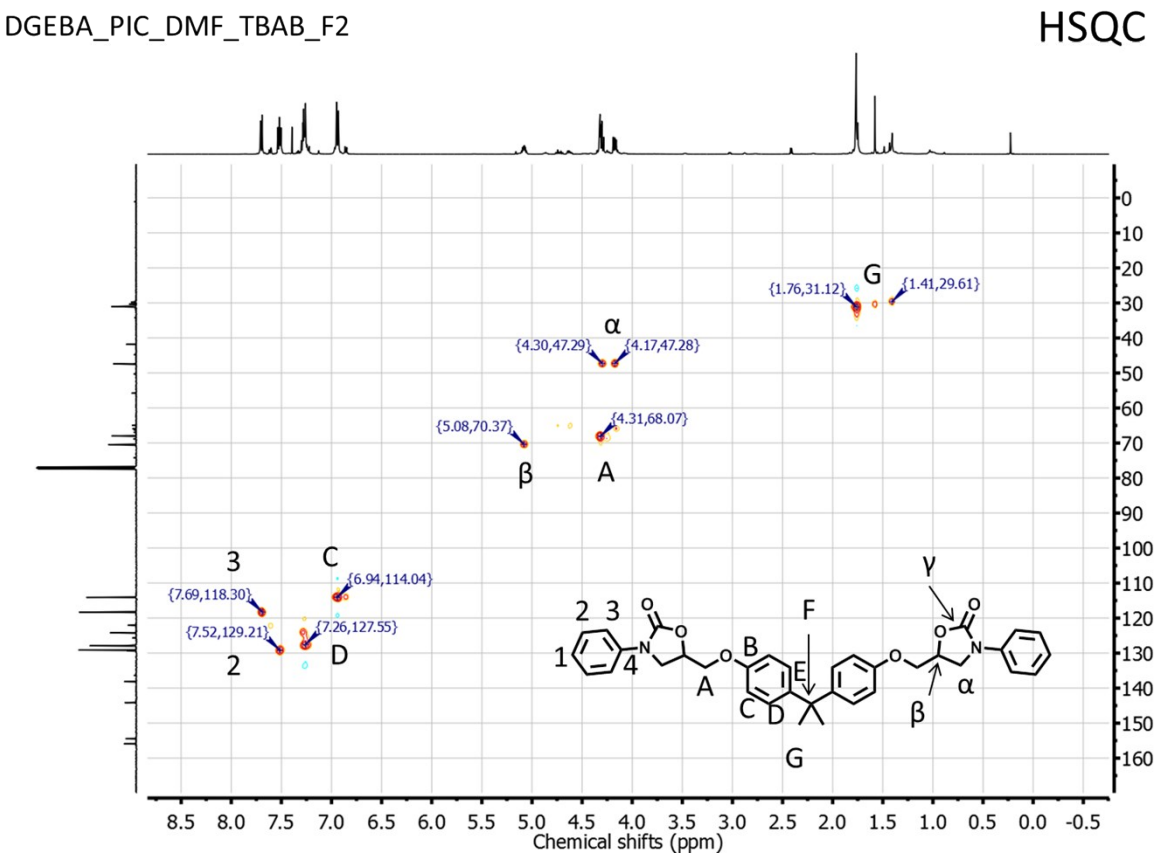

Figure S12 Heteronuclear Single Quantum Correlation (HSQC) NMR spectrum of DGEBA_PIC_DMF_TBAB_F2.

^{1}H NMR spectra of the DGEBA and major fraction of the DGEBA reactions

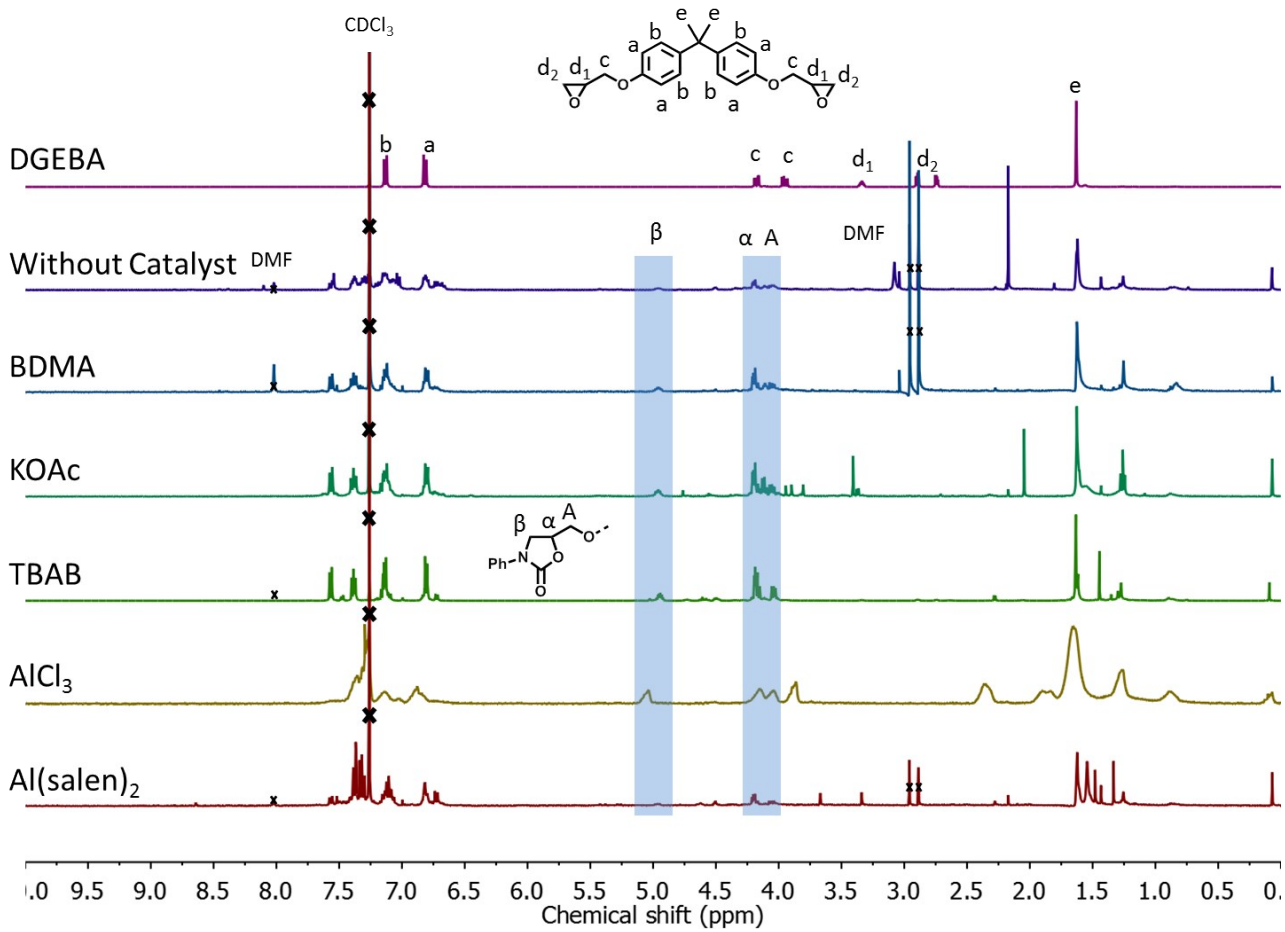

Figure S13 ^{1}H NMR spectra of DGEBA and the main fraction of DGEBA reaction without catalyst and with BDMA, KOAc, TBAB, $AlCl_3$ or $Al(salen)_2$.

Determination of the ^{1}H oxazolidone peak for Mundex

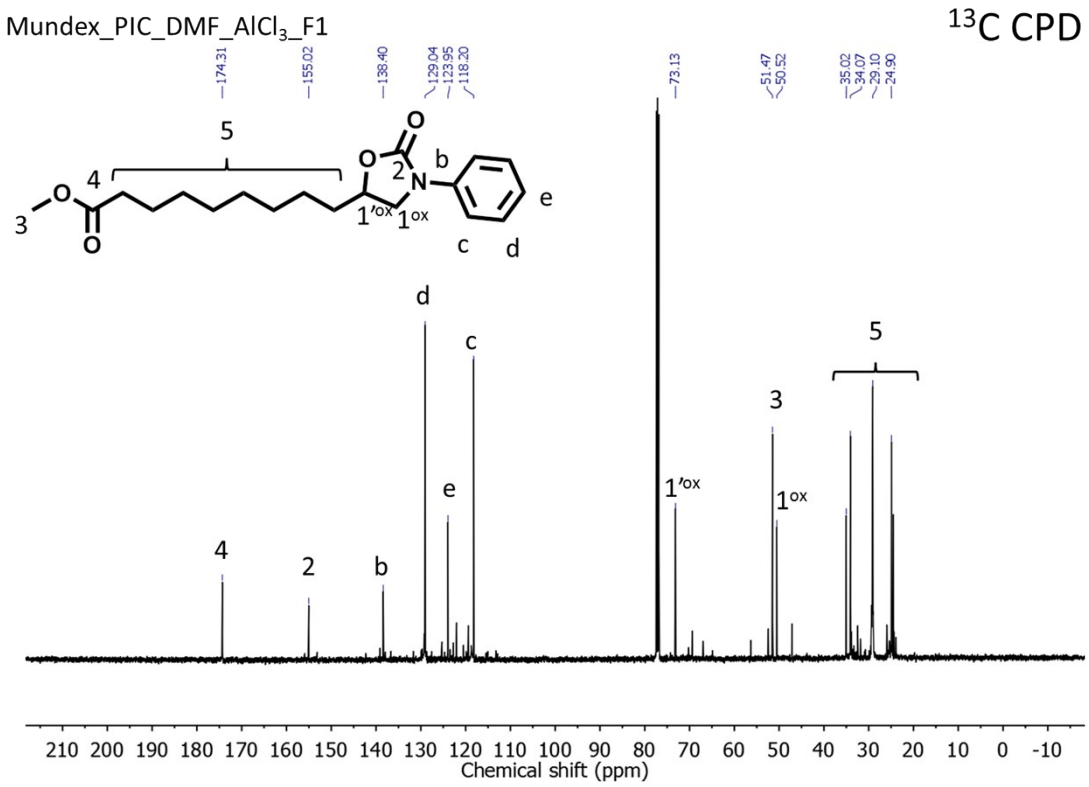

Figure S14 ^{13}C NMR Composite Programmed Decoupling (CPD) spectrum of Mundex_PIC_DMF_$AlCl_3$_F1.

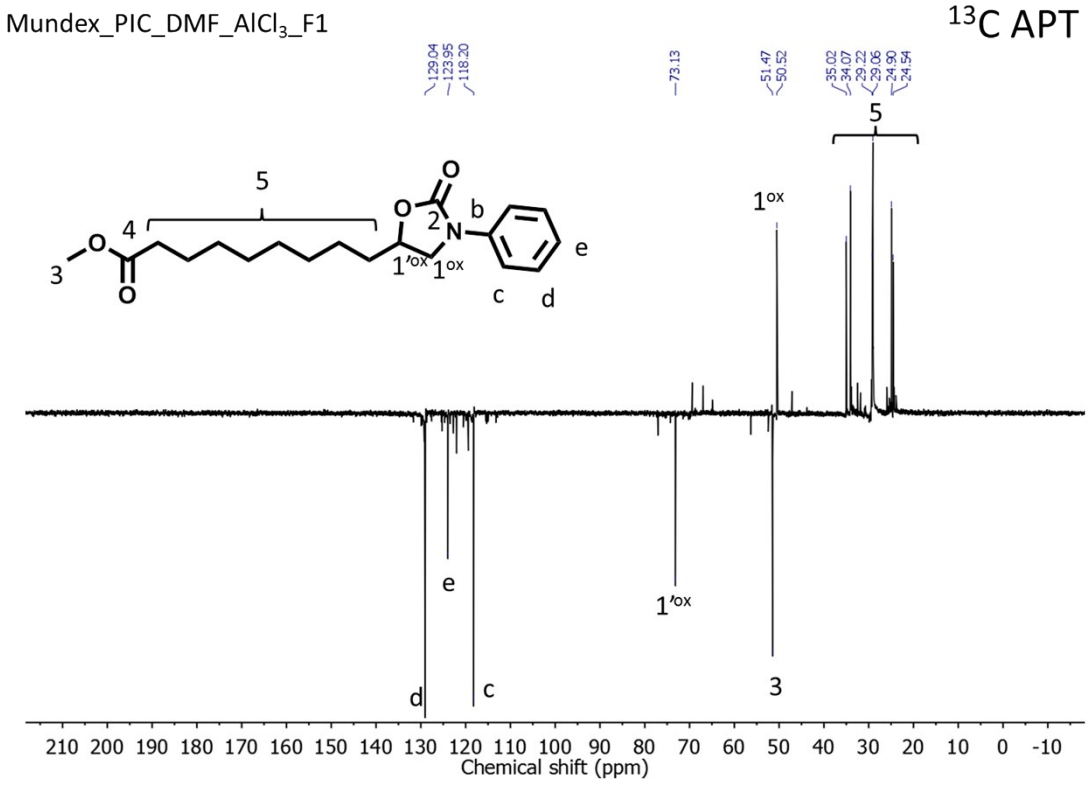

Figure S15 ^{13}C NMR Attached Proton test (APT) spectrum of Mundex_PIC_DMF_$AlCl_3$_F1.

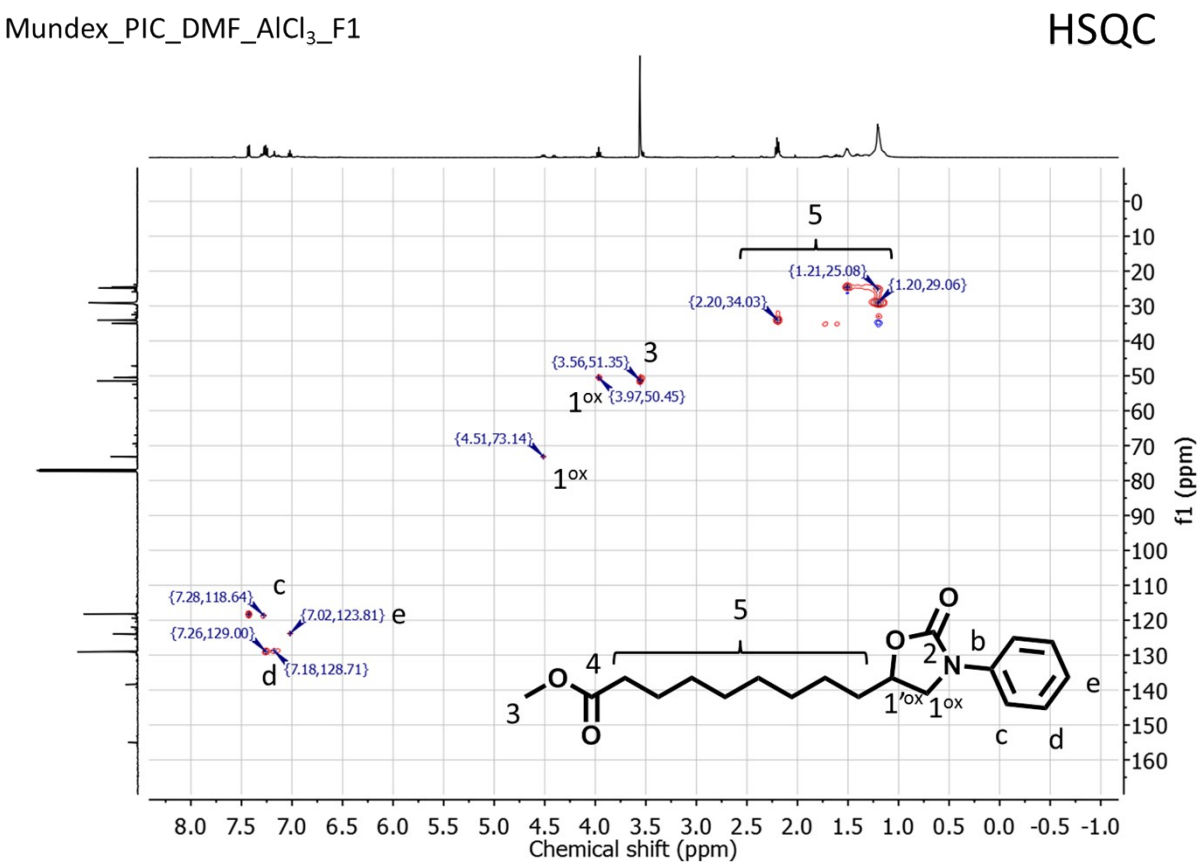

Figure S16 Heteronuclear Single Quantum Correlation (HSQC) NMR spectrum of Mundex_PIC_DMF_$AlCl_3$_F1.

NMR spectra of the Mundex minor fractions

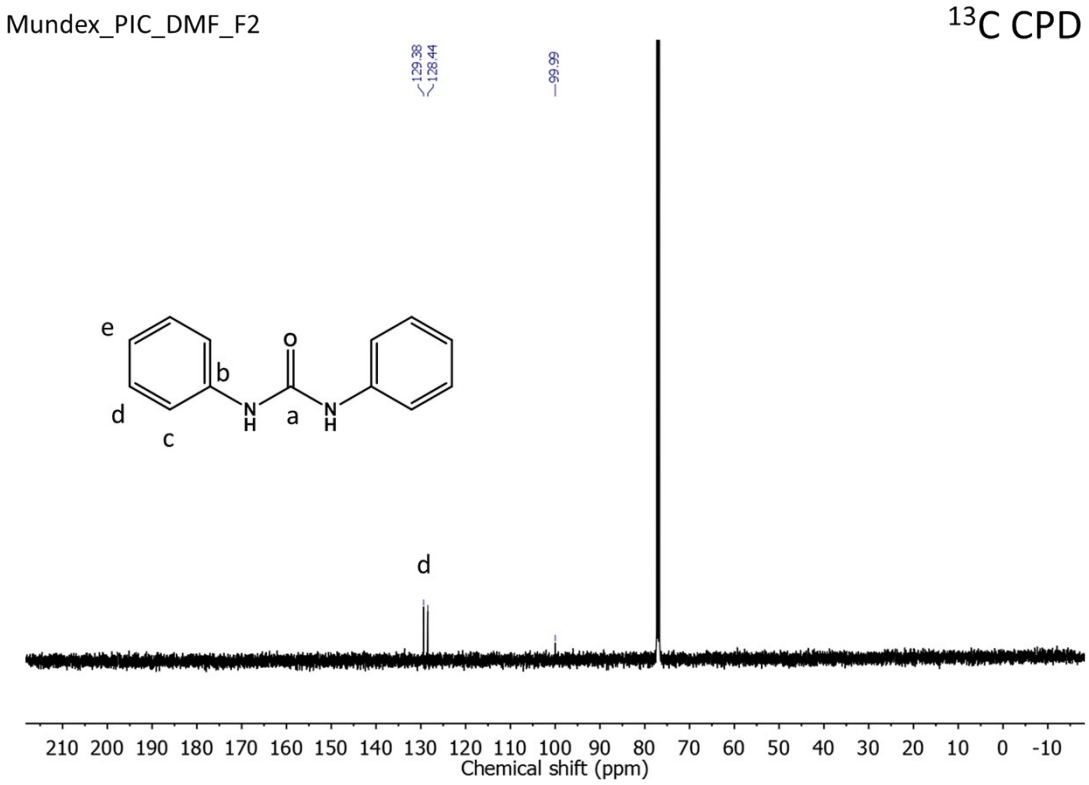

Figure S17 ^{13}C NMR Composite Programmed Decoupling (CPD) spectrum of Mundex_PIC_DMF _F2.

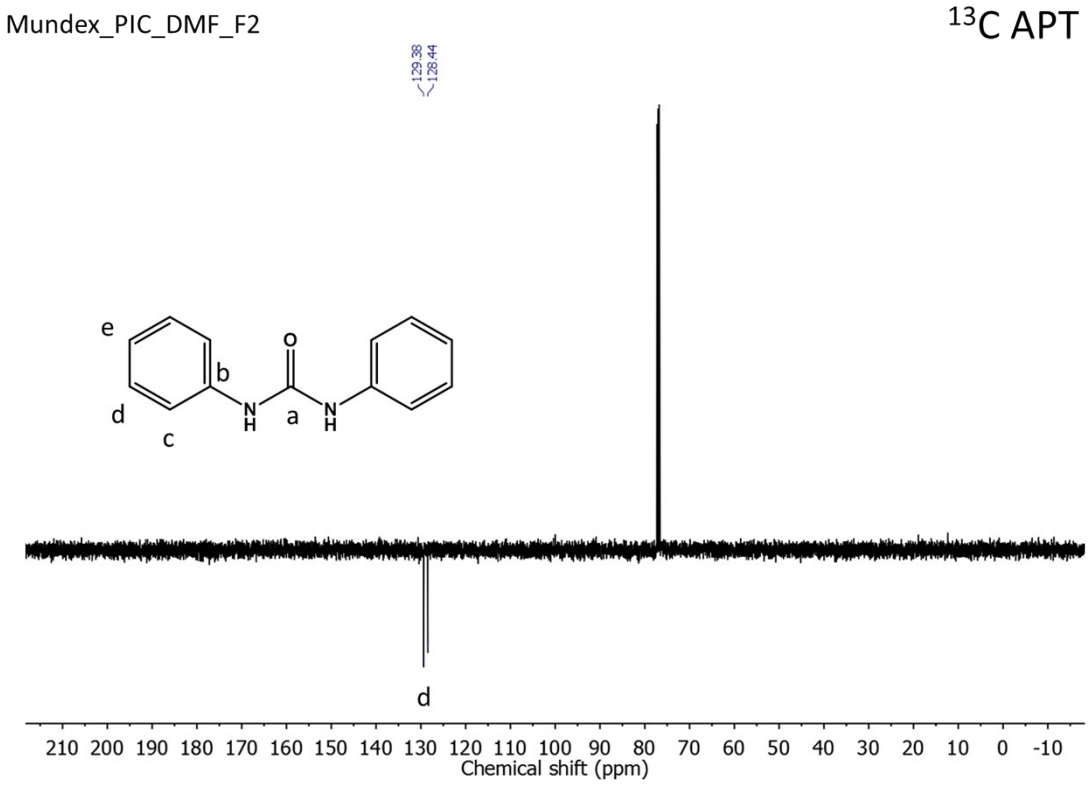

Figure S18 ^{13}C NMR Attached Proton test (APT) spectrum of Mundex_PIC_DMF _F2.

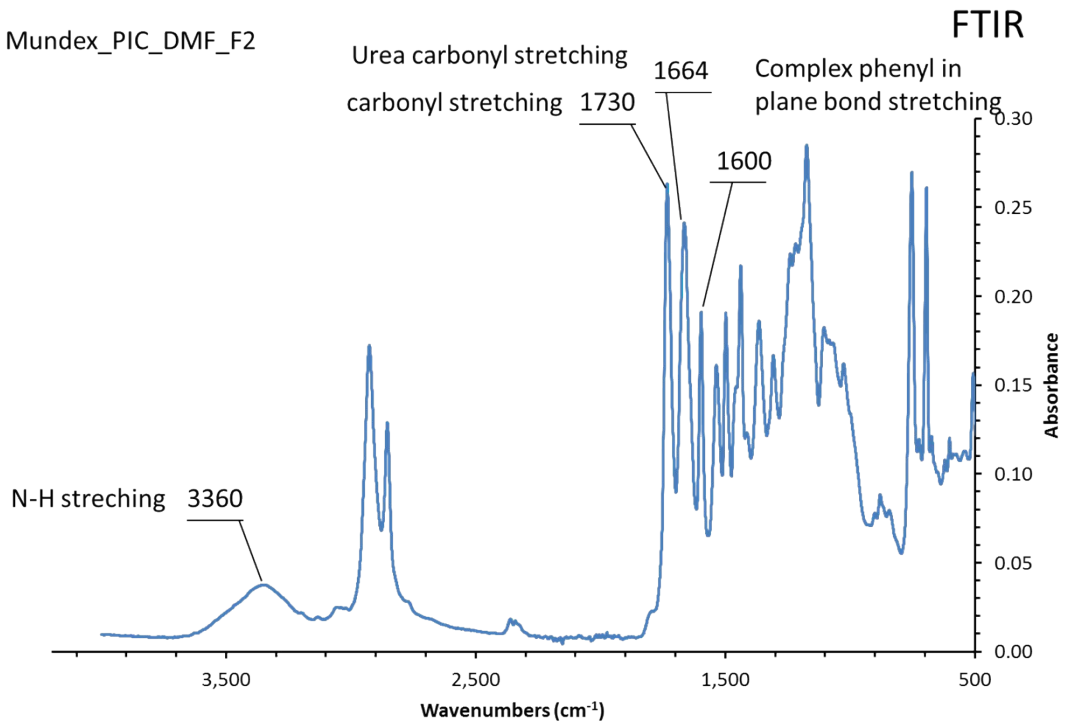

Figure S19 FTIR spectrum of Mundex_PIC_DMF _F2.

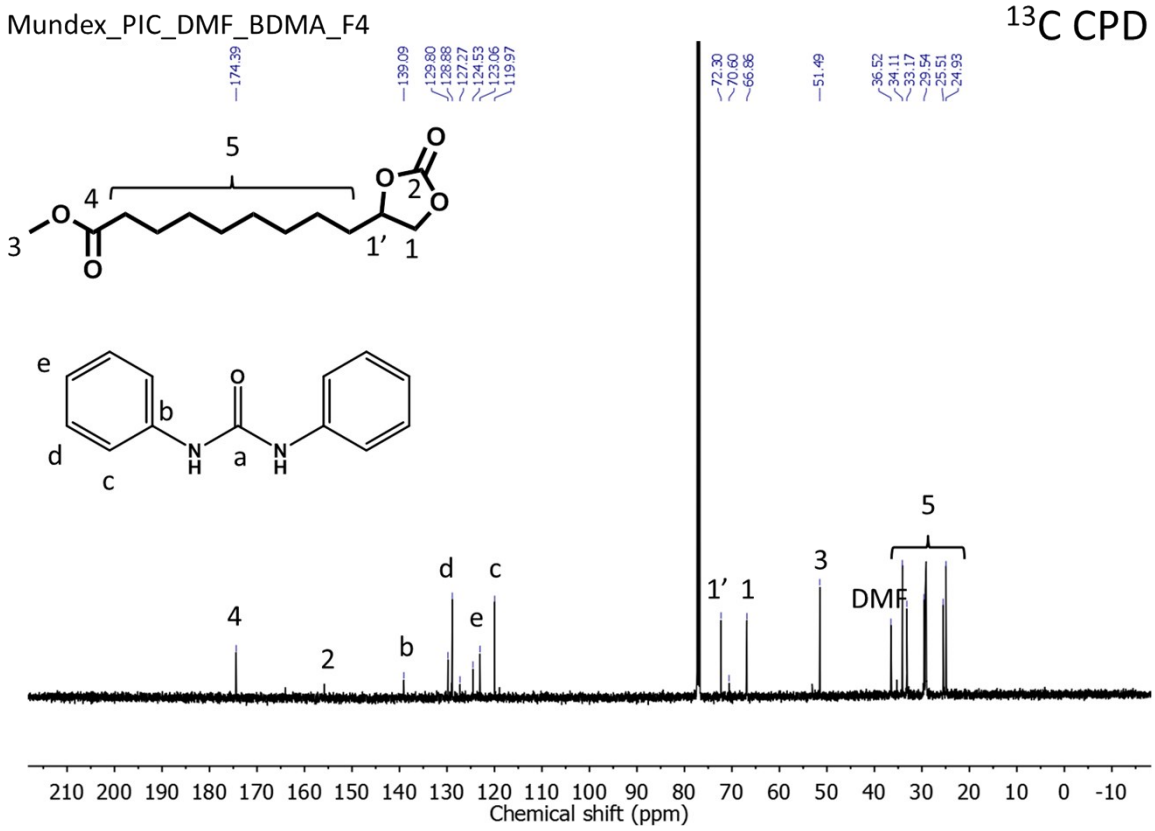

Figure S20 ^{13}C NMR Composite Programmed Decoupling (CPD) spectrum of Mundex_PIC_BDMA _F2.

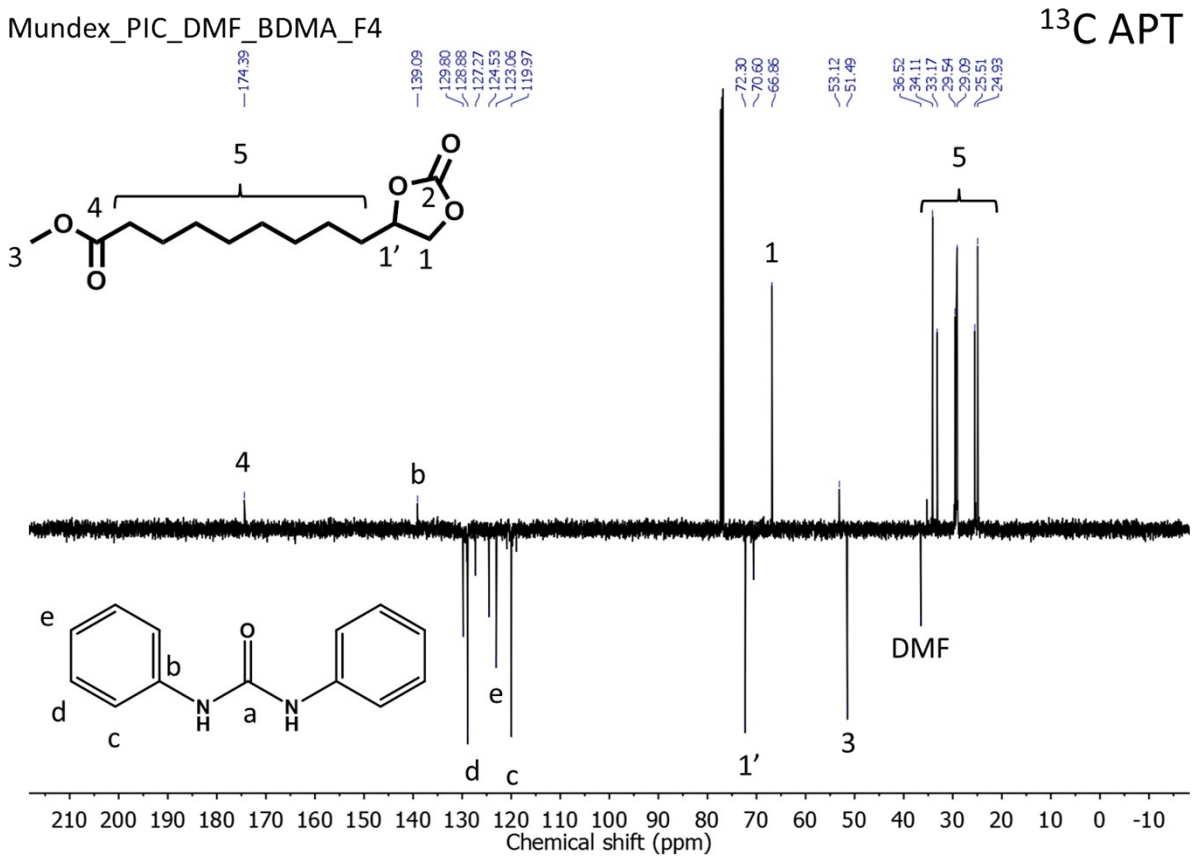

Figure S21 ^{13}C NMR Attached Proton test (APT) spectrum of Mundex_PIC_BDMA _F2.

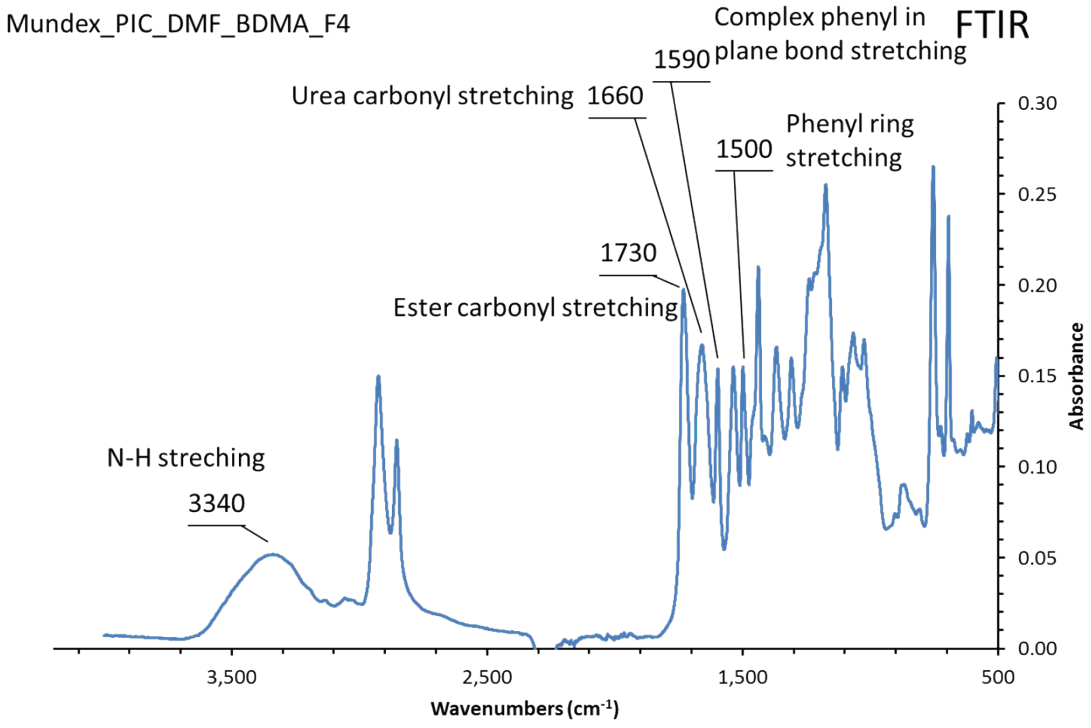

Figure S22 FTIR spectrum of Mundex_PIC_BDMA _F4.

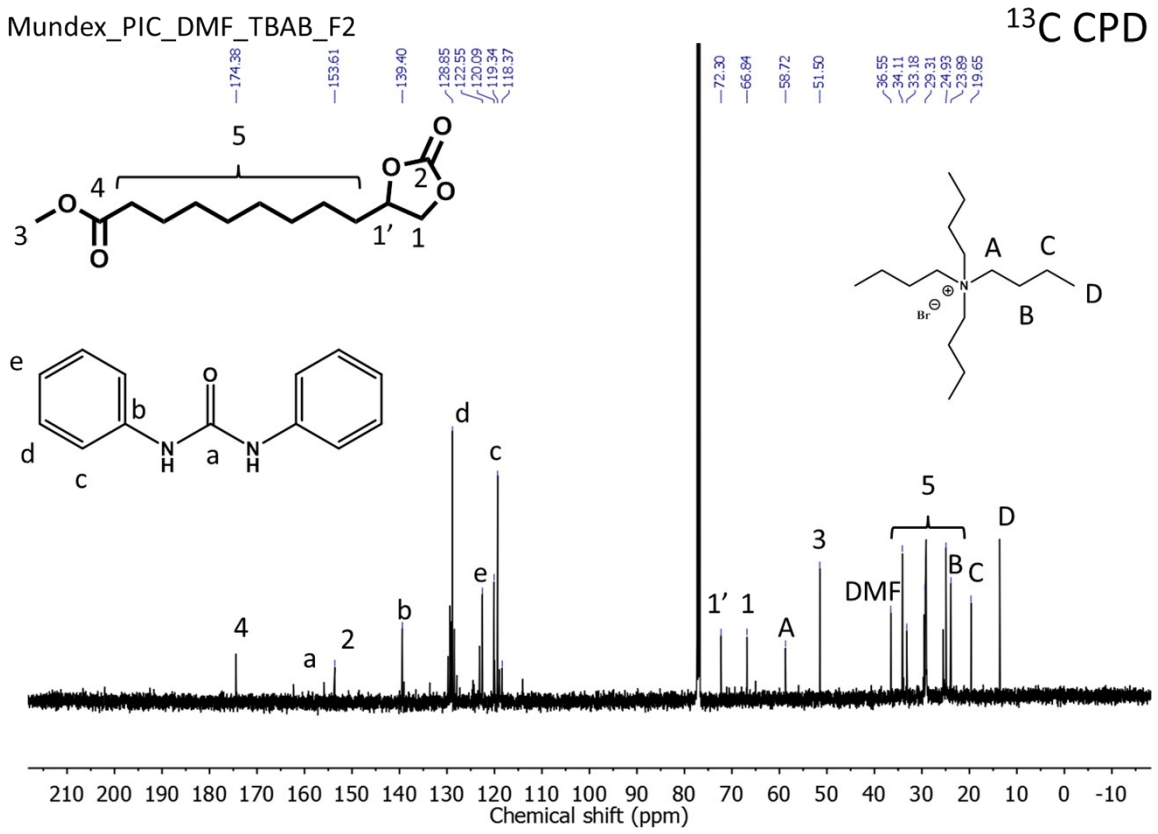

Figure S23 ^{13}C NMR Composite Programmed Decoupling (CPD) spectrum of Mundex_PIC_TBAB _F2.

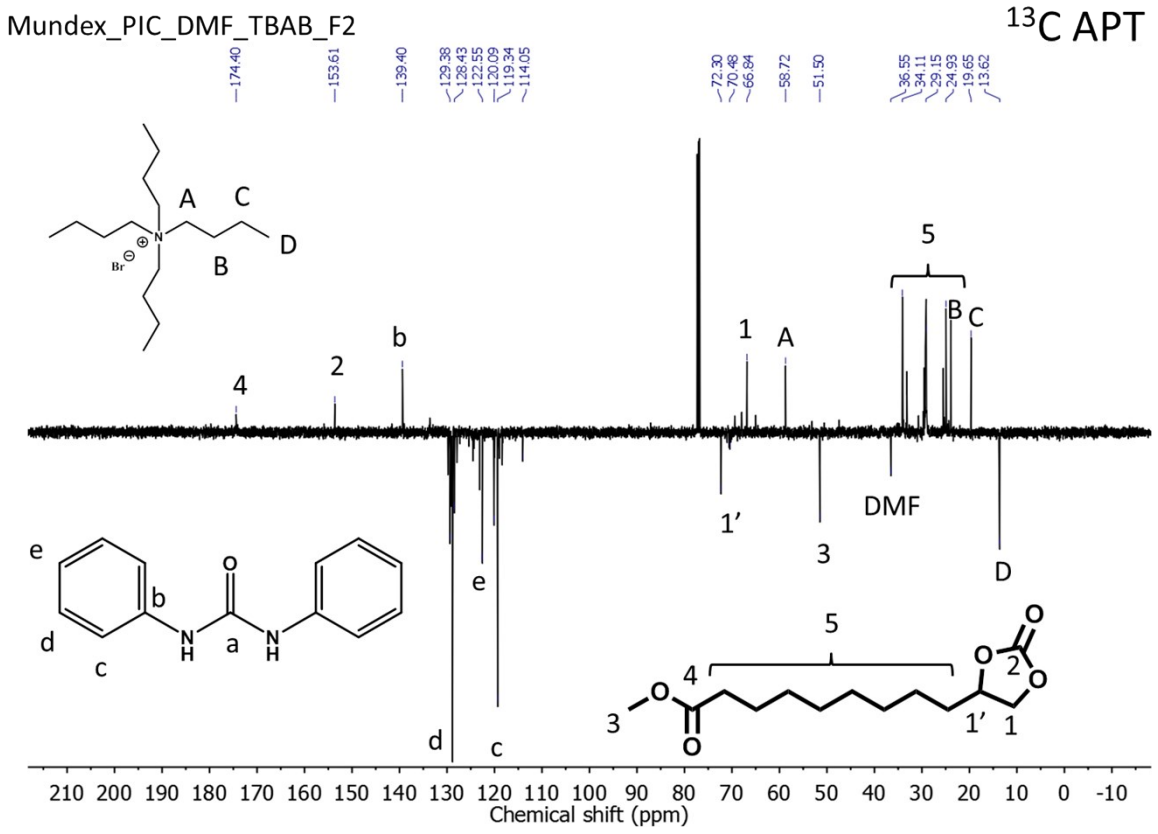

Figure S24 ^{13}C NMR Attached Proton test (APT) spectrum of Mundex_PIC_TBAB _F2.

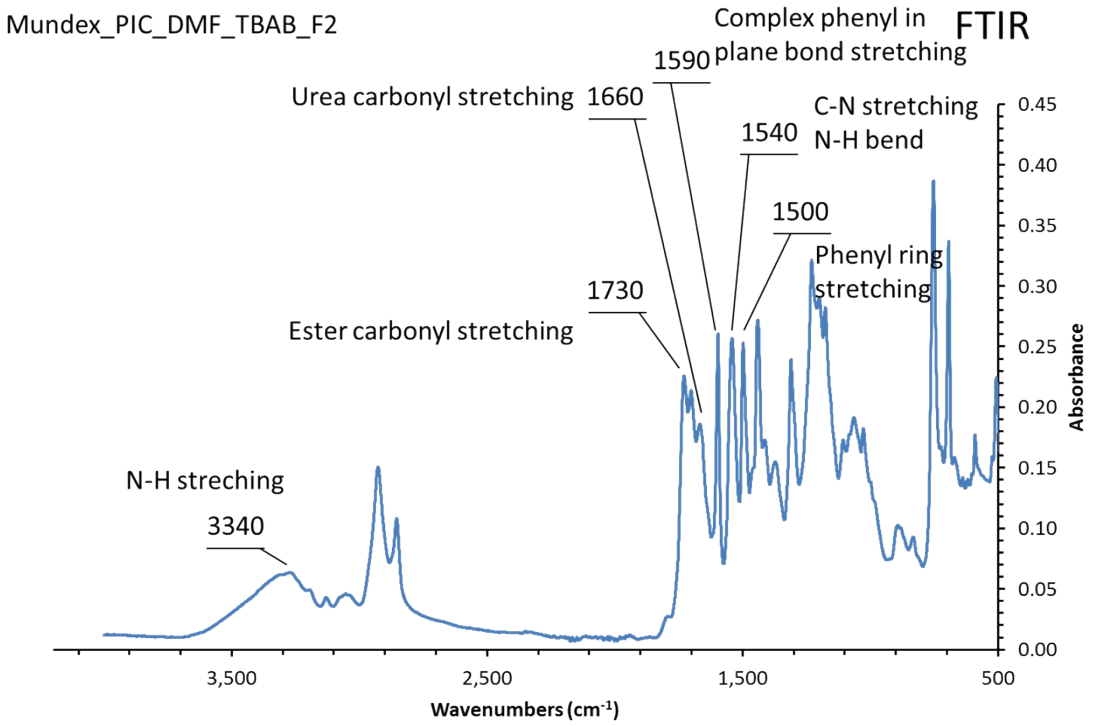

Figure S25 FTIR spectrum of Mundex_PIC_TBAB _F4.

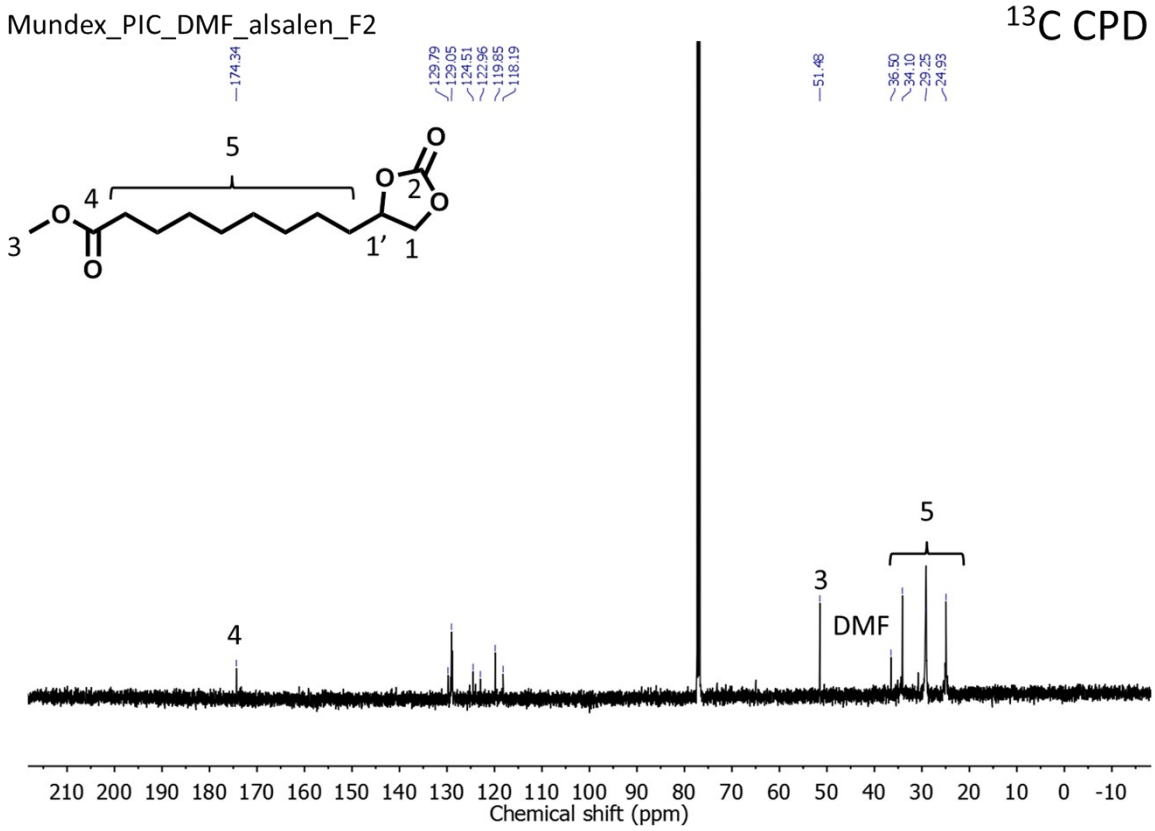

Figure S26 ^{13}C NMR Composite Programmed Decoupling (CPD) spectrum of Mundex_PIC_Al(salen)$_2$ _F2.

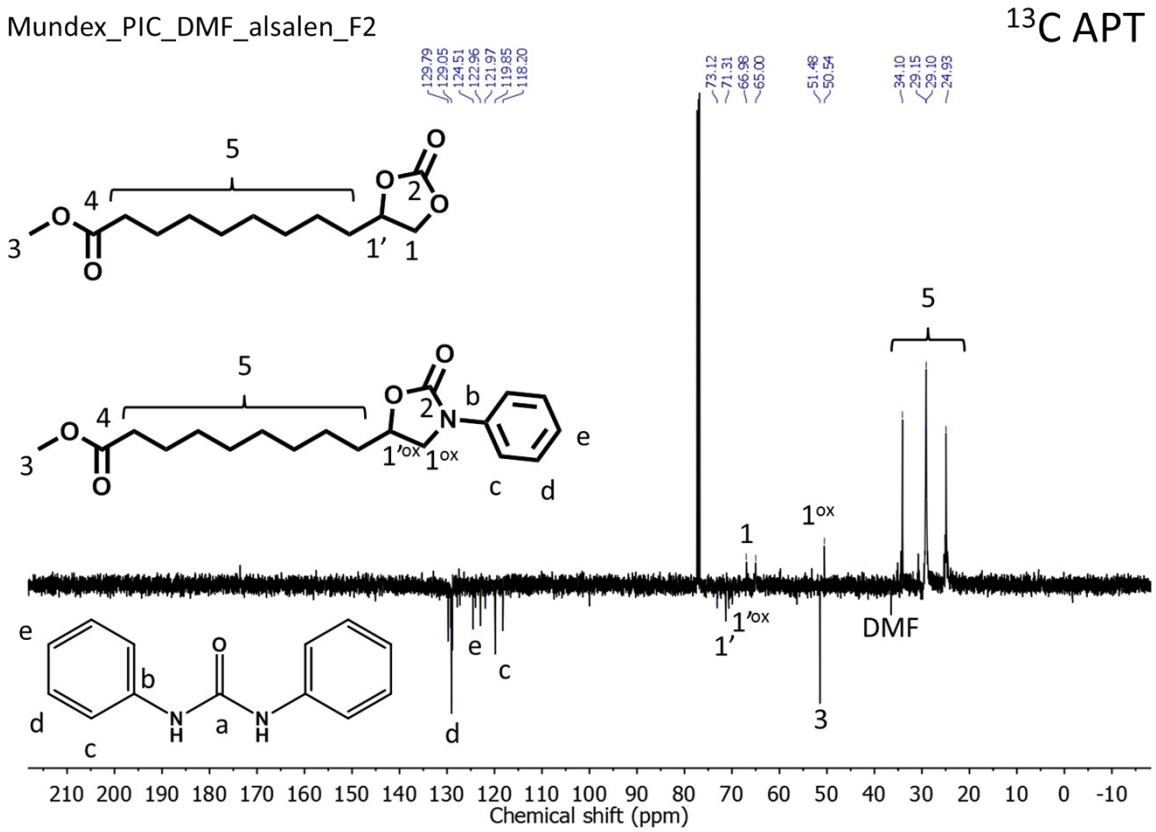

Figure S27 ^{13}C NMR Attached Proton test (APT) spectrum of Mundex_PIC_Al(salen)$_2$ _F2.

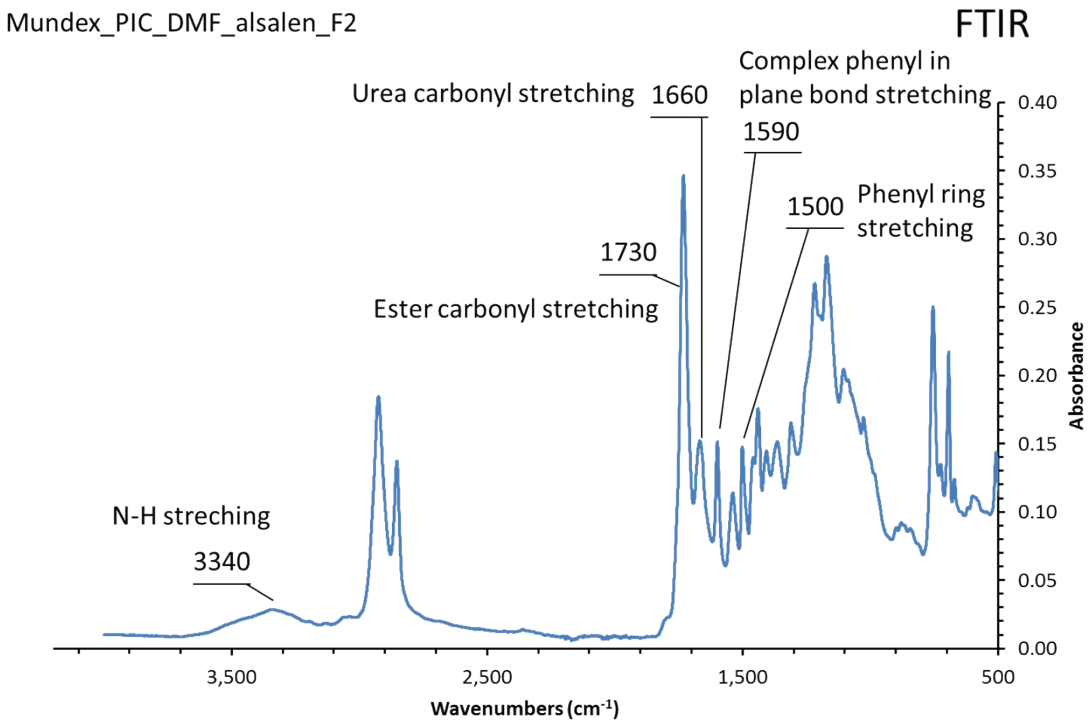

Figure S28 FTIR spectrum of Mundex_PIC_ Al(salen)$_2$ _F4.

Table S4 Products in mass fraction of the Mundex reactions.

	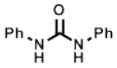 Urea	 Carbonate	 Oxazolidone	Other
Without cat	6%		54%	40%
BDMA	3%	3%	72%	22%
KOAc			73%	27%
TBAB	4%	4%	60%	32%
$ALCl_3$			69%	31%
$Al(salen)_2$	5%	6%	54%	35%

Complete NMR analysis of EVHOSO-Al(salen)$_2$

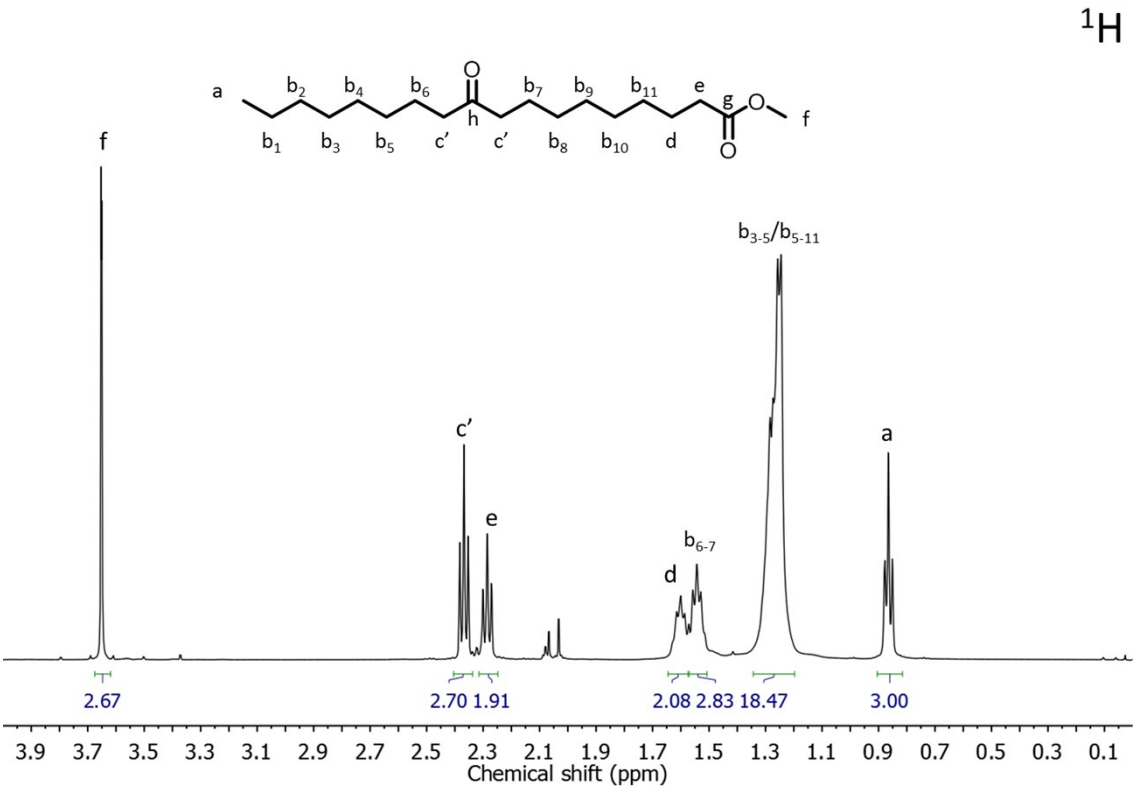

Figure S29 ^{1}H NMR spectrum of EVHOSO-Al(salen)$_2$.

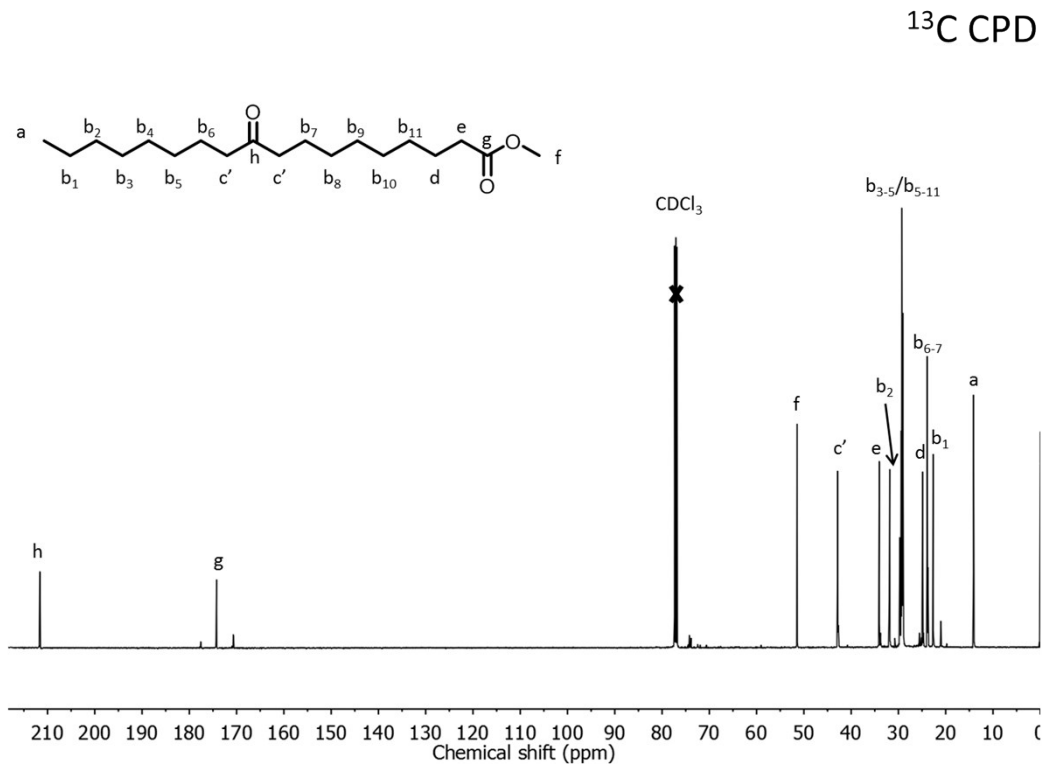

Figure S30 ^{13}C NMR Composite Programmed Decoupling (CPD) spectrum of EVHOSO-Al(salen)$_2$.

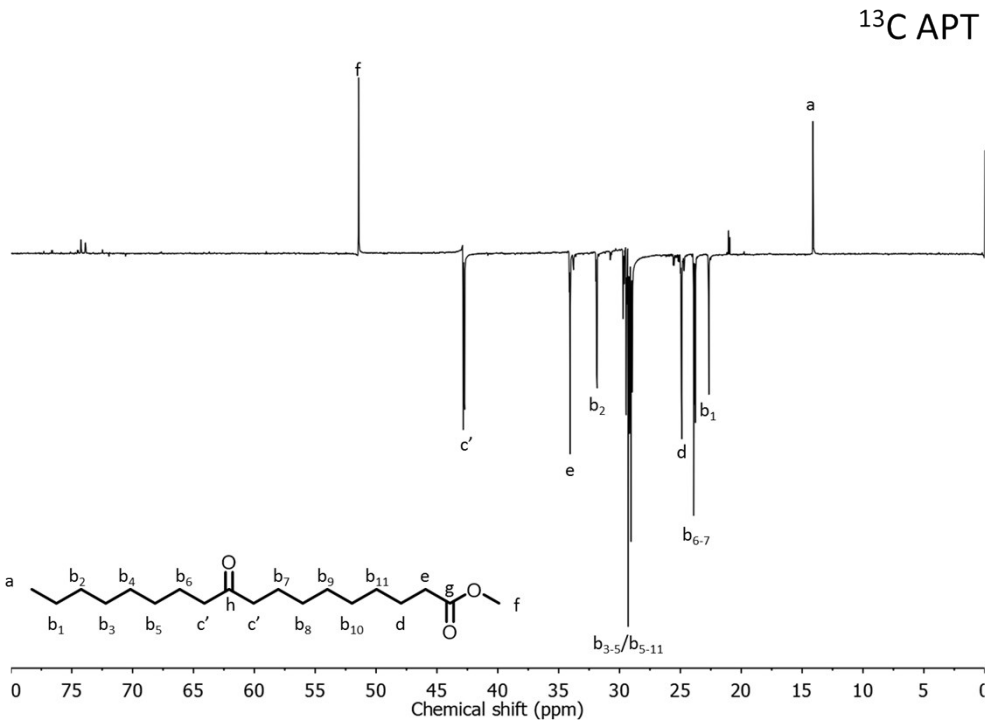

Figure S31 ^{13}C Attached Proton test (APT) NMR spectrum of EVHOSO-Al(salen)$_2$.

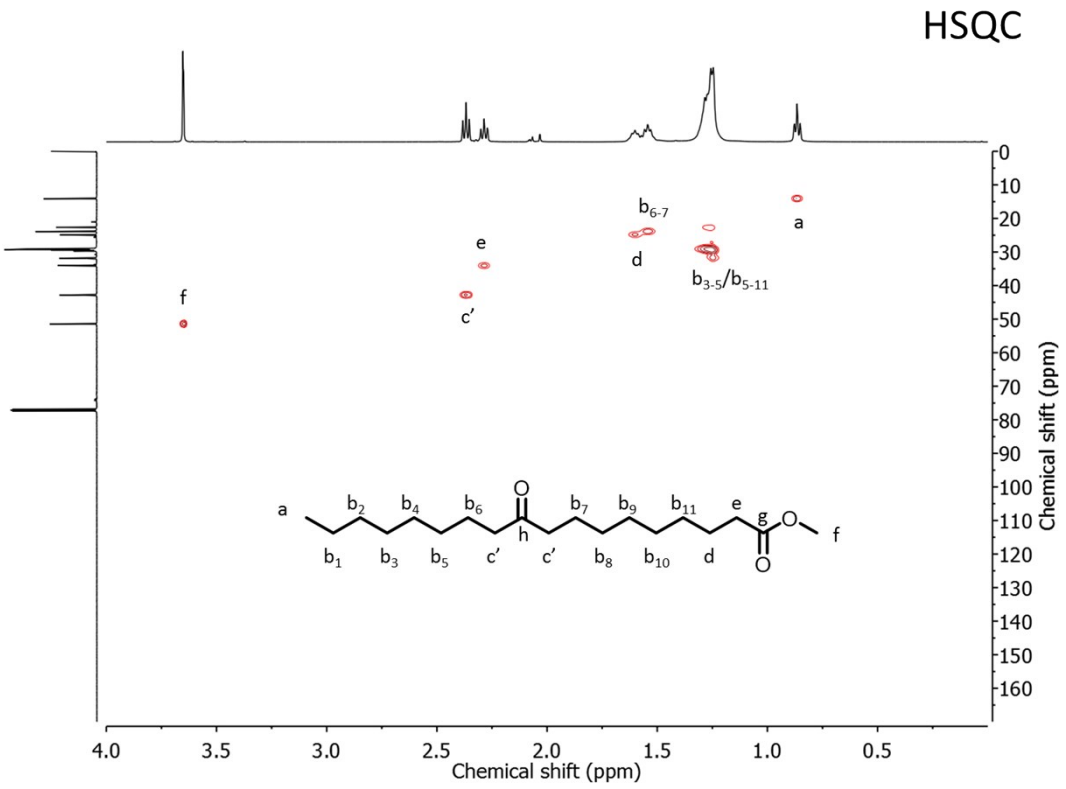

Figure S32 Heteronuclear Single Quantum Correlation (HSQC) NMR spectrum of EVHOSO-Al(salen)$_2$.

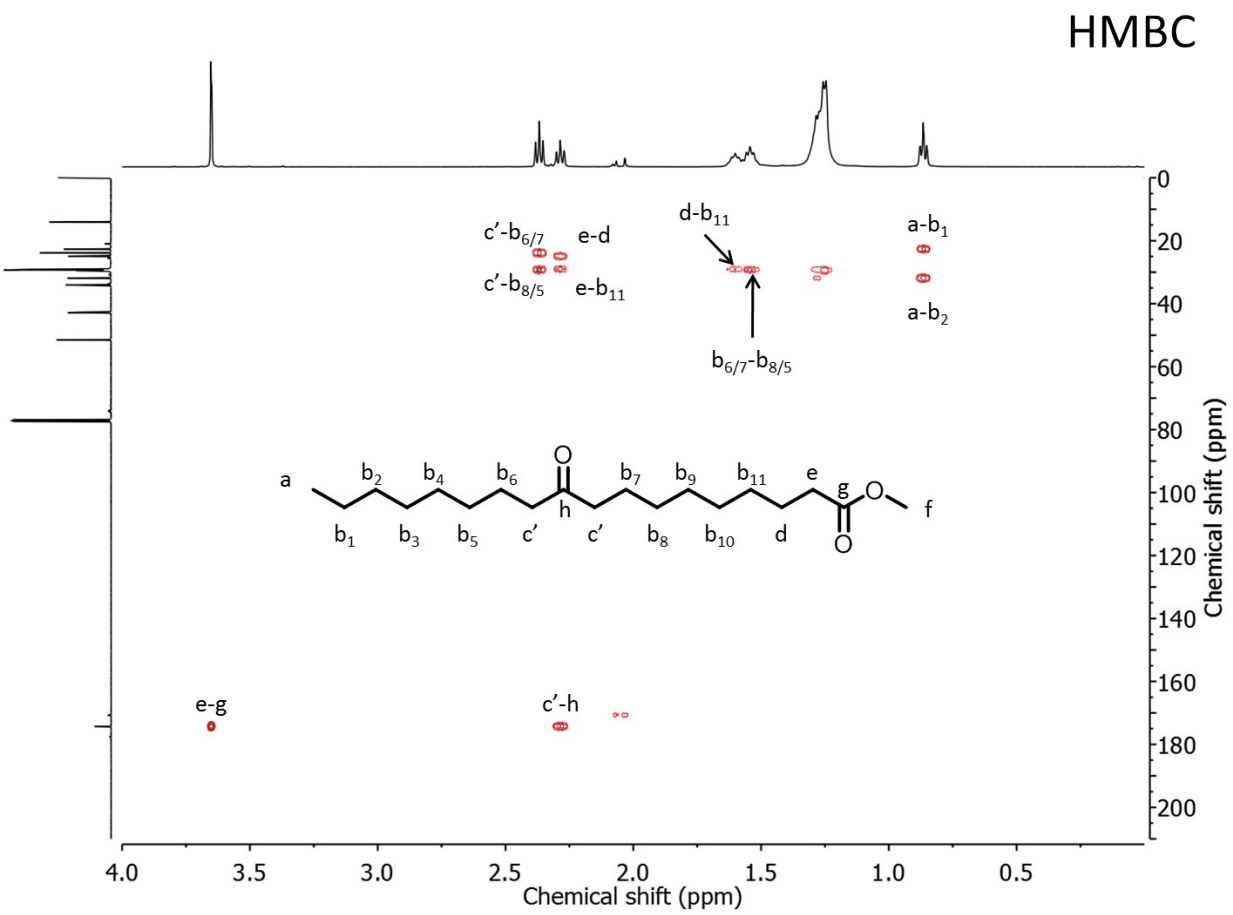

Figure S33 Heteronuclear Multiple Bond Correlation (HMBC) NMR spectrum of EVHOSO-Al(salen)$_2$.

NMR spectra of the EVHOSO minor fractions

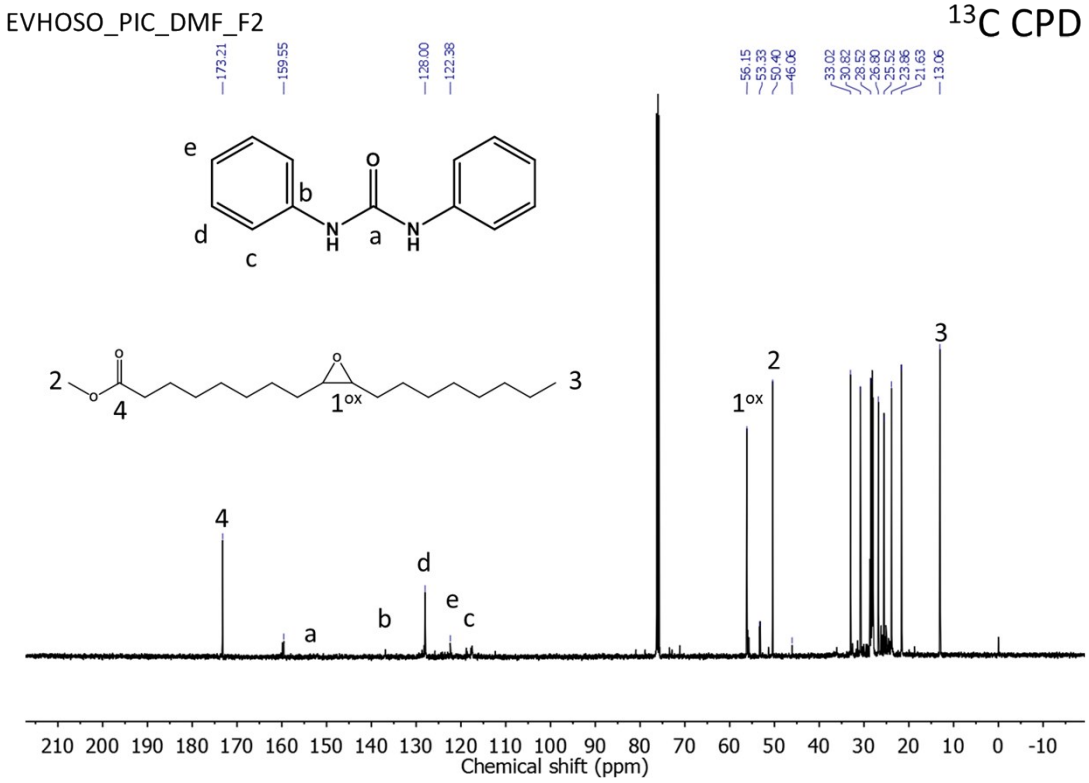

Figure S34 ^{13}C NMR Composite Programmed Decoupling (CPD) spectrum of EVHOSO_PIC_DMF_F2.

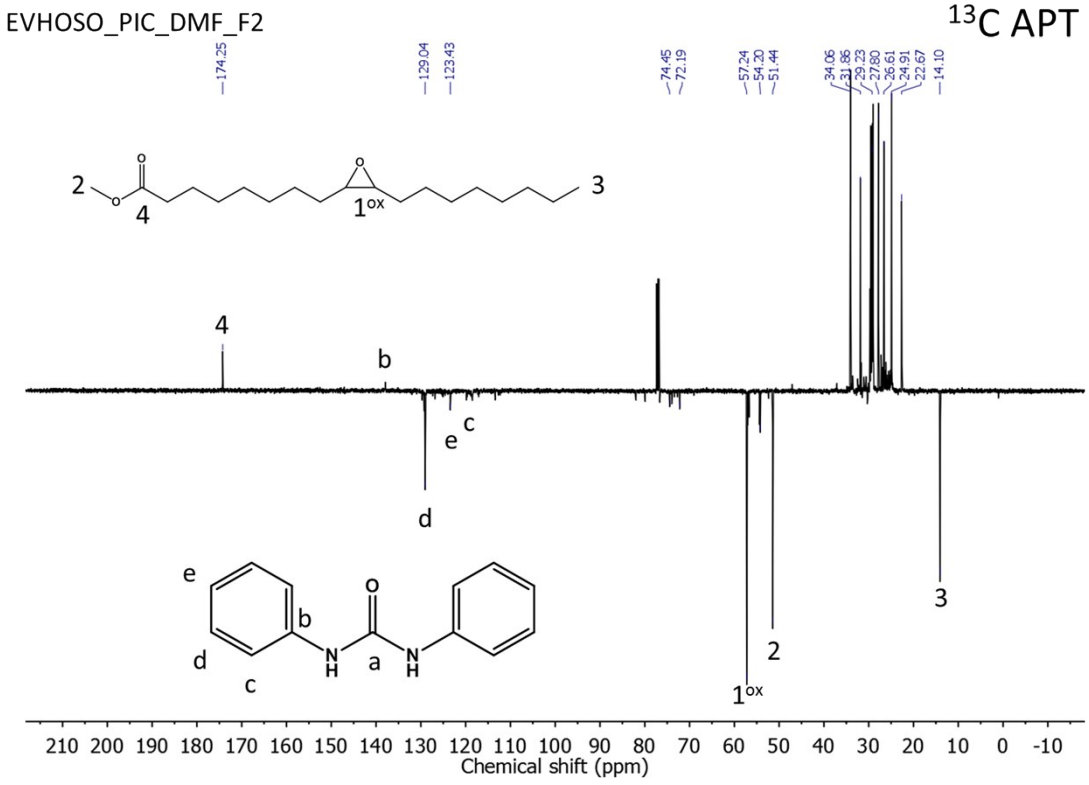

Figure S35 ^{13}C NMR Attached Proton test (APT) spectrum of EVHOSO_PIC_ DMF_F2.

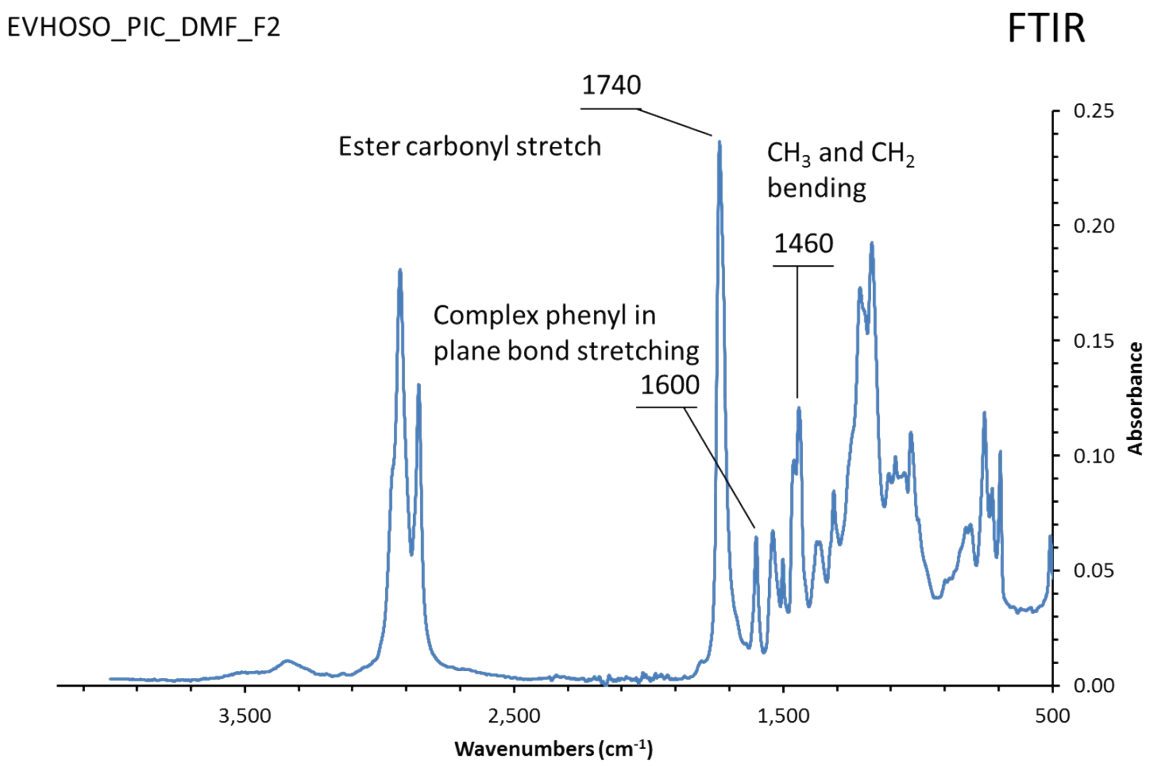

Figure S36 FTIR spectrum of EVHOSO_PIC_DMF_F2.

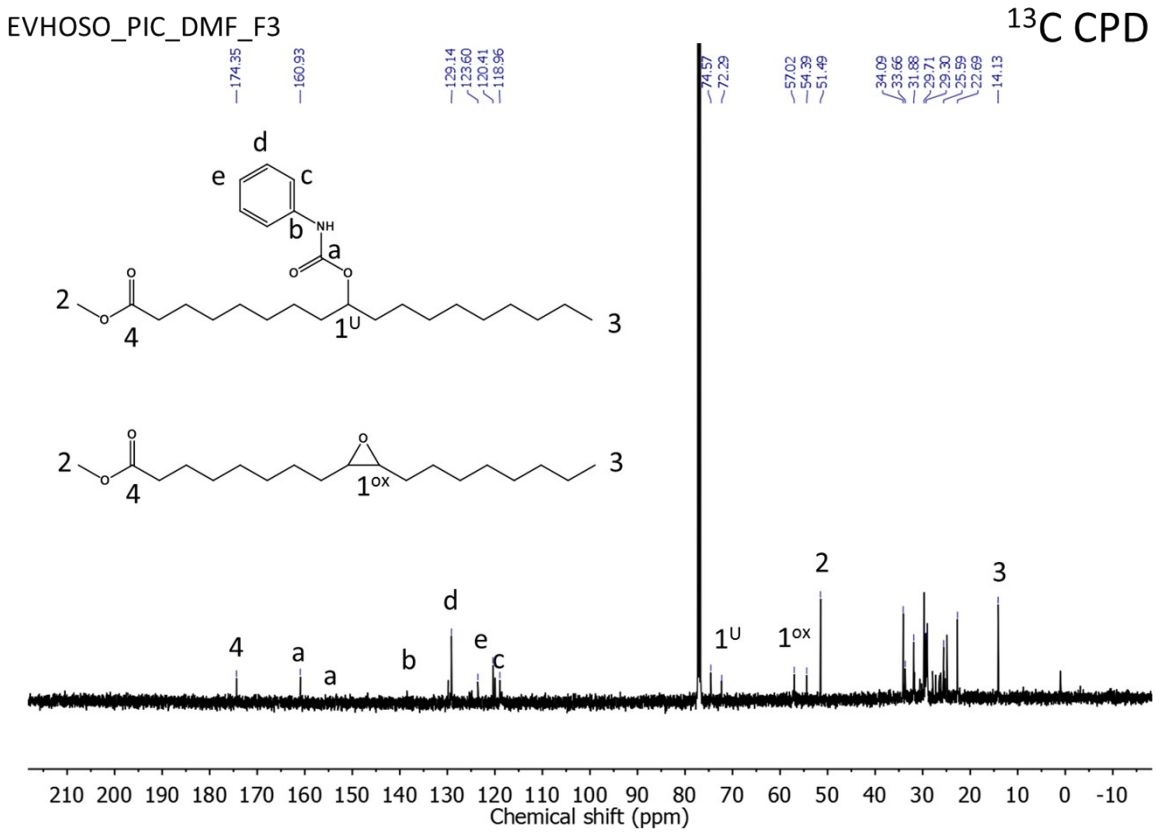

Figure S37 ^{13}C NMR Composite Programmed Decoupling (CPD) spectrum of EVHOSO_PIC_DMF_F3.

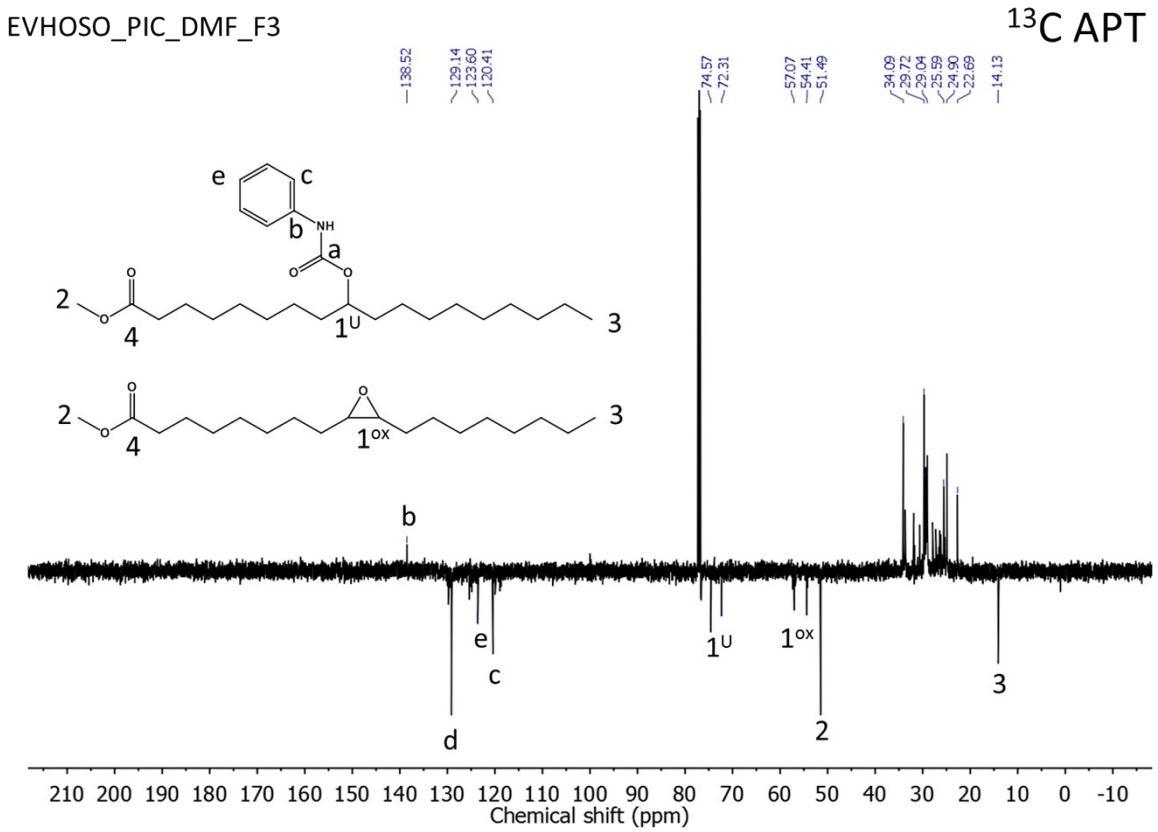

Figure S38 ^{13}C NMR Attached Proton test (APT) spectrum of EVHOSO_PIC_DMF_F3.

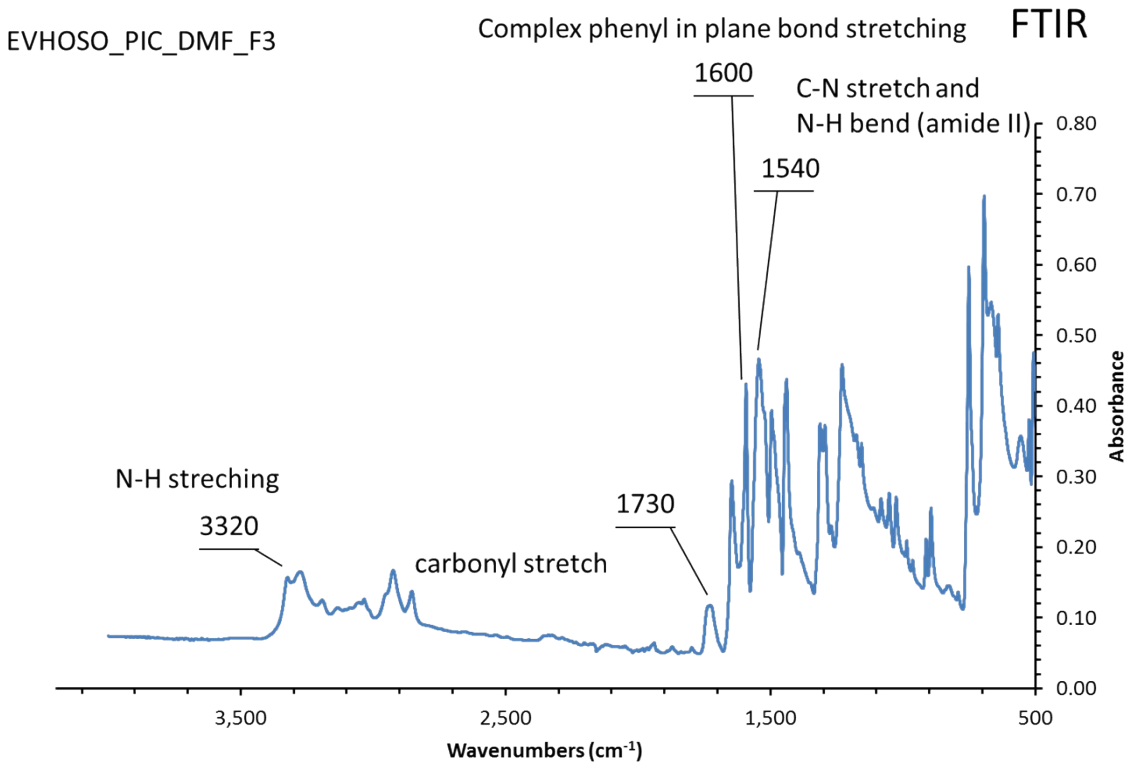

Figure S39 FTIR spectrum of EVHOSO_PIC_DMF_F3.

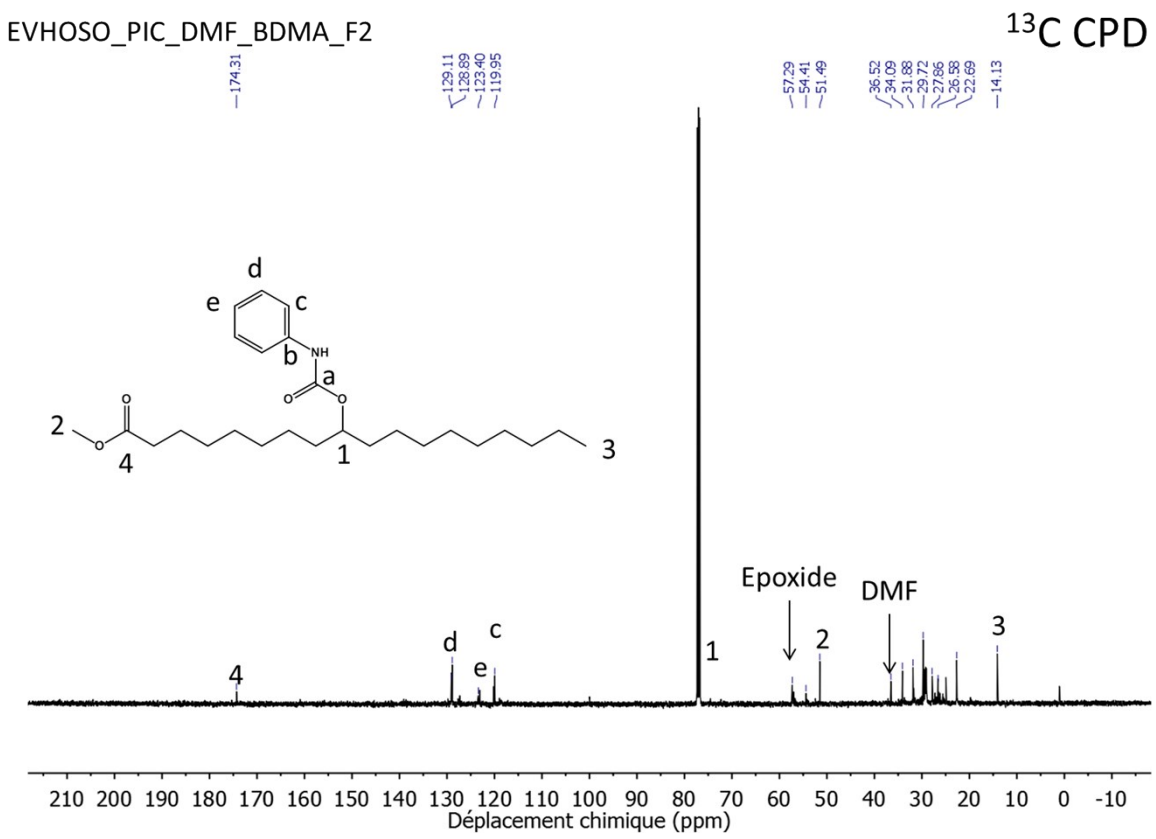

Figure S40 ^{13}C NMR Composite Programmed Decoupling (CPD) spectrum of EVHOSO_PIC_BDMA_F2.

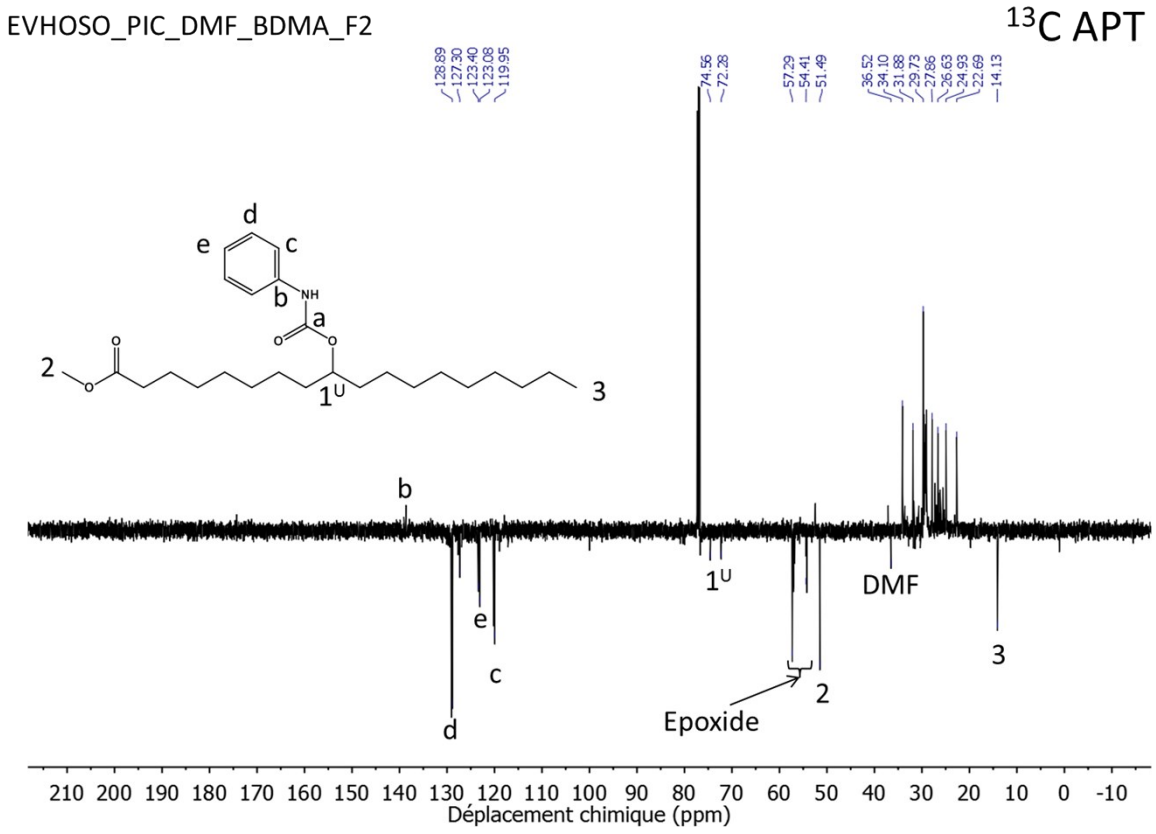

Figure S41 ^{13}C NMR Attached Proton test (APT) spectrum of EVHOSO_PIC_BDMA_F2.

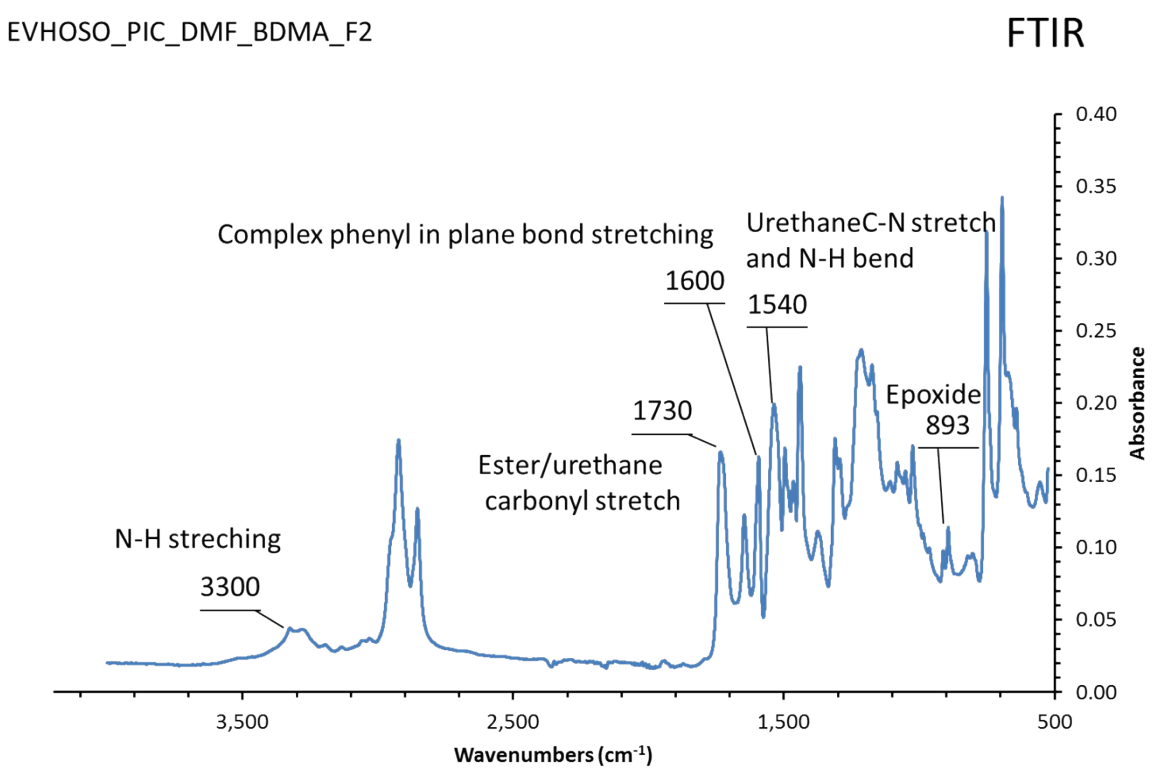

Figure S42 FTIR spectrum of EVHOSO_PIC_BDMA_F2.

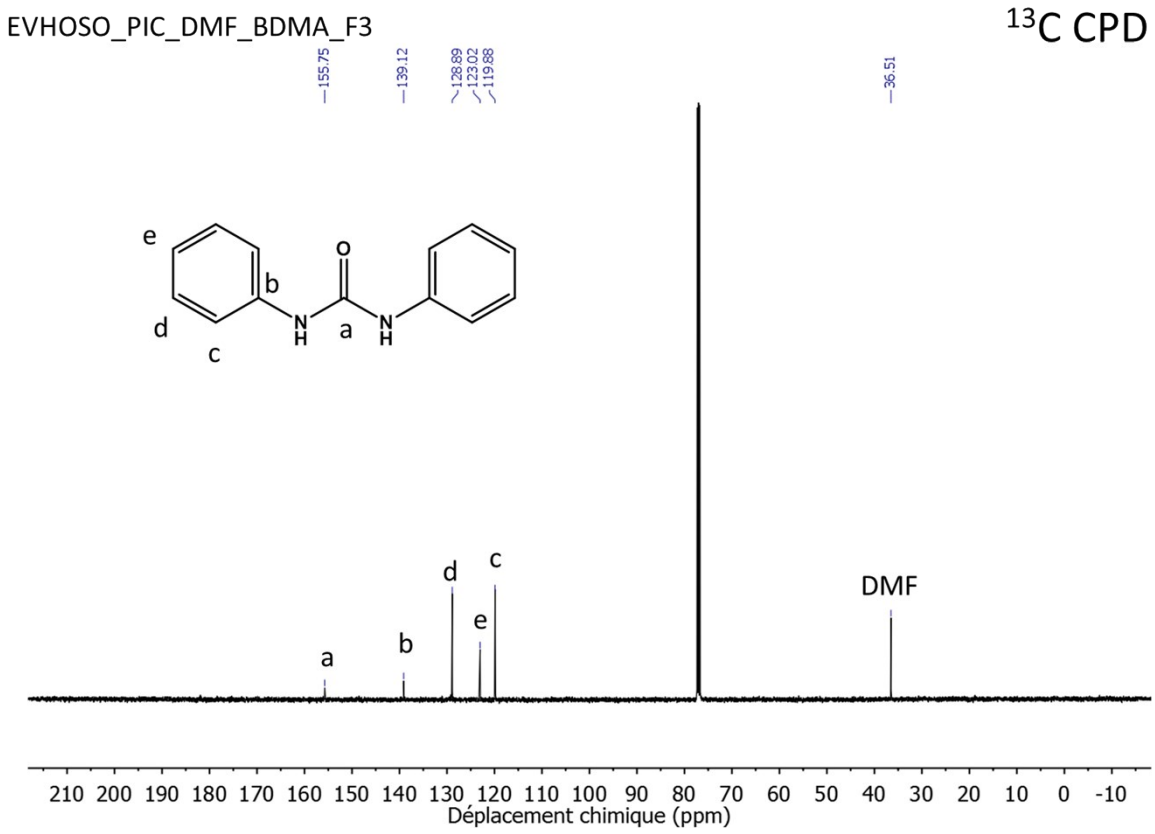

Figure S43 ^{13}C NMR Composite Programmed Decoupling (CPD) spectrum of EVHOSO_PIC_BDMA_F3.

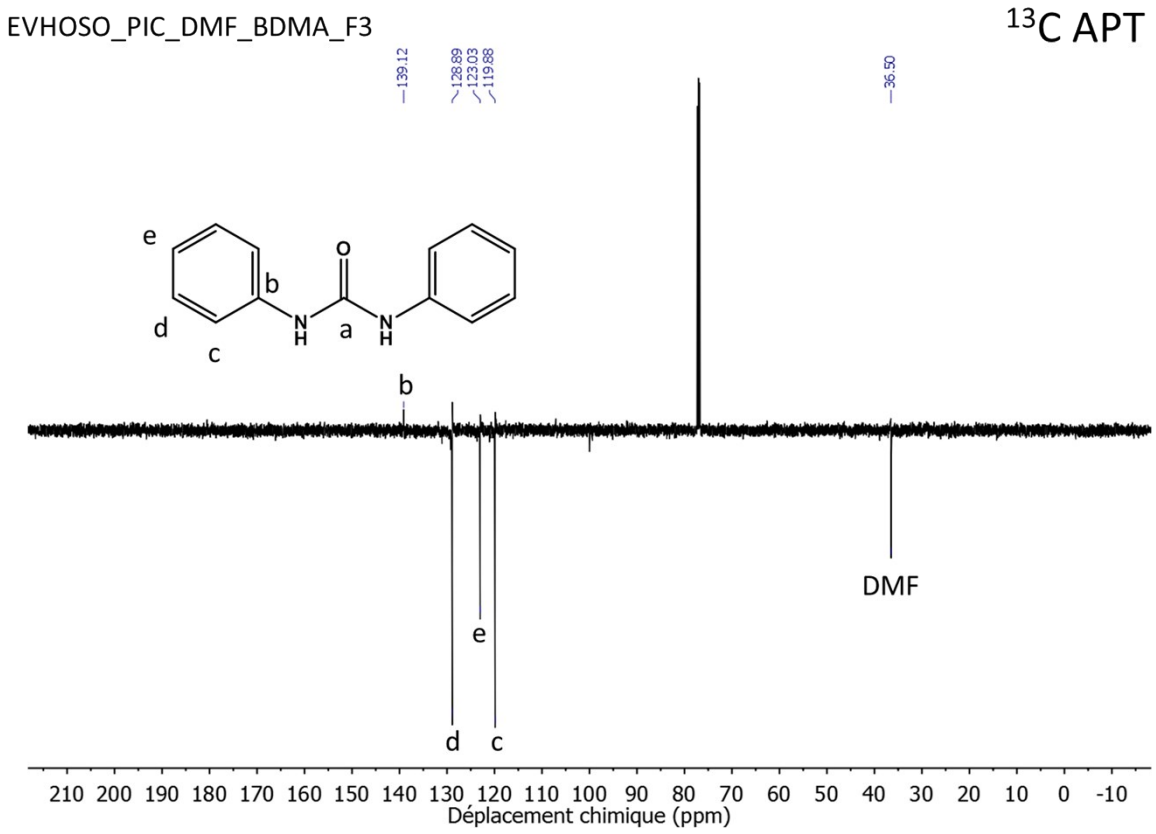

Figure S44 ^{13}C NMR Attached Proton test (APT) spectrum of EVHOSO_PIC_BDMA_F3.

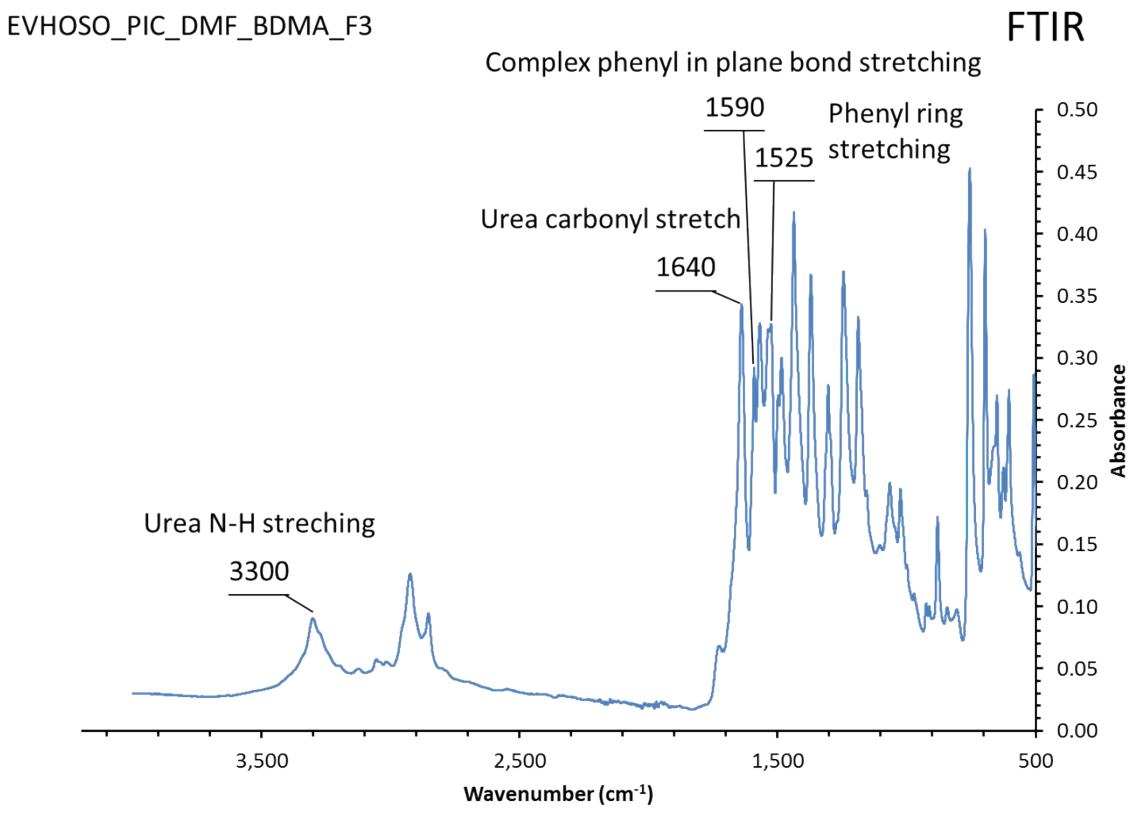

Figure S45 FTIR spectrum of EVHOSO_PIC_BDMA_F3.

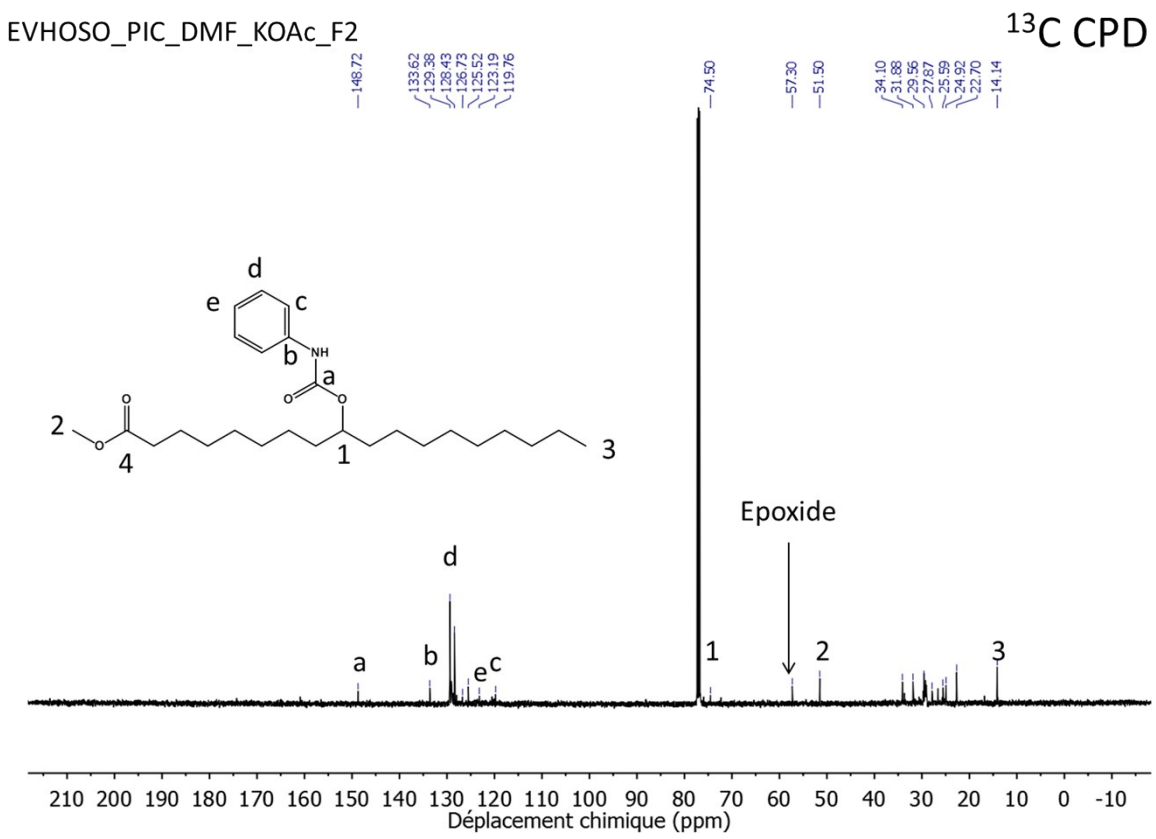

Figure S46 ^{13}C NMR Composite Programmed Decoupling (CPD) spectrum of EVHOSO_PIC_KOAc_F2.

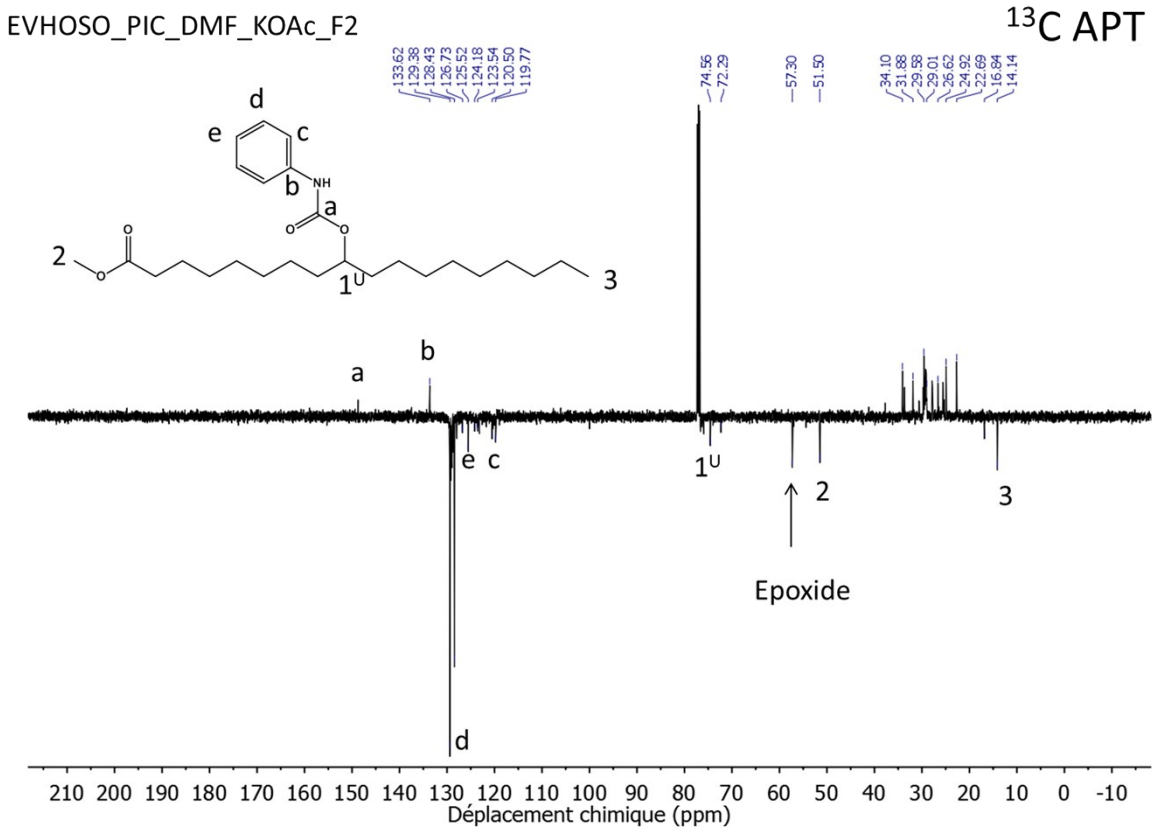

Figure S47 ^{13}C NMR Attached Proton test (APT) spectrum of EVHOSO_PIC_KOAc_F2.

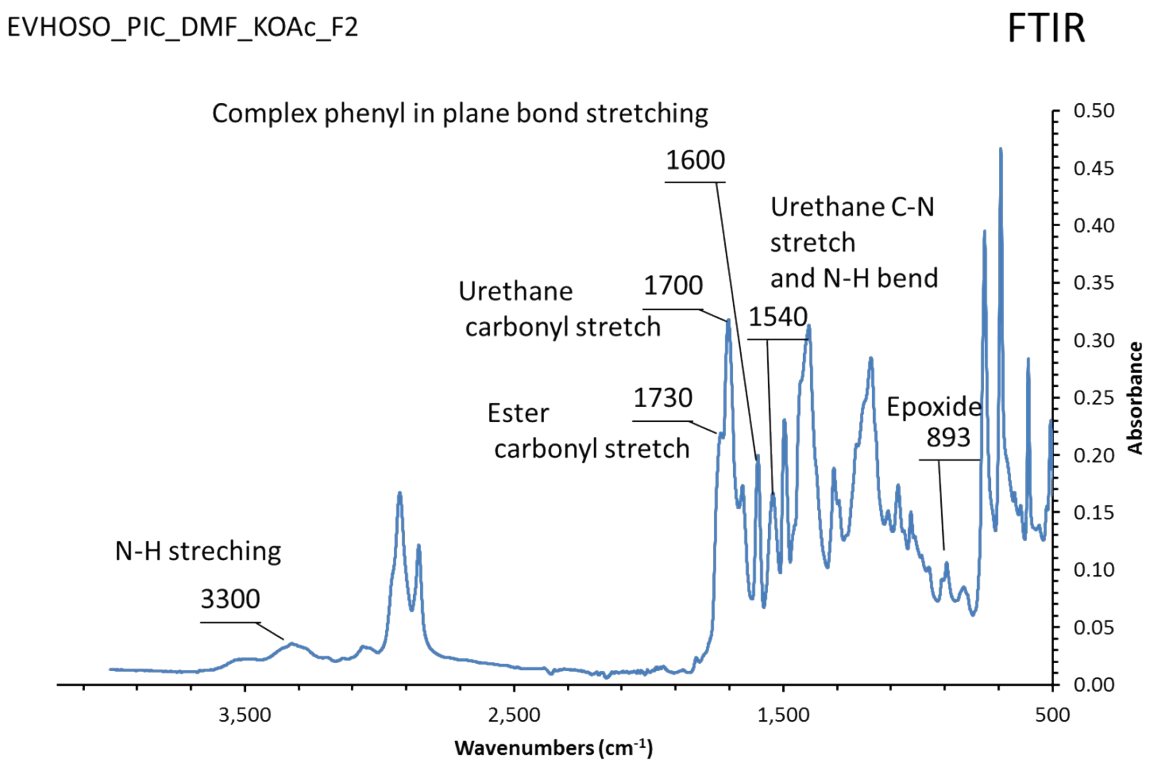

Figure S48 FTIR spectrum of EVHOSO_PIC_KOAc_F2.

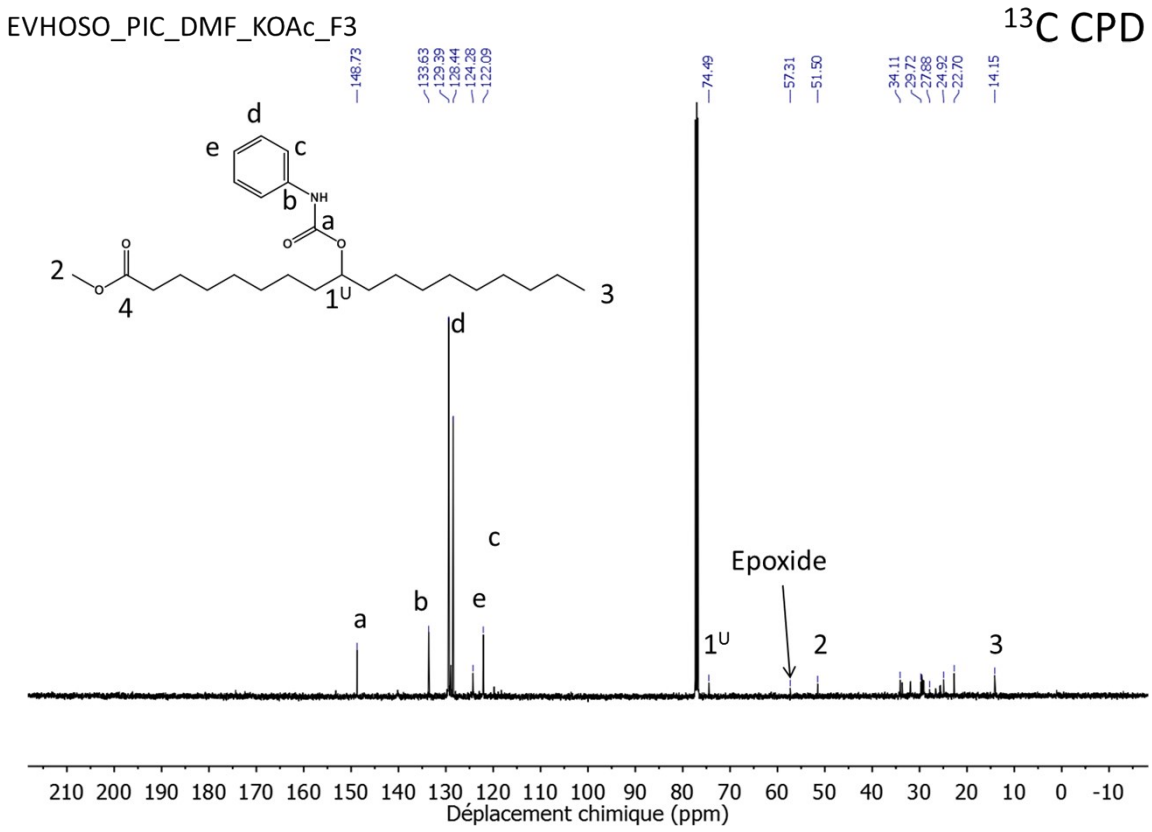

Figure S49 ^{13}C NMR Composite Programmed Decoupling (CPD) spectrum of EVHOSO_PIC_KOAc_F3.

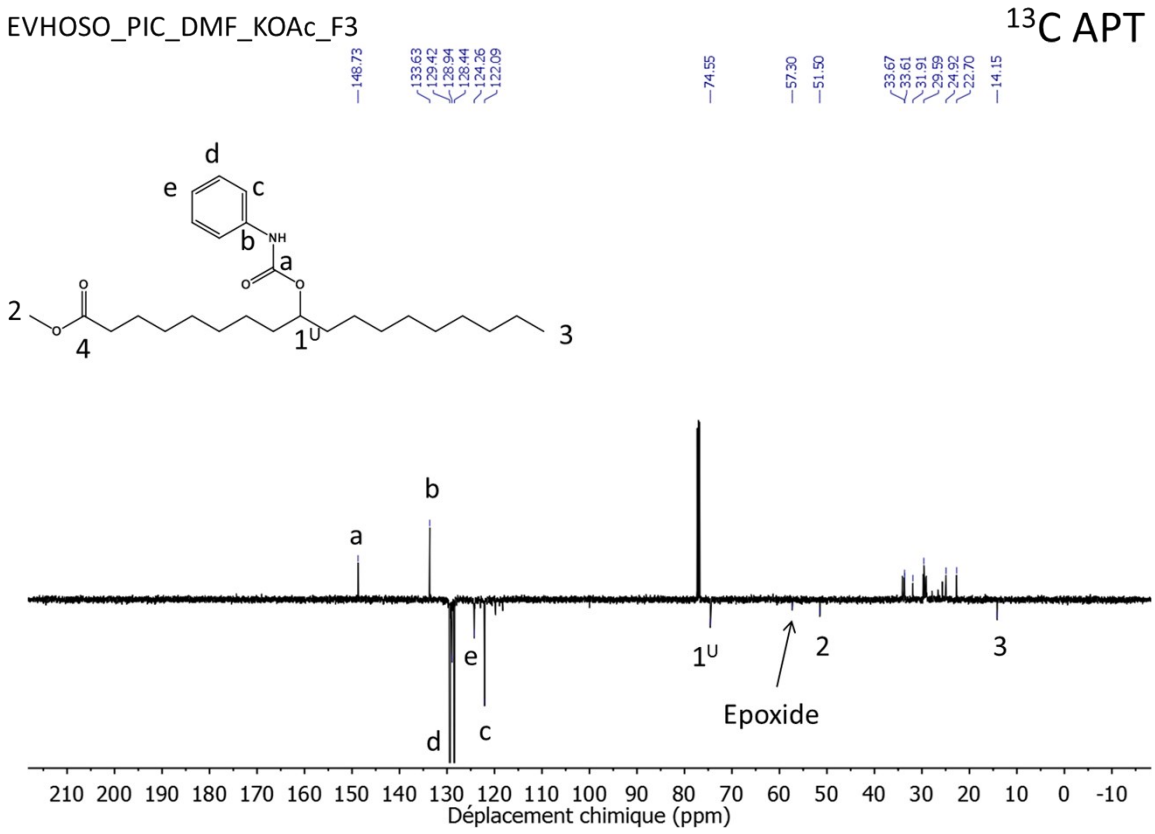

Figure S50 ^{13}C NMR Attached Proton test (APT) spectrum of EVHOSO_PIC_KOAc_F3.

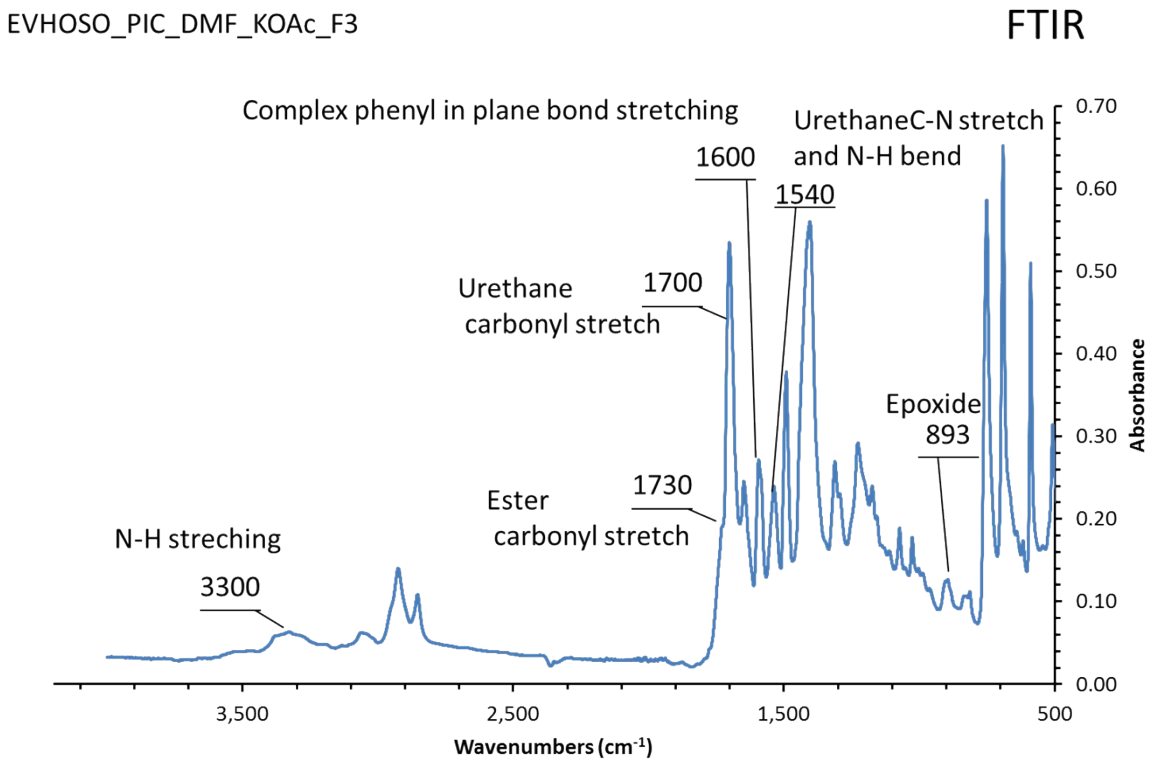

Figure S51 FTIR spectrum of EVHOSO_PIC_KOAc_F3.

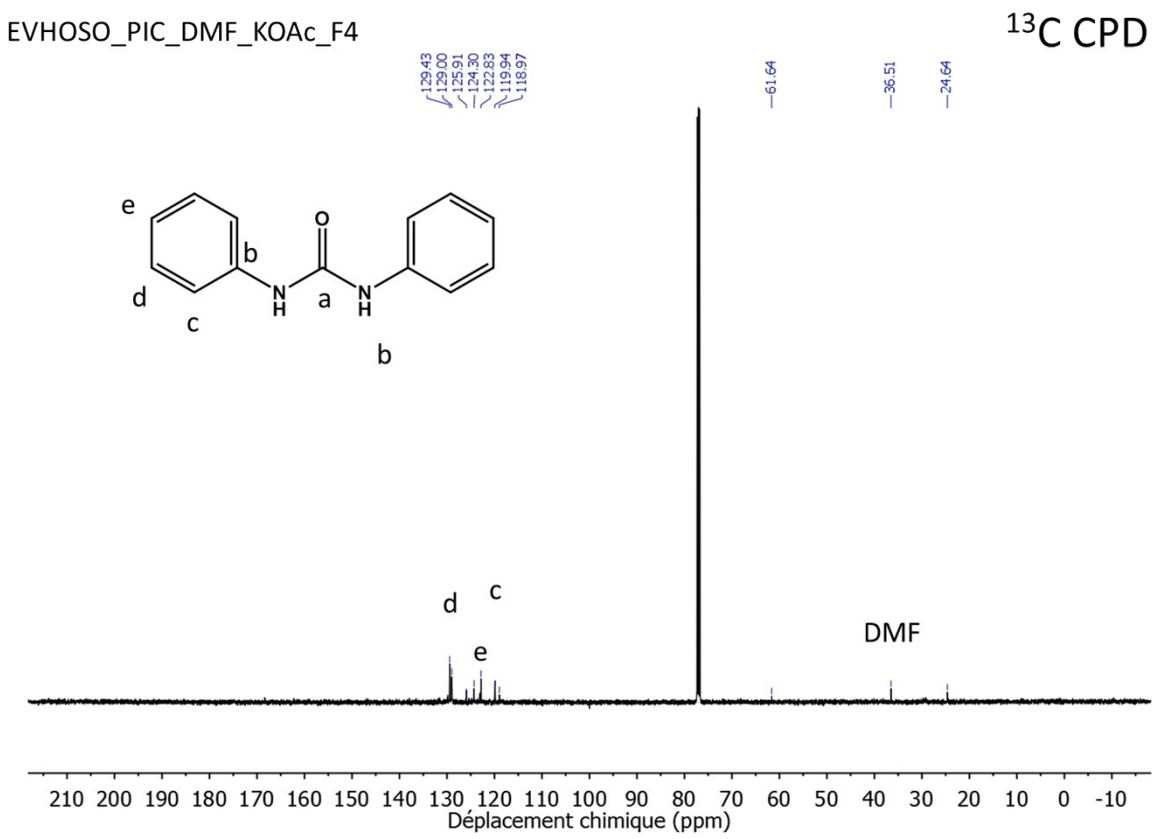

Figure S52 ^{13}C NMR Composite Programmed Decoupling (CPD) spectrum of EVHOSO_PIC_KOAc_F4.

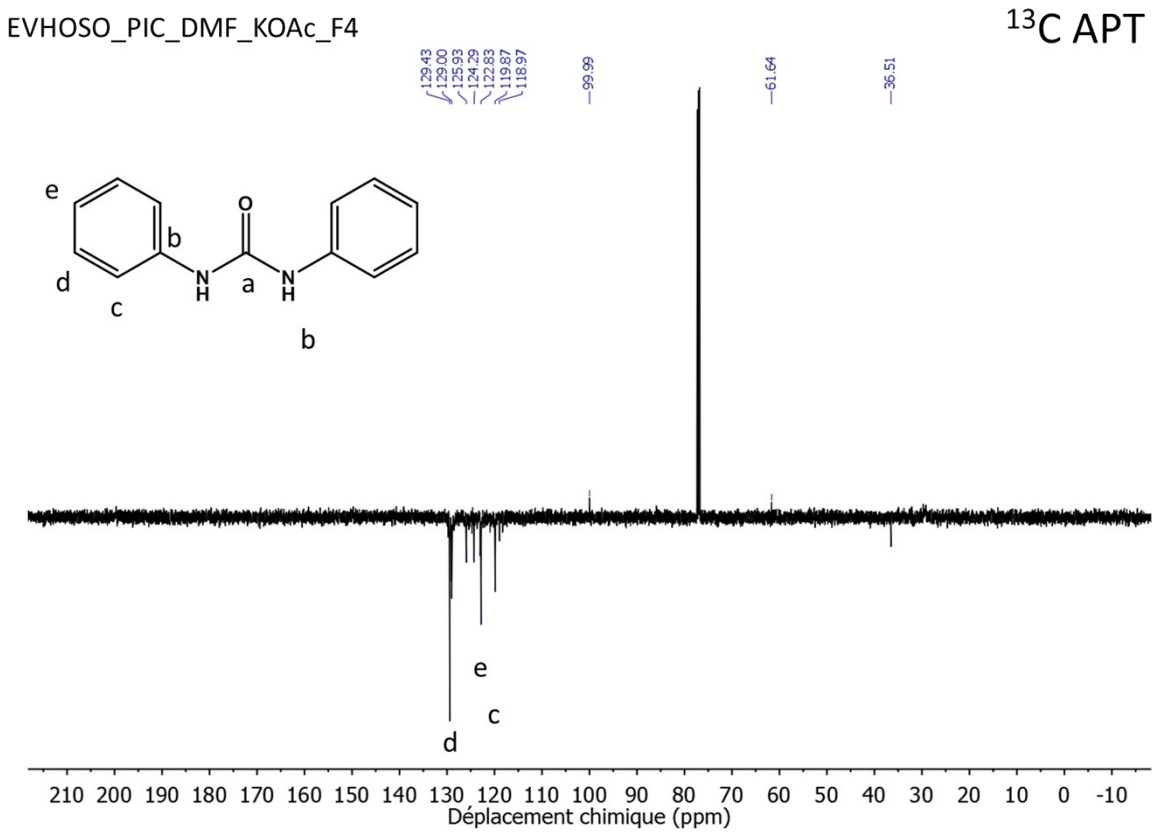

Figure S53 ^{13}C NMR Attached Proton test (APT) spectrum of EVHOSO_PIC_KOAc_F4.

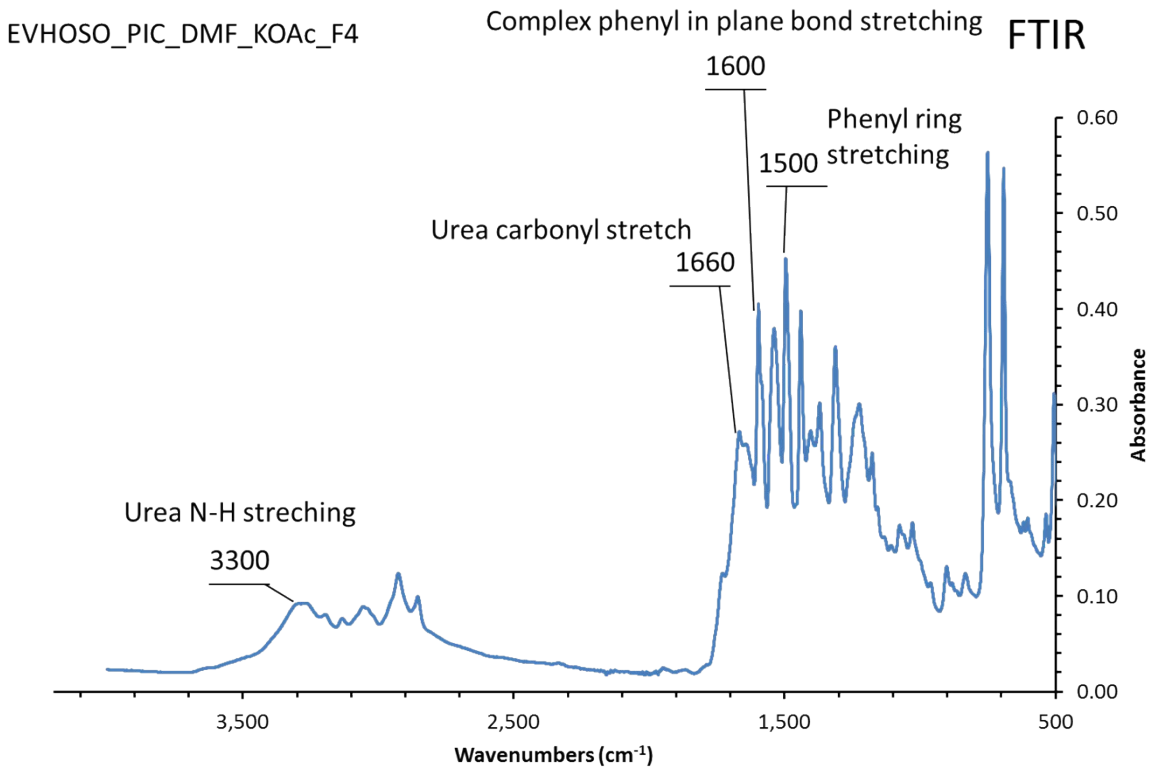

Figure S54 FTIR spectrum of EVHOSO_PIC_KOAc_F4.

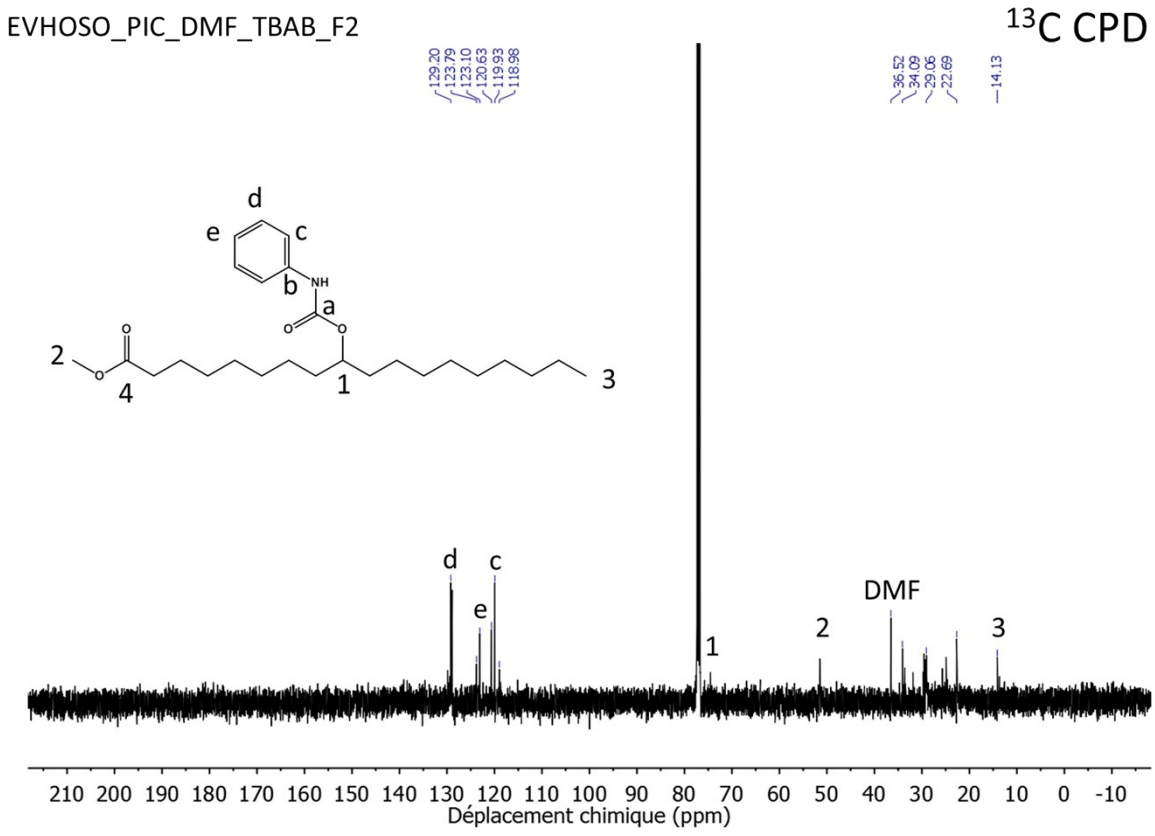

Figure S55 ^{13}C NMR Composite Programmed Decoupling (CPD) spectrum of EVHOSO_PIC_TBAB_F2.

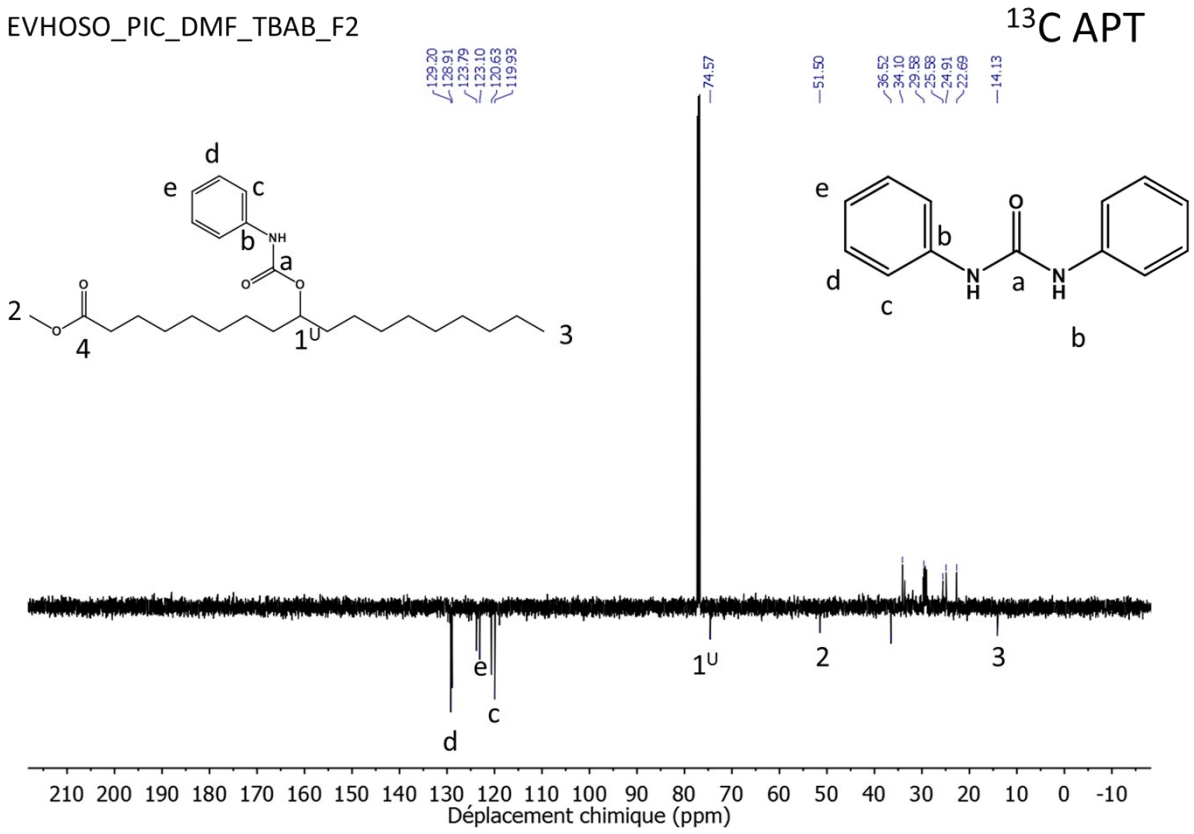

Figure S56 ^{13}C NMR Attached Proton test (APT) spectrum of EVHOSO_PIC_TBAB_F2.

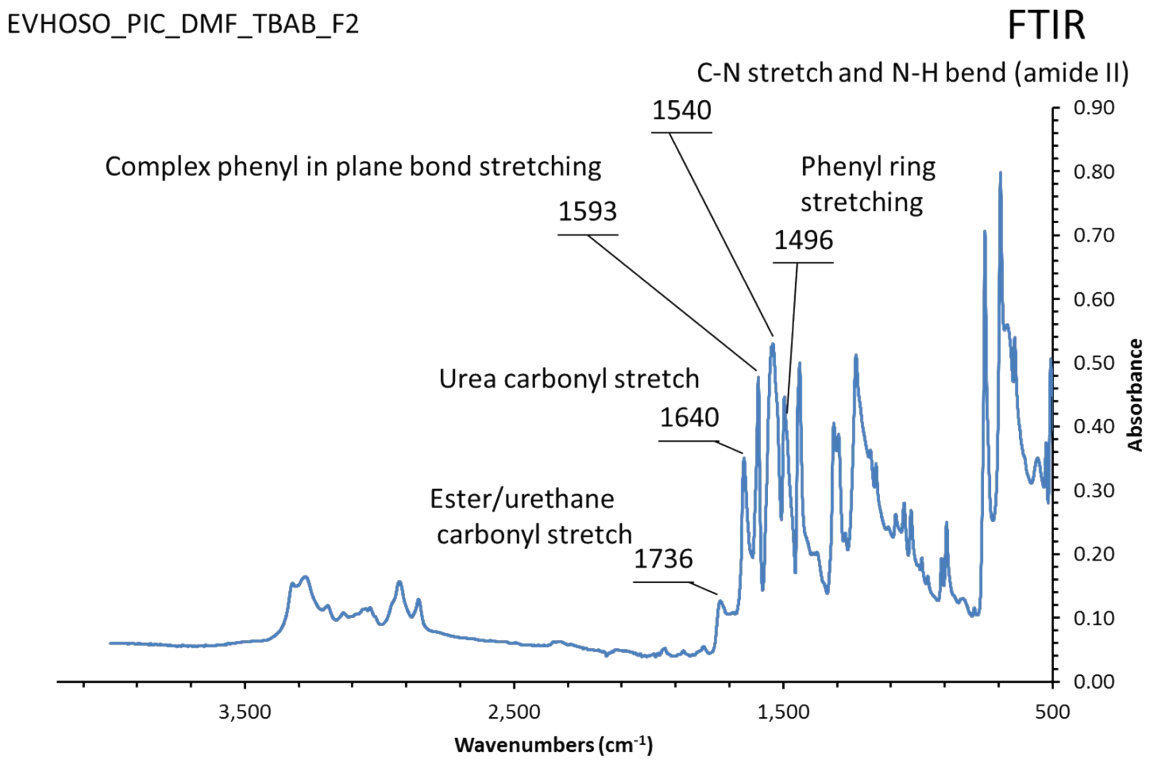

Figure S57 FTIR spectrum of EVHOSO_PIC_TBAB_F2.

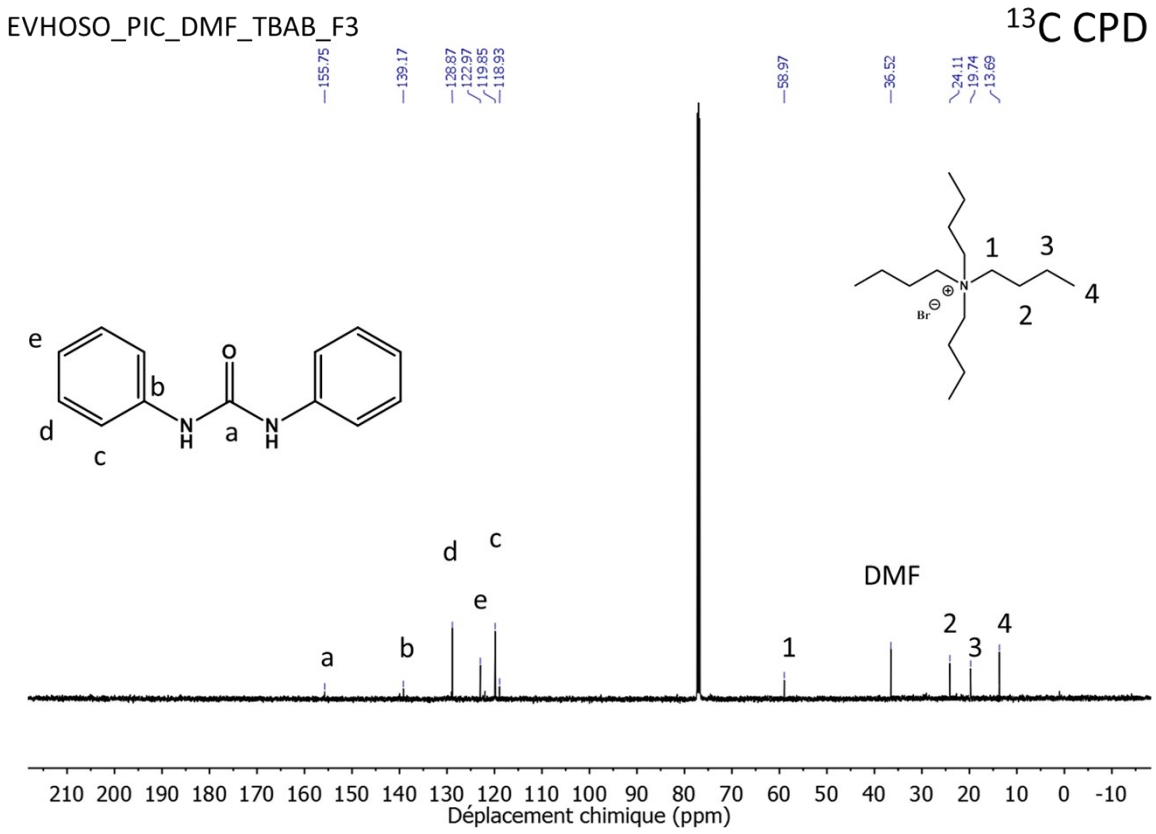

Figure S58 ^{13}C NMR Composite Programmed Decoupling (CPD) spectrum of EVHOSO_PIC_TBAB_F3.

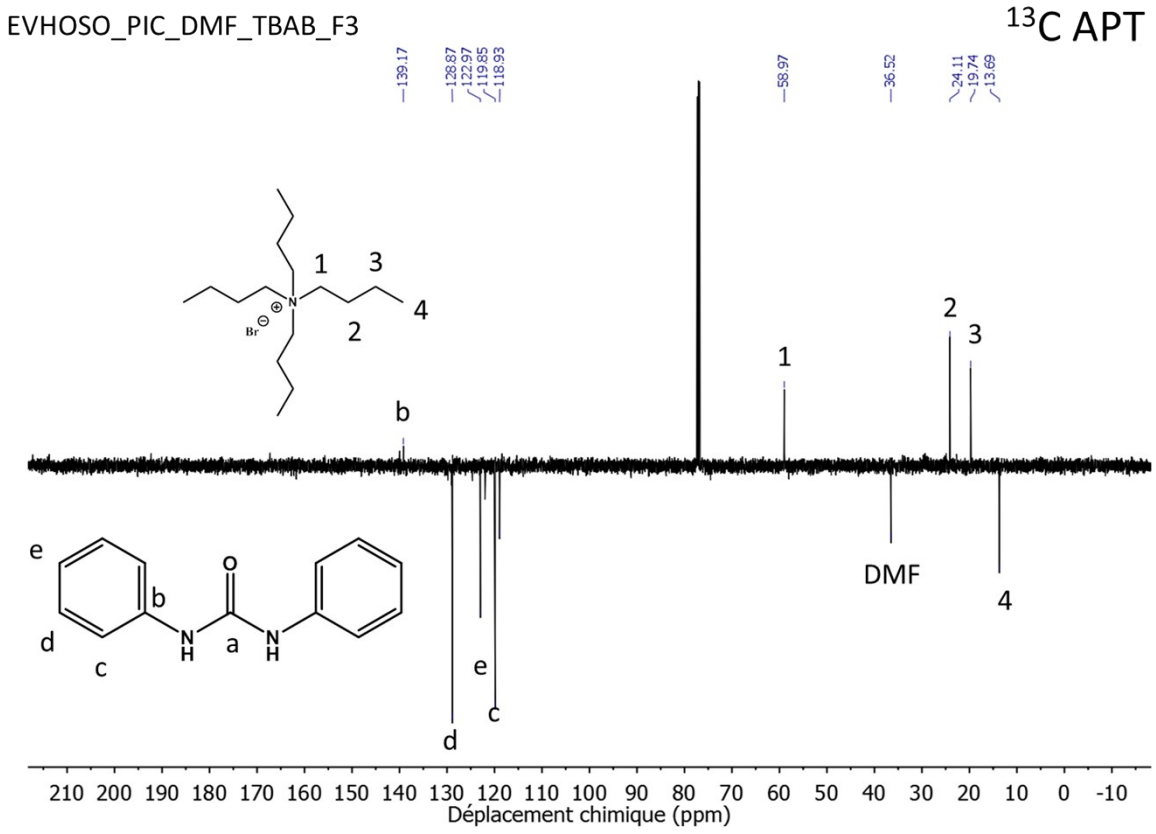

Figure S59 ^{13}C NMR Attached Proton test (APT) spectrum of EVHOSO_PIC_TBAB_F3.

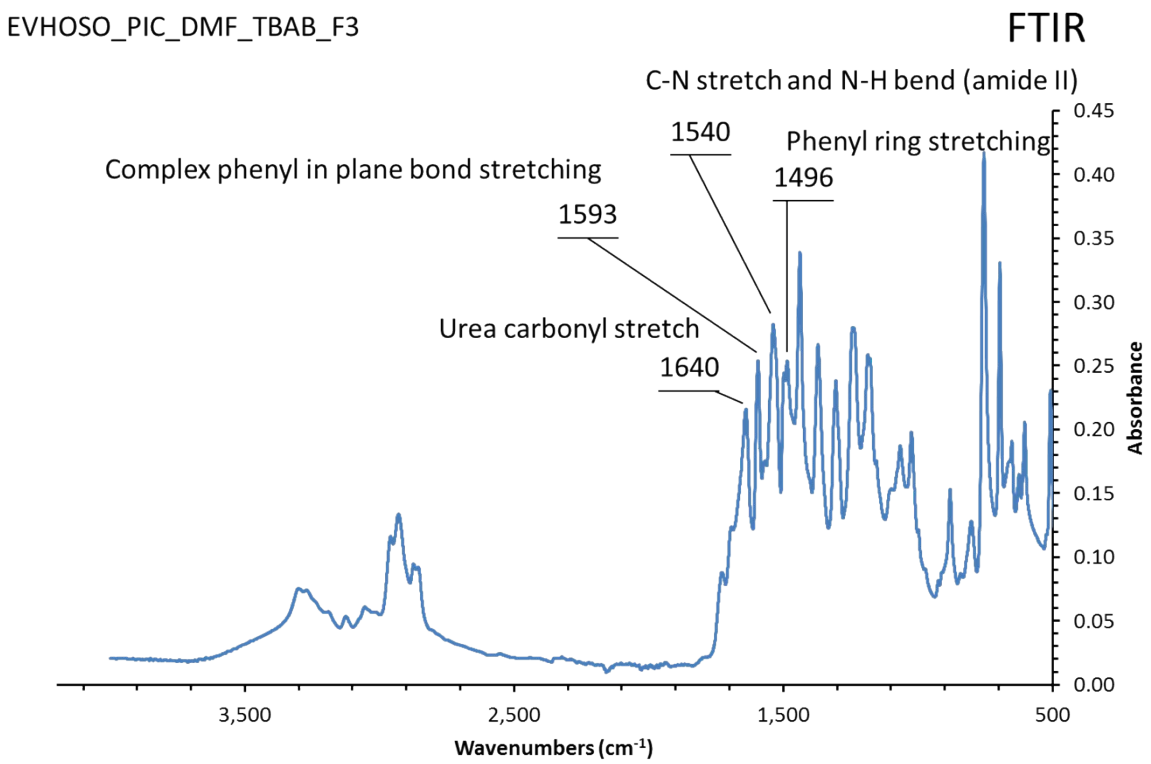

Figure S60 FTIR spectrum of EVHOSO_PIC_TBAB_F3.

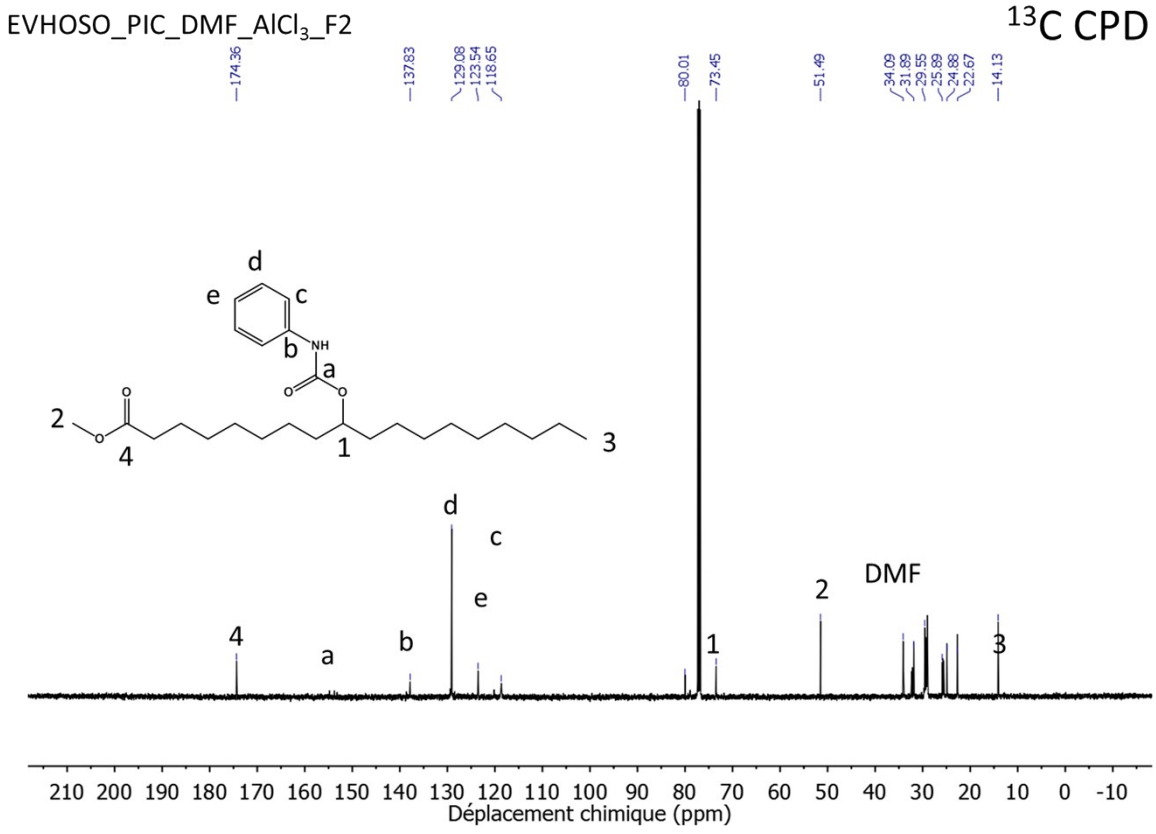

Figure S61 ^{13}C NMR Composite Programmed Decoupling (CPD) spectrum of EVHOSO_PIC_$AlCl_3$_F2.

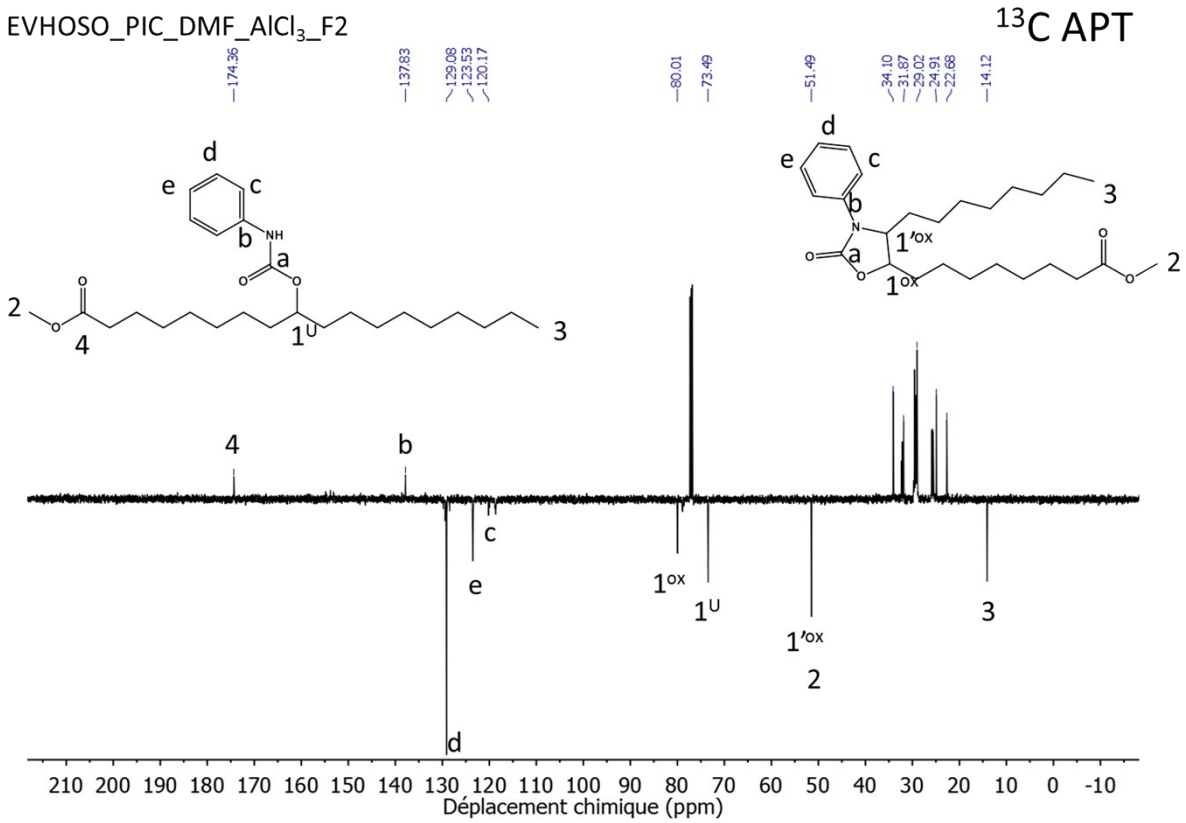

Figure S62 ^{13}C NMR Attached Proton test (APT) spectrum of EVHOSO_PIC_AlCl$_3$_F2.

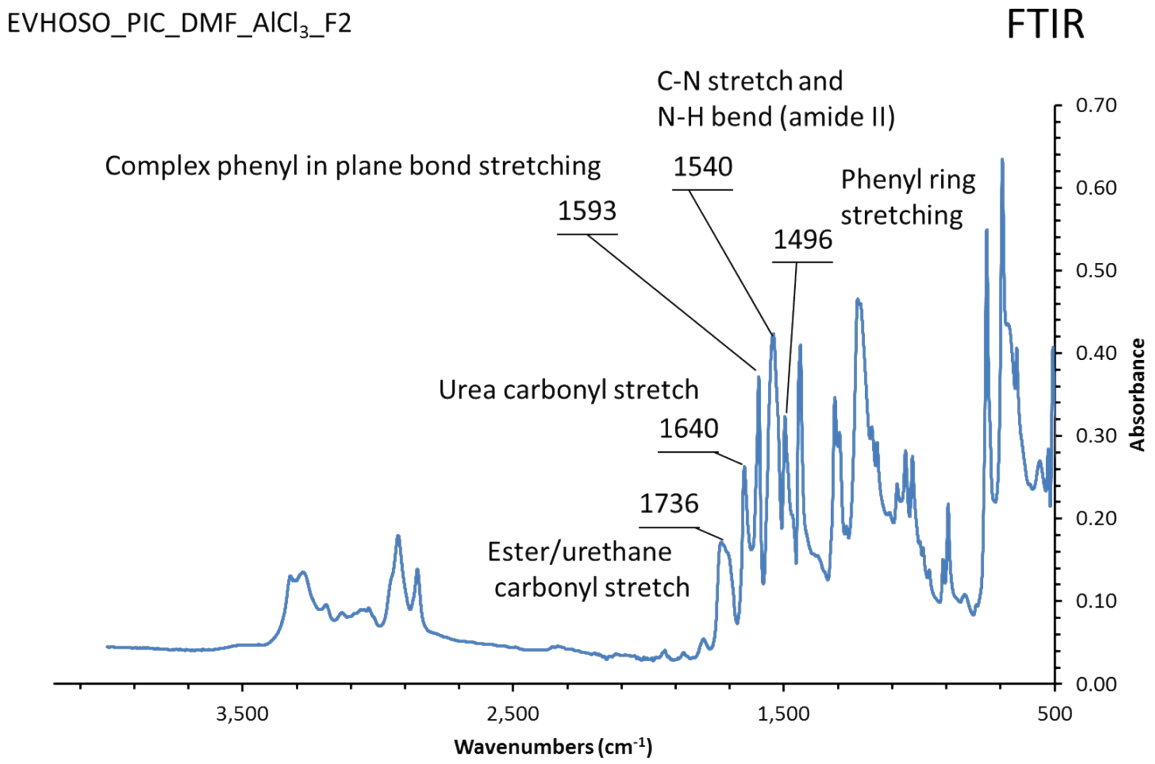

Figure S63 FTIR spectrum of EVHOSO_PIC_AlCl$_3$_F2.

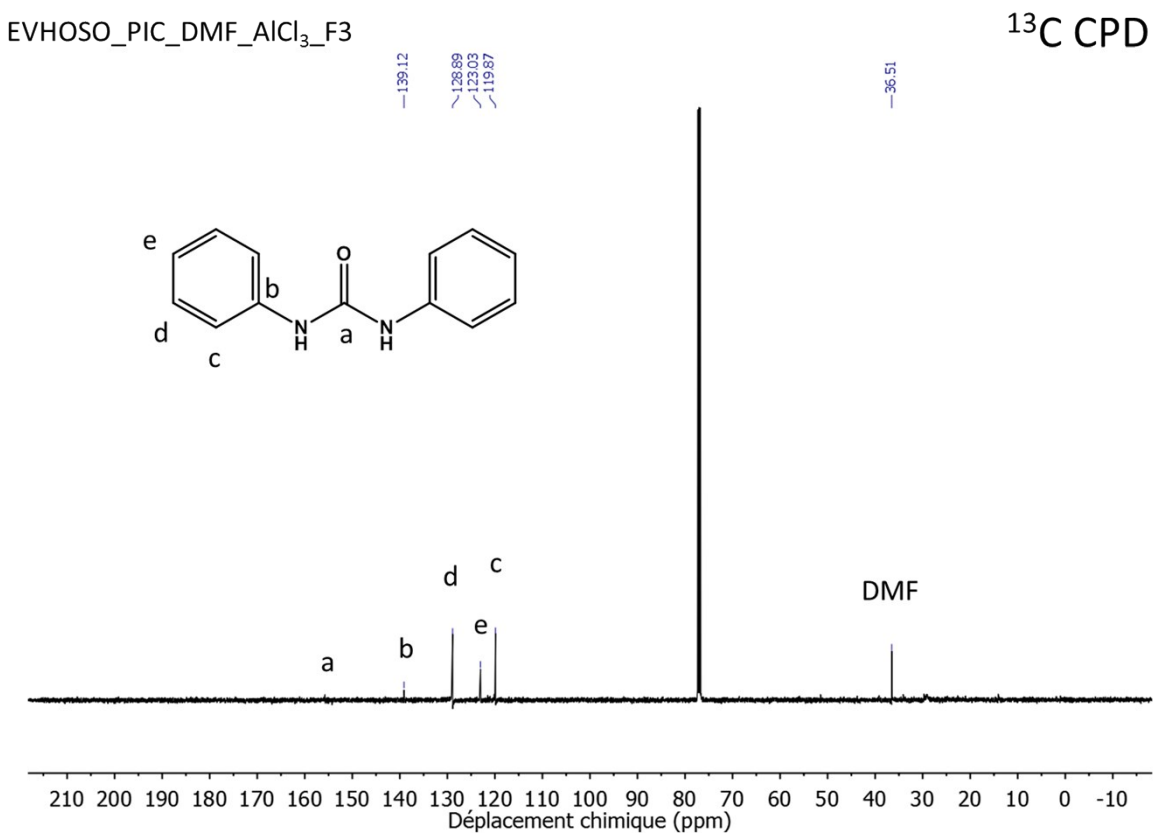

Figure S64 ^{13}C NMR Composite Programmed Decoupling (CPD) spectrum of EVHOSO_PIC_$AlCl_3$_F3.

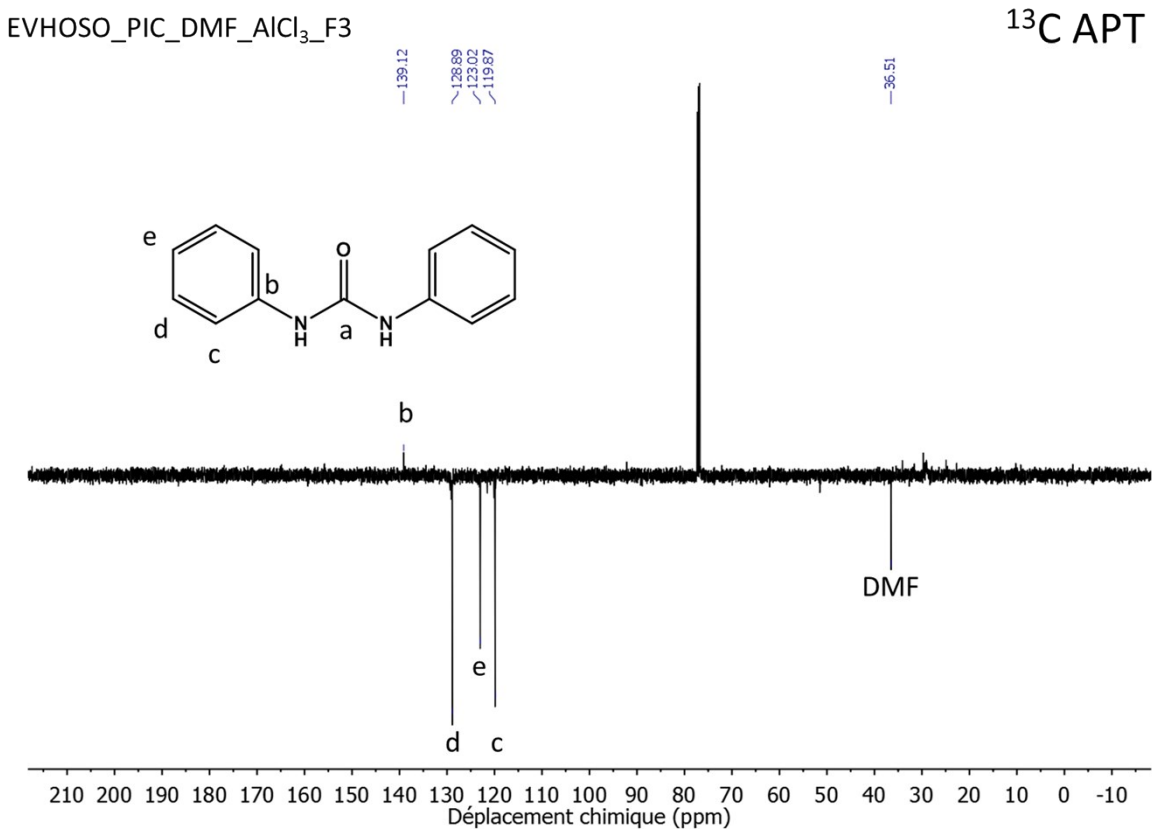

Figure S65 ^{13}C NMR Attached Proton test (APT) spectrum of EVHOSO_PIC_$AlCl_3$_F3.

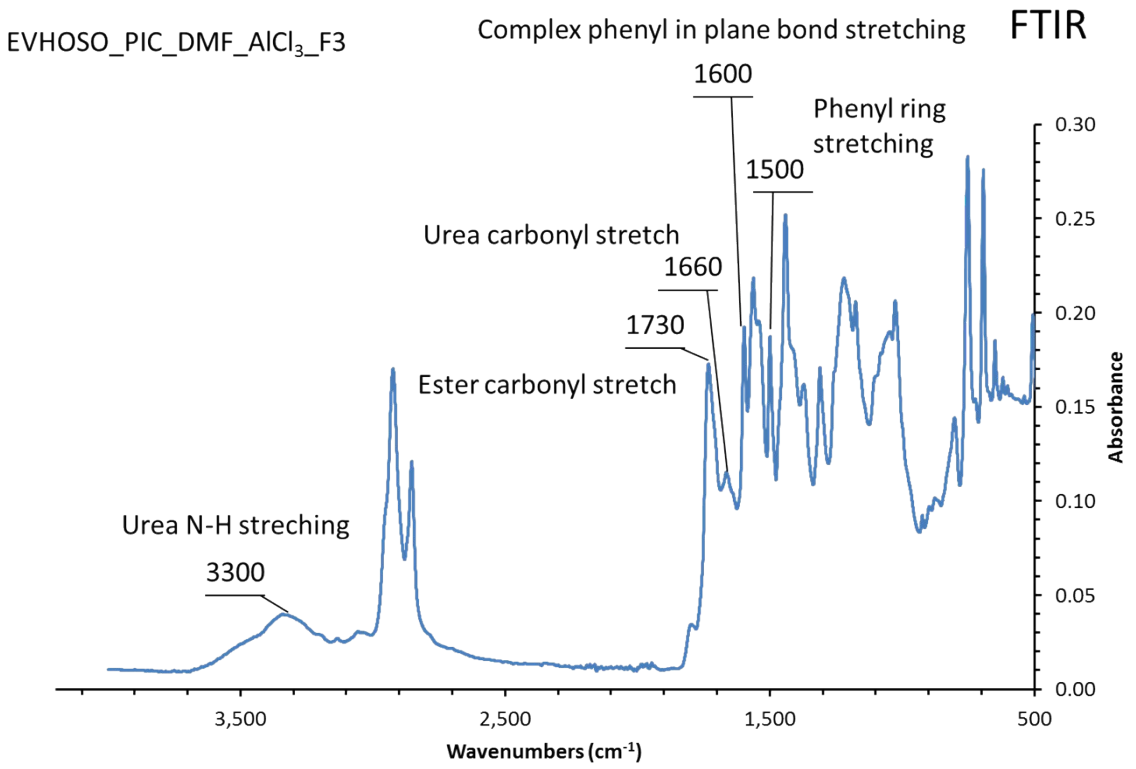

Figure S66 FTIR spectrum of EVHOSO_PIC_$AlCl_3$_F3.

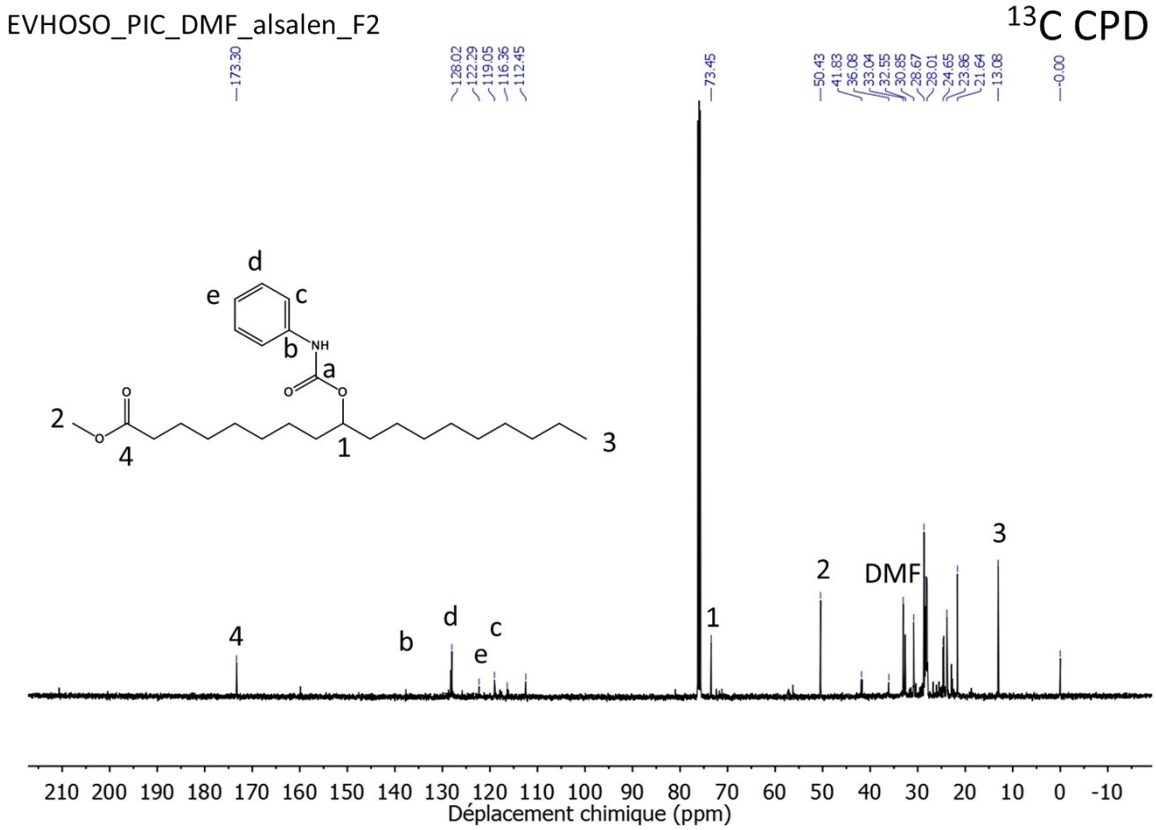

Figure S67 ^{13}C NMR Composite Programmed Decoupling (CPD) spectrum of EVHOSO_PIC_Al(salen)$_2$_F2.

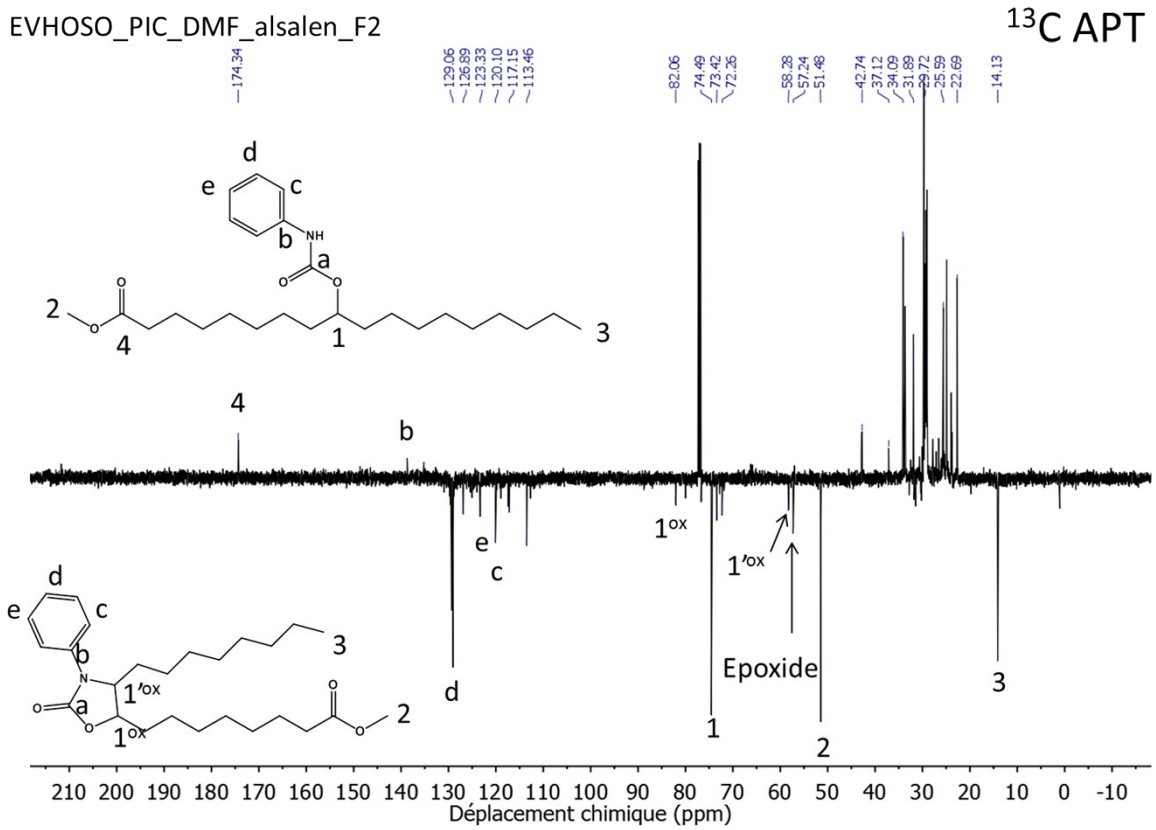

Figure S68 ^{13}C NMR Attached Proton test (APT) spectrum of EVHOSO_PIC_Al(salen)$_2$_F2.

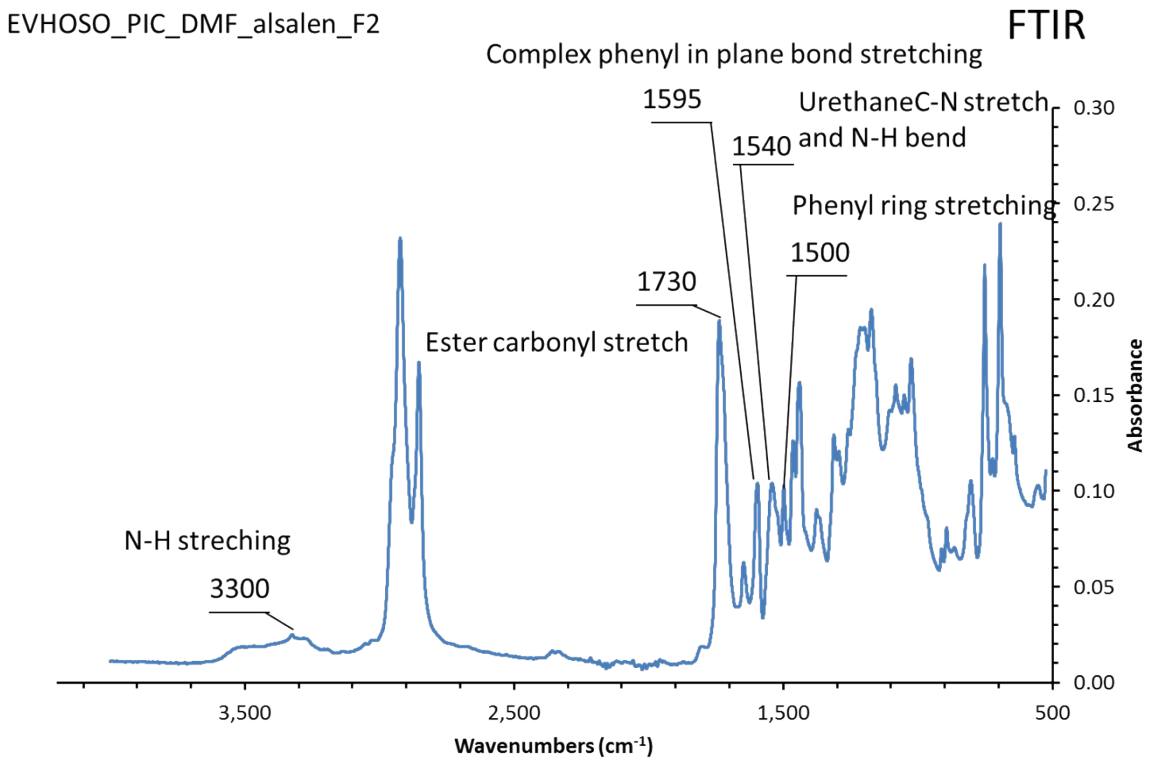

Figure S69 FTIR spectrum of EVHOSO_PIC_Al(salen)$_2$_F2.

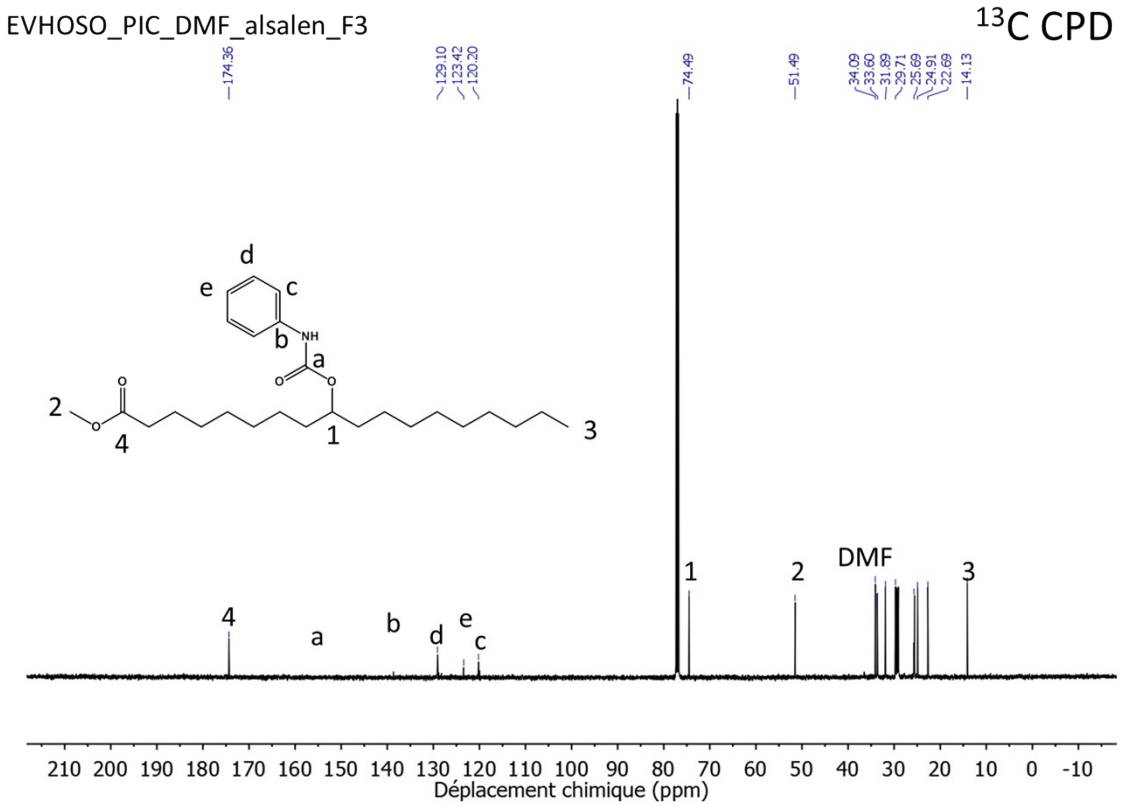

Figure S70 ^{13}C NMR Composite Programmed Decoupling (CPD) spectrum of EVHOSO_PIC_Al(salen)$_2$_F3.

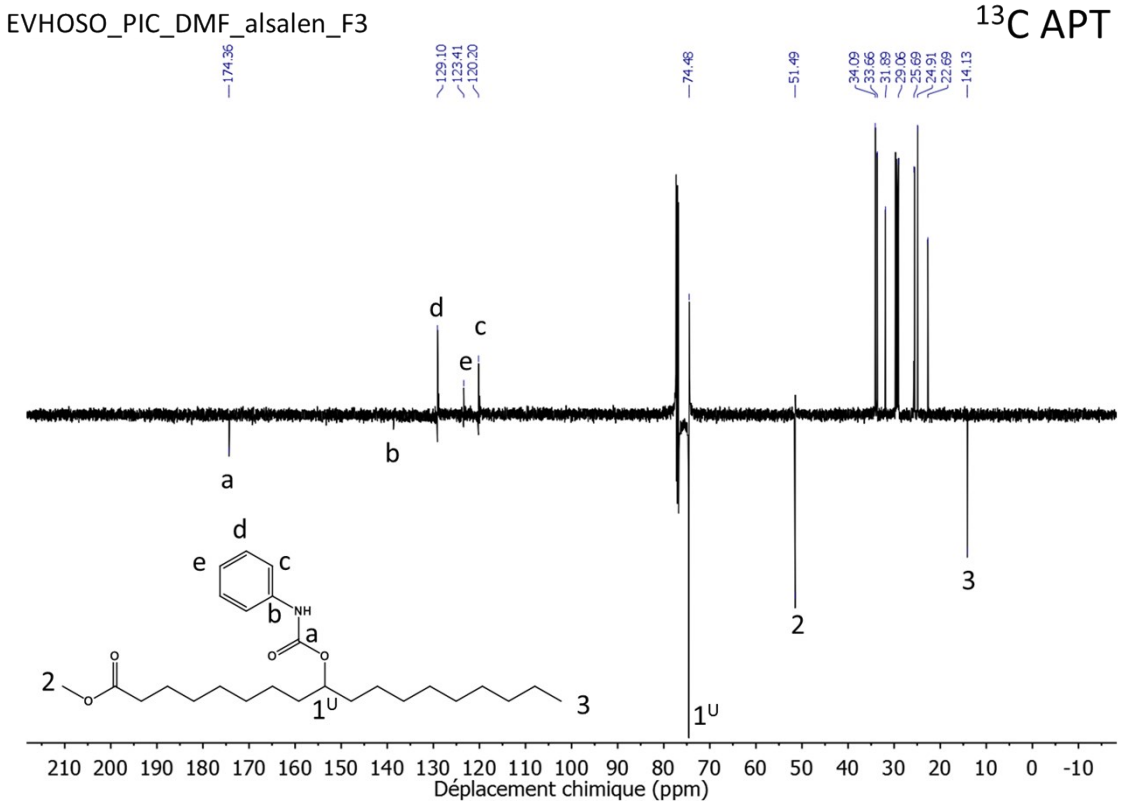

Figure S71 ^{13}C NMR Attached Proton test (APT) spectrum of EVHOSO_PIC_Al(Salen)$_2$_F3.

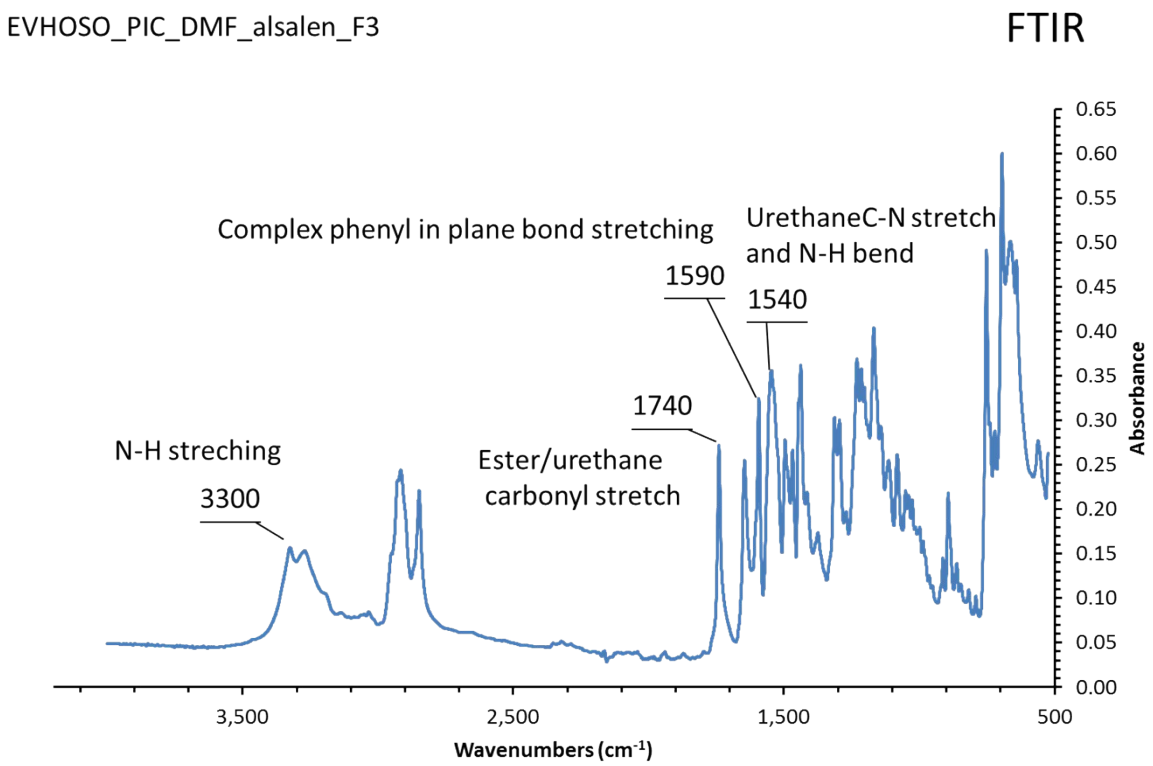

Figure S72 FTIR spectrum of EVHOSO_PIC_Al(salen)$_2$_F3.

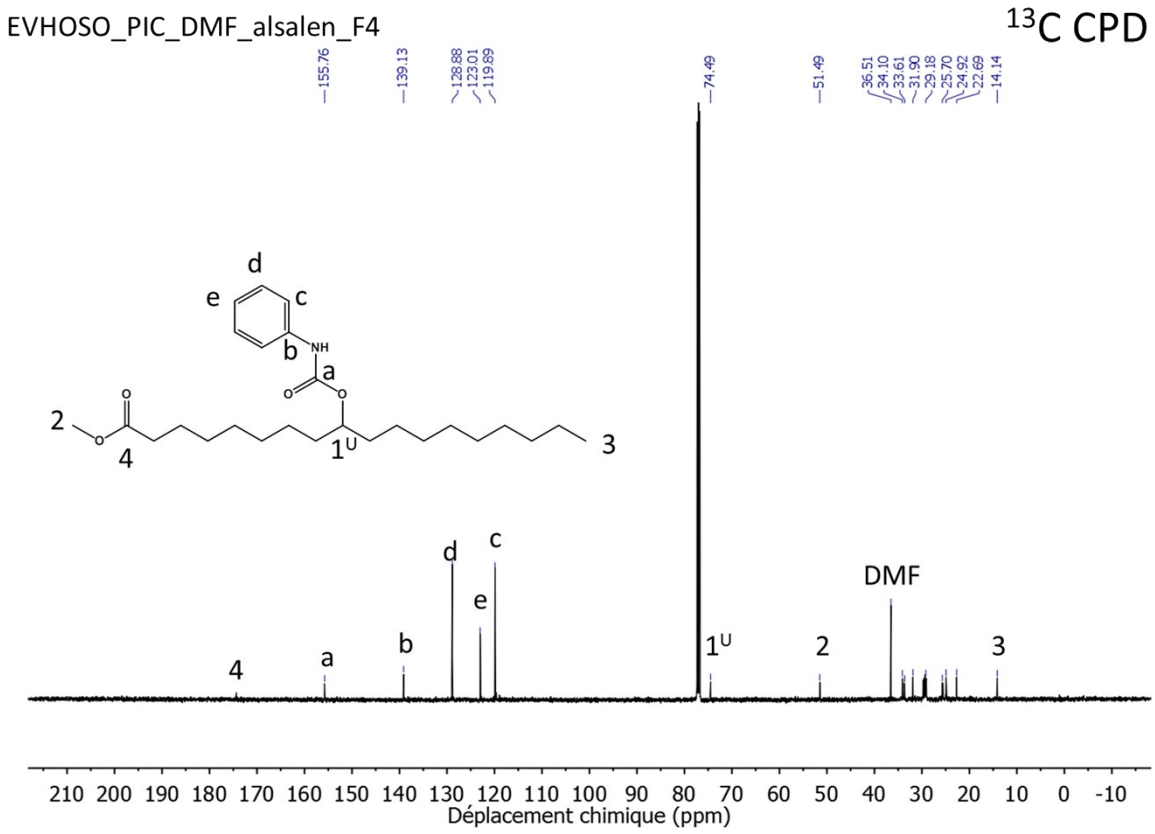

Figure S73 ^{13}C NMR Composite Programmed Decoupling (CPD) spectrum of EVHOSO_PIC_Al(salen)$_2$_F4.

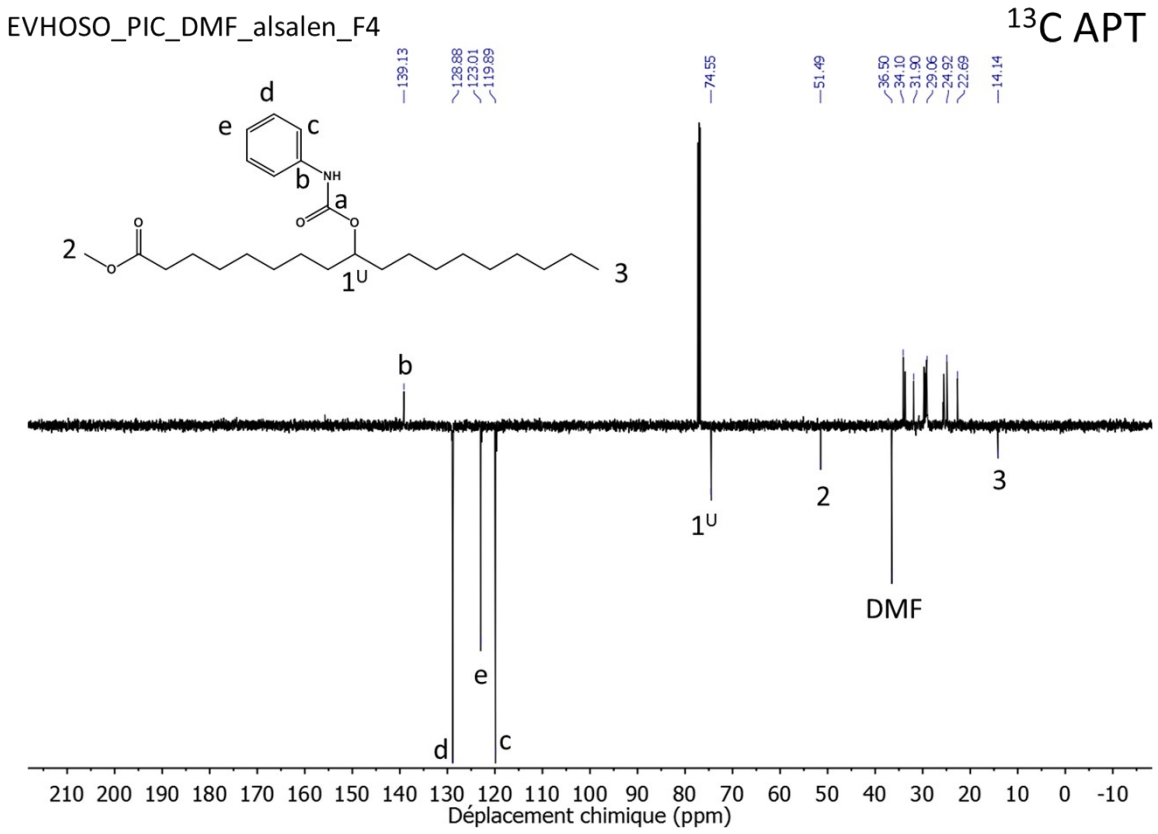

Figure S74 ^{13}C NMR Attached Proton test (APT) spectrum of EVHOSO_PIC_Al(salen)$_2$_F4.

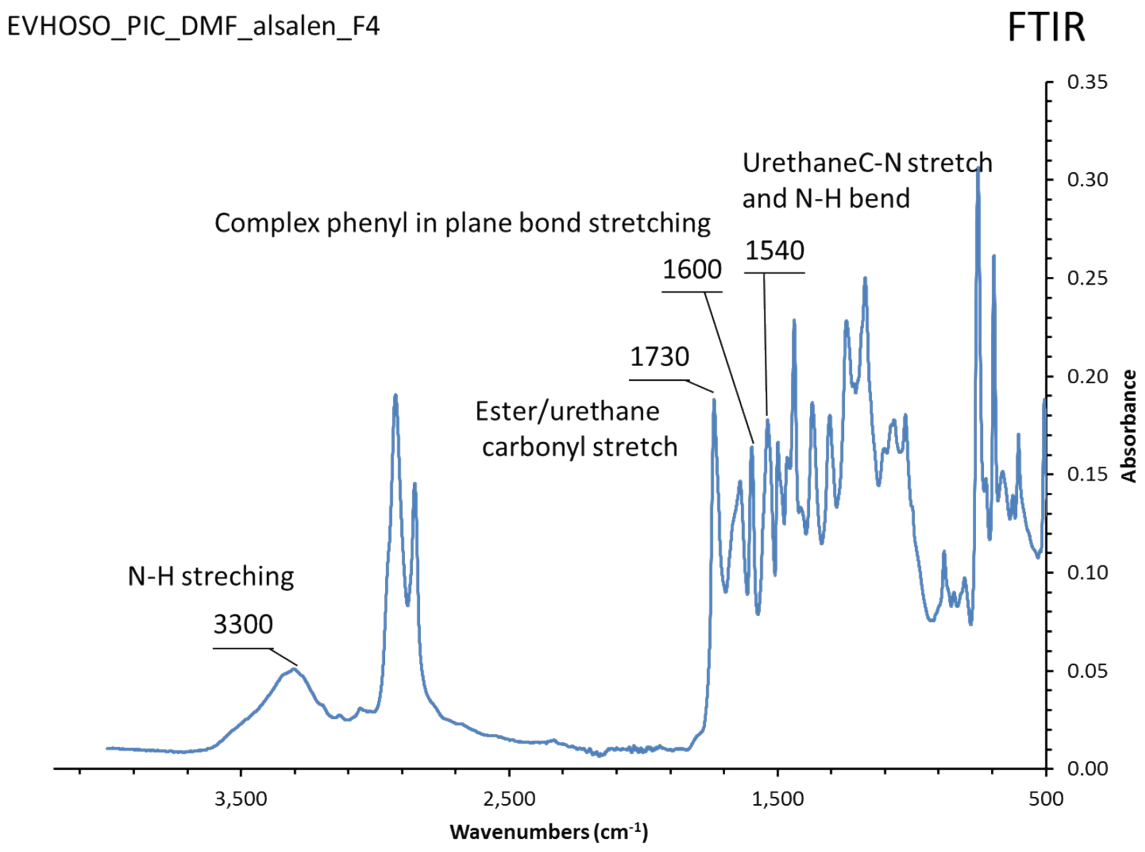

Figure S75 FTIR spectrum of EVHOSO_PIC_Al(salen)$_2$_F4.